

**@ Electronic Supplementary Information @**

**Enantioselective recognition of inherently chiral calix[4]arene  
crown-6 carboxylic acid cone conformer towards chiral  
aminoalcohols**

Ke Yang<sup>a</sup>, Si-Zhe Li<sup>a</sup>, Yin-Hu Wang<sup>a</sup>, Wen-Zhen Zhang<sup>a</sup>, Zhan-Hui Xu<sup>c</sup>,  
Xiang-Yong Zhou<sup>b</sup>, Rong-Xiu Zhu<sup>b,\*</sup>, Jun Luo<sup>a,\*</sup>, Qian Wan<sup>a,\*</sup>

<sup>a</sup> *Tongji School of Pharmacy, Huazhong University of Science and Technology, No. 13 Hangkong Road, Wuhan 430030, PR China*

<sup>b</sup> *Institute of Theoretical Chemistry, School of Chemistry and Chemical Engineering, Shandong University, Jinan 250100, PR China*

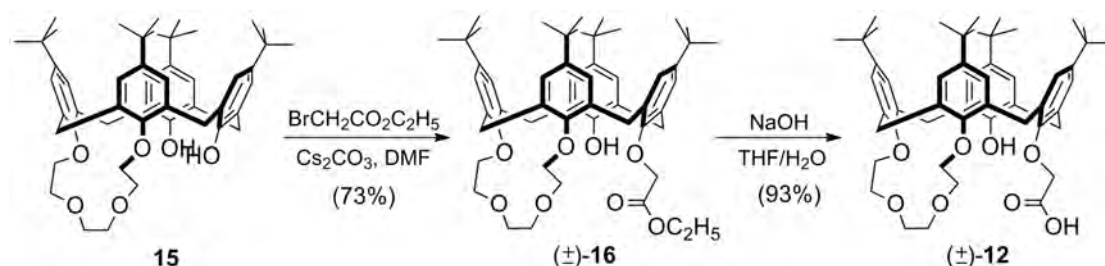
<sup>c</sup> *College of Chemistry and Molecular Engineering, Zhengzhou University, No. 100 Kexue Road, Zhengzhou 450001, PR China*

\*E-mail addresses: rxzhu@sdu.edu.cn (R.-X. Zhu); lawdream1975@163.com (J. Luo); wanqian@hust.edu.cn (Q. Wan)

## Part A. Synthesis

### A-1. Synthesis of (±)-12

Compound (±)-12 was synthesized according to the two-step procedure for the synthesis of its debutylated analogues<sup>1</sup>, starting from 15<sup>2</sup> (Scheme S-1).



**Scheme S-1** Synthesis of (±)-12 starting from 15.

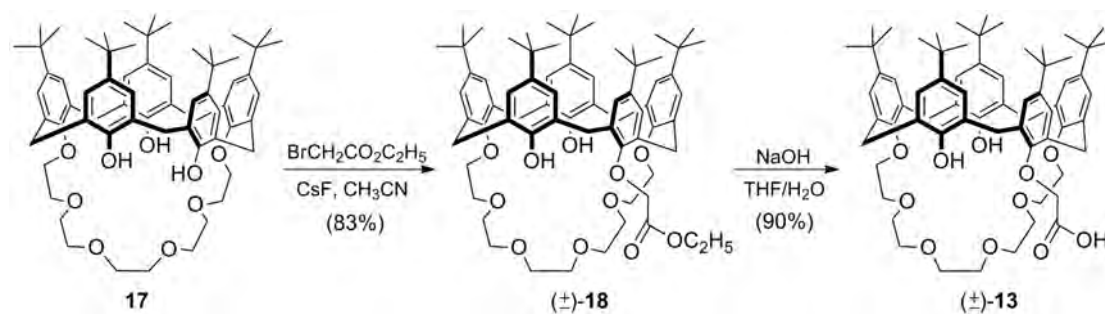
*Synthesis of (±)-16:* To a stirred mixture of 15 (4.69 g, 6.15 mmol), Cs<sub>2</sub>CO<sub>3</sub> (2.00 g, 6.15 mmol) in dry DMF (400 mL) was added BrCH<sub>2</sub>CO<sub>2</sub>C<sub>2</sub>H<sub>5</sub> (816 μL, 7.38 mmol) and the reaction mixture was heated at 60 °C overnight. The solvent was removed under reduced pressure and the residue was partitioned between CH<sub>2</sub>Cl<sub>2</sub> and H<sub>2</sub>O. The organic layer was dried over anhydrous Na<sub>2</sub>SO<sub>4</sub>. Purification by column chromatography (SiO<sub>2</sub>, petroleum ether/ethyl acetate = 4:1 v/v) gave (±)-16 as a white solid in 73% yield (3.88 g). Mp 231–233 °C (CH<sub>2</sub>Cl<sub>2</sub>/CH<sub>3</sub>OH). Anal. Calcd for C<sub>54</sub>H<sub>72</sub>O<sub>8</sub>·0.1CH<sub>2</sub>Cl<sub>2</sub>: C, 75.76; H, 8.49. Found C, 75.69; H, 8.53. <sup>1</sup>H NMR (400 MHz, CDCl<sub>3</sub>): δ 7.16 (d, 1H, *J* = 2.4 Hz, ArH), 7.13 (d, 1H, *J* = 2.4 Hz, ArH), 7.08 (d, 1H, *J* = 2.4 Hz, ArH), 7.02 (d, 1H, *J* = 2.4 Hz, ArH), 6.70 (d, 1H, *J* = 2.4 Hz, ArH), 6.63 (d, 1H, *J* = 2.4 Hz, ArH), 6.41 (s, 2H, ArH), 5.96 (s, 1H, OH), 4.57 (d, 1H, *J* = 15.6 Hz, 1H, ArOCH<sub>2</sub>CO<sub>2</sub>), 4.53 (d, 1H, *J* = 12.4 Hz, ArCH<sub>2</sub>Ar), 4.50 (d, 1H, *J* = 12.8 Hz, ArCH<sub>2</sub>Ar), 4.43 (d, 1H, *J* = 12.8 Hz, ArCH<sub>2</sub>Ar), 4.42 (d, 1H, *J* = 15.6 Hz, 1H, ArOCH<sub>2</sub>CO<sub>2</sub>), 4.43–3.72 (m, 12H, OCH<sub>2</sub>CH<sub>2</sub>O), 4.27 (t, *J* = 7.6 Hz, 2H, CO<sub>2</sub>CH<sub>2</sub>CH<sub>3</sub>), 4.20 (d, 1H, *J* = 13.2 Hz, ArCH<sub>2</sub>Ar), 3.30 (d, 1H, *J* = 13.4 Hz, ArCH<sub>2</sub>Ar), 3.23 (d, 1H, *J* = 13.2 Hz, ArCH<sub>2</sub>Ar), 3.19 (d, 2H, *J* = 11.4 Hz, ArCH<sub>2</sub>Ar), 1.32 (t, 3H, *J* = 7.6 Hz, CO<sub>2</sub>CH<sub>2</sub>CH<sub>3</sub>), 1.33 (s, 9H, C(CH<sub>3</sub>)<sub>3</sub>), 1.32 (s, 9H, C(CH<sub>3</sub>)<sub>3</sub>), 0.91 (s, 9H, C(CH<sub>3</sub>)<sub>3</sub>), 0.74 (s, 9H, C(CH<sub>3</sub>)<sub>3</sub>). <sup>13</sup>C NMR (100 MHz, CDCl<sub>3</sub>): δ 169.6,

153.6, 152.4, 150.7, 150.1, 146.2, 145.8, 145.2, 141.3, 136.1, 135.6, 133.0, 131.8, 131.7, 131.6, 129.6, 127.8, 125.8, 125.7, 125.5, 125.3, 125.2, 124.7, 124.6, 75.3, 72.31, 72.27, 71.8, 69.9, 69.5, 69.0, 61.0, 34.1, 33.8, 33.6, 31.8, 31.7, 31.4, 31.1, 31.0, 30.2, 14.3. MS (ESI):  $m/z$  871.9 ( $M + Na^+$ , 100%).

*Synthesis of (±)-12*: To a solution of NaOH (108 mg, 2.7 mmol) in THF/H<sub>2</sub>O (10 mL/10 mL) was added (±)-**16** (234 mg, 0.27 mmol) and the reaction mixture was heated to 60 °C for 5h. After evaporation of the solvent under reduced pressure, the residue was partitioned between 10% HCl and CH<sub>2</sub>Cl<sub>2</sub>. The organic layer was dried over anhydrous Na<sub>2</sub>SO<sub>4</sub>. Purification by column chromatography (SiO<sub>2</sub>, petroleum ether/ethyl acetate = from 3:1 to 1:1 v/v) gave (±)-**12** as a white solid in 93% yield (210 mg). Mp 148–150 °C (CH<sub>2</sub>Cl<sub>2</sub>/CH<sub>3</sub>OH). <sup>1</sup>H NMR (400 MHz, CDCl<sub>3</sub>): δ 7.73 (s, 1H, OH), 7.06 (d, 1H,  $J = 2.0$  Hz, ArH), 7.02 (d, 1H,  $J = 2.0$  Hz, ArH), 6.96 (d, 1H,  $J = 2.4$  Hz, ArH), 6.95 (d, 1H,  $J = 2.4$  Hz, ArH), 6.93 (d, 1H,  $J = 2.0$  Hz, ArH), 6.90 (d, 2H,  $J = 1.6$  Hz, ArH), 6.87 (d, 1H,  $J = 2.0$  Hz, ArH), 4.87 (d, 1H,  $J = 16.4$  Hz, ArOCH<sub>2</sub>CO<sub>2</sub>), 4.83 (d, 1H,  $J = 13.2$  Hz, ArCH<sub>2</sub>Ar), 4.39 (d, 1H,  $J = 15.6$  Hz, ArOCH<sub>2</sub>CO<sub>2</sub>), 4.27 (d, 1H,  $J = 12.8$  Hz, ArCH<sub>2</sub>Ar), 4.19 (d, 1H,  $J = 13.2$  Hz, ArCH<sub>2</sub>Ar), 4.08 (d, 1H,  $J = 13.6$  Hz, ArCH<sub>2</sub>Ar), 4.24–3.79 (m, 12H, OCH<sub>2</sub>CH<sub>2</sub>O), 3.41 (d, 1H,  $J = 13.6$  Hz, ArCH<sub>2</sub>Ar), 3.31 (d, 1H,  $J = 13.2$  Hz, ArCH<sub>2</sub>Ar), 3.28 (d, 1H,  $J = 13.6$  Hz, ArCH<sub>2</sub>Ar), 3.27 (d, 1H,  $J = 12.4$  Hz, ArCH<sub>2</sub>Ar), 1.21 (s, 9H, C(CH<sub>3</sub>)<sub>3</sub>), 1.12 (s, 9H, C(CH<sub>3</sub>)<sub>3</sub>), 1.09 (s, 9H, C(CH<sub>3</sub>)<sub>3</sub>), 1.08 (s, 9H, C(CH<sub>3</sub>)<sub>3</sub>). <sup>13</sup>C NMR (100 MHz, CDCl<sub>3</sub>): δ 170.9, 152.3, 151.2, 150.3, 149.1, 147.3, 146.9, 146.0, 142.8, 135.0, 134.1, 134.0, 133.7, 132.4, 132.24, 132.22, 129.2, 128.3, 126.4, 126.0, 125.70, 125.67, 125.5, 125.1, 75.3, 74.4, 71.7, 70.45, 70.36, 70.2, 69.2, 34.1, 34.0, 33.9, 32.8, 32.4, 31.6, 31.5, 31.30, 31.27, 31.2, 29.8. MS (ESI):  $m/z$  843.8 ( $M + Na^+$ , 100%). Anal. Calcd for C<sub>52</sub>H<sub>68</sub>O<sub>8</sub>: C, 76.06; H, 8.35. Found C, 76.04; H, 8.39.

## A-2. Synthesis of (±)-13

Compound (±)-**13** was synthesized according to the two-step procedure for the synthesis of its crown-5 analogues<sup>3</sup>, starting from **17**<sup>4</sup> (Scheme S-2).



**Scheme S-2** Synthesis of (±)-13 starting from 17.

*Synthesis of (±)-18:* A mixture of **17** (476 mg, 0.47 mmol), CsF (143 mg, 0.94 mmol) and BrCH<sub>2</sub>CO<sub>2</sub>C<sub>2</sub>H<sub>5</sub> (62 μL, 0.56 mmol) in THF (50 mL) was refluxed for 2d. After evaporation of the solvent under reduced pressure, the residue was partitioned between CH<sub>2</sub>Cl<sub>2</sub> and 3.6% HCl. The organic layer was dried over anhydrous MgSO<sub>4</sub>. Purification by column chromatography (SiO<sub>2</sub>, petroleum ether/acetone = 6:1 v/v) gave (±)-**18** as a white solid in 83% yield (429 mg). Mp 96–98 °C. <sup>1</sup>H NMR (CDCl<sub>3</sub>, 400 MHz): δ 7.23 (d, 1H, *J* = 2.4 Hz, ArH), 7.14 (s, 2H, ArH), 7.13 (s, 1H, OH), 7.11 (d, 1H, *J* = 2.4 Hz, ArH), 7.10 (d, 1H, *J* = 2.4 Hz, ArH), 7.04 (d, 1H, *J* = 2.4 Hz, ArH), 6.97 (d, 1H, *J* = 2.0 Hz, ArH), 6.90 (d, 1H, *J* = 2.0 Hz, ArH), 6.58 (s, 1H, OH), 6.47 (d, 1H, *J* = 2.0 Hz, ArH), 6.42 (d, 1H, *J* = 1.6 Hz, ArH), 4.59 (d, 1H, *J* = 15.6 Hz, ArOCH<sub>2</sub>CO<sub>2</sub>), 4.56–4.47 (m, 3H, ArCH<sub>2</sub>Ar, ArOCH<sub>2</sub>CO<sub>2</sub>), 4.44 (d, 1H, *J* = 14.0 Hz, ArCH<sub>2</sub>Ar), 4.42 (d, 2H, *J* = 14.0 Hz, ArCH<sub>2</sub>Ar), 4.31 (q, 2H, *J* = 7.2 Hz, CO<sub>2</sub>CH<sub>2</sub>CH<sub>3</sub>), 4.17–3.67 (m, 20H, OCH<sub>2</sub>CH<sub>2</sub>O), 3.40 (d, 2H, *J* = 16.4 Hz, ArCH<sub>2</sub>Ar), 3.36 (d, 1H, *J* = 15.2 Hz, ArCH<sub>2</sub>Ar), 3.34 (d, 1H, *J* = 15.6 Hz, ArCH<sub>2</sub>Ar), 3.30 (d, 1H, *J* = 14.8 Hz, ArCH<sub>2</sub>Ar), 1.35 (t, 3H, *J* = 7.2 Hz, CO<sub>2</sub>CH<sub>2</sub>CH<sub>3</sub>), 1.33 (s, 9H, C(CH<sub>3</sub>)<sub>3</sub>), 1.25 (s, 9H, C(CH<sub>3</sub>)<sub>3</sub>), 1.16 (s, 9H, C(CH<sub>3</sub>)<sub>3</sub>), 0.98 (s, 9H, C(CH<sub>3</sub>)<sub>3</sub>), 0.56 (s, 9H, C(CH<sub>3</sub>)<sub>3</sub>). <sup>13</sup>C NMR (CDCl<sub>3</sub>, 100MHz): δ 169.7, 151.7, 151.6, 150.4, 150.2, 149.5, 146.5, 146.40, 146.36, 142.0, 141.5, 134.4, 133.5, 133.0, 132.7, 132.6, 132.5, 128.0, 127.4, 127.1, 126.9, 126.34, 126.32, 126.13, 126.06, 125.6, 125.2, 125.02, 124.96, 124.8, 124.3, 74.4, 73.2, 71.3, 71.1, 71.0, 70.9, 70.8, 70.7, 70.5, 70.1, 61.1, 34.1, 34.0, 33.9, 33.8, 33.7, 31.7, 31.6, 31.4, 31.2, 31.1, 30.8, 30.5, 30.1, 30.01, 29.98, 14.3. MS (ESI) *m/z*: 1138.7 (M + K<sup>+</sup>, 100%). Anal. Calcd for C<sub>69</sub>H<sub>94</sub>O<sub>11</sub>: C,

75.38; H, 8.62. Found C, 75.31; H, 8.72.

*Synthesis of (±)-13*: To a solution of NaOH (313 mg, 7.8 mmol) in THF/H<sub>2</sub>O (25 mL/25 mL) was added (±)-**18** (430 mg, 0.39 mmol) and the reaction mixture was heated to 60 °C overnight. After evaporation of the solvent under reduced pressure, the residue was partitioned between 10% HCl and CH<sub>2</sub>Cl<sub>2</sub>. The organic layer was dried over anhydrous MgSO<sub>4</sub>. Purification by column chromatography (SiO<sub>2</sub>, petroleum ether/acetone = 2:1 v/v) gave (±)-**13** as a white solid in 90% yield (377 mg). Mp 123–125 °C. <sup>1</sup>H NMR (CDCl<sub>3</sub>, 400 MHz): δ 7.29 (d, 1H, *J* = 2.0 Hz, ArH), 7.23 (d, 1H, *J* = 2.0 Hz, ArH), 7.20–7.19 (m, 2H, ArH), 7.15–7.14 (m, 2H, ArH), 7.04 (d, 1H, *J* = 2.0 Hz, ArH), 6.89 (s, 1H, OH), 6.83 (d, 1H, *J* = 1.6 Hz, ArH), 6.82 (d, 1H, *J* = 2.0 Hz, ArH), 6.68 (d, 1H, *J* = 1.6 Hz, ArH), 6.50 (s, 1H, OH), 4.53 (d, 1H, *J* = 15.2 Hz, ArCH<sub>2</sub>Ar), 4.49 (d, 1H, *J* = 15.2 Hz, ArCH<sub>2</sub>Ar), 4.45 (d, 1H, *J* = 14.0 Hz, ArCH<sub>2</sub>Ar), 4.42 (d, 1H, *J* = 13.6 Hz, ArCH<sub>2</sub>Ar), 4.26–3.64 (m, 22H, ArOCH<sub>2</sub>CO<sub>2</sub>, OCH<sub>2</sub>CH<sub>2</sub>O), 4.08 (d, 1H, *J* = 13.2 Hz, ArCH<sub>2</sub>Ar), 3.50 (d, 1H, *J* = 13.6 Hz, ArCH<sub>2</sub>Ar), 3.41 (d, 1H, *J* = 15.6 Hz, ArCH<sub>2</sub>Ar), 3.38 (d, 1H, *J* = 14.0 Hz, ArCH<sub>2</sub>Ar), 3.37 (d, 1H, *J* = 14.4 Hz, ArCH<sub>2</sub>Ar), 3.36 (d, 1H, *J* = 14.8 Hz, ArCH<sub>2</sub>Ar), 1.34 (s, 9H, C(CH<sub>3</sub>)<sub>3</sub>), 1.27 (s, 9H, C(CH<sub>3</sub>)<sub>3</sub>), 1.26 (s, 9H, C(CH<sub>3</sub>)<sub>3</sub>), 0.95 (s, 9H, C(CH<sub>3</sub>)<sub>3</sub>), 0.78 (s, 9H, C(CH<sub>3</sub>)<sub>3</sub>). <sup>13</sup>C NMR (CDCl<sub>3</sub>, 100MHz): δ 170.7, 151.4, 150.6, 150.1, 150.0, 149.2, 146.82, 146.79, 146.5, 142.3, 141.6, 133.9, 133.7, 132.9, 132.7, 132.3, 127.2, 127.1, 126.7, 126.5, 126.4, 126.2, 125.9, 125.6, 125.5, 125.3, 125.2, 124.5, 74.24, 74.19, 71.1, 71.0, 70.7, 70.61, 70.57, 70.3, 70.2, 34.2, 34.0, 33.9, 31.9, 31.7, 31.6, 31.5, 31.1, 31.0, 30.3, 29.44, 29.38, 29.3. MS (ESI) *m/z*: 1094.3 (M + Na<sup>+</sup>, 100%). Anal. Calcd for C<sub>67</sub>H<sub>90</sub>O<sub>11</sub>·0.5H<sub>2</sub>O: C, 74.48; H, 8.49. Found C, 74.52; H, 8.53.

## References

1. Cao, Y.-D.; Luo, J.; Zheng, Q.-Y.; Chen, C.-F.; Wang, M.-X.; Huang, Z.-T. *J. Org. Chem.* **2004**, *69*, 206.
2. Arduini, A.; Domiano, L.; Pochini, A.; Secchi, A.; Ungaro, R.; Ugozzoli, F.; Struck, O.; Verboom, W.; Reinhoudt, D. N. *Tetrahedron* **1997**, *53*, 3767.

3. Arnecke, R.; Böhmer, V.; Ferguson, G.; Pappalardo, S. *Tetrahedron Lett.* **1996**, *37*, 1497.
4. Kraft, D.; Arnecke, R.; Böhmer, V.; Vogt, W. *Tetrahedron* **1993**, *49*, 6019.

## Part B. NMR spectra of new compounds

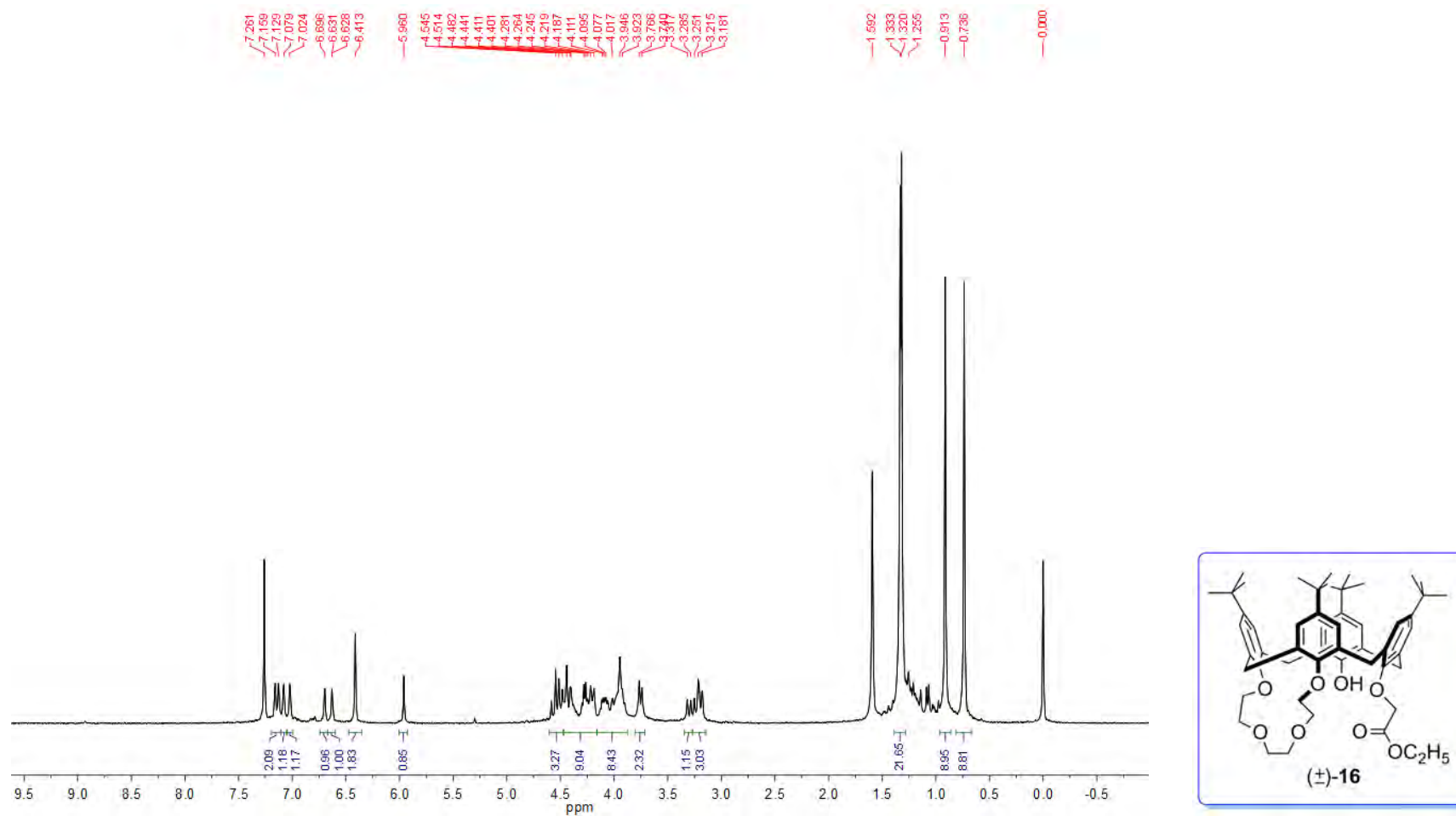


**Fig. S-1** <sup>1</sup>H NMR spectrum of (±)-16 (CDCl<sub>3</sub>, 400 MHz, 25 °C).

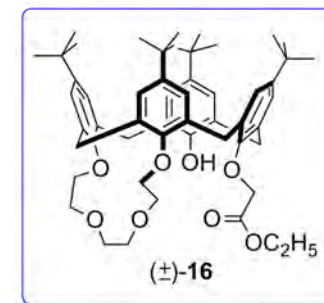
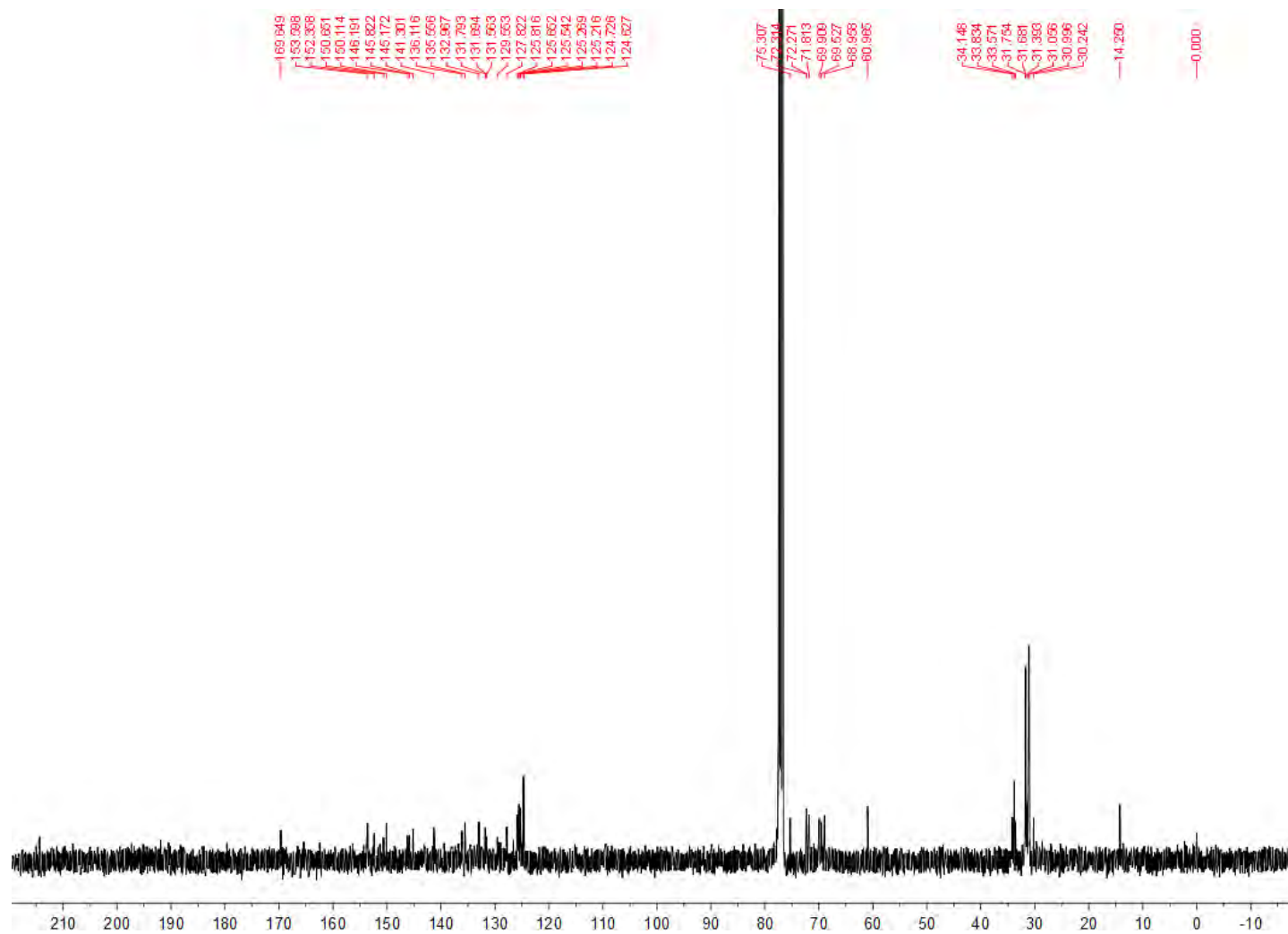


**Fig. S-2**  $^{13}\text{C}$  NMR spectrum of (±)-**16** ( $\text{CDCl}_3$ , 100 MHz, 25 °C).



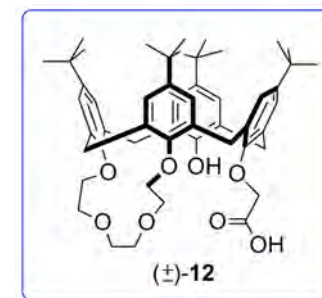
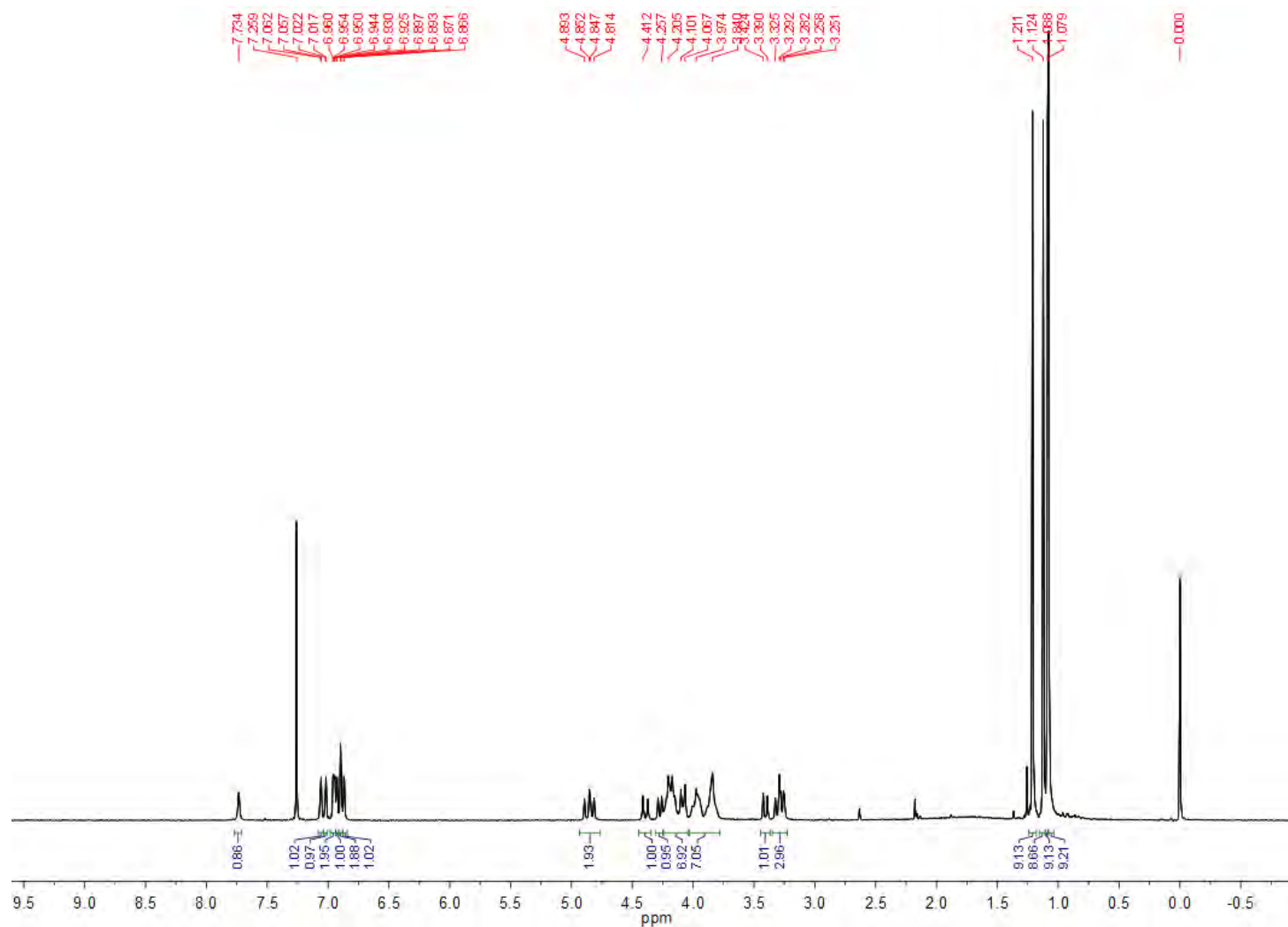


**Fig. S-3**  $^1\text{H}$  NMR spectrum of (±)-12 ( $\text{CDCl}_3$ , 400 MHz, 25 °C).

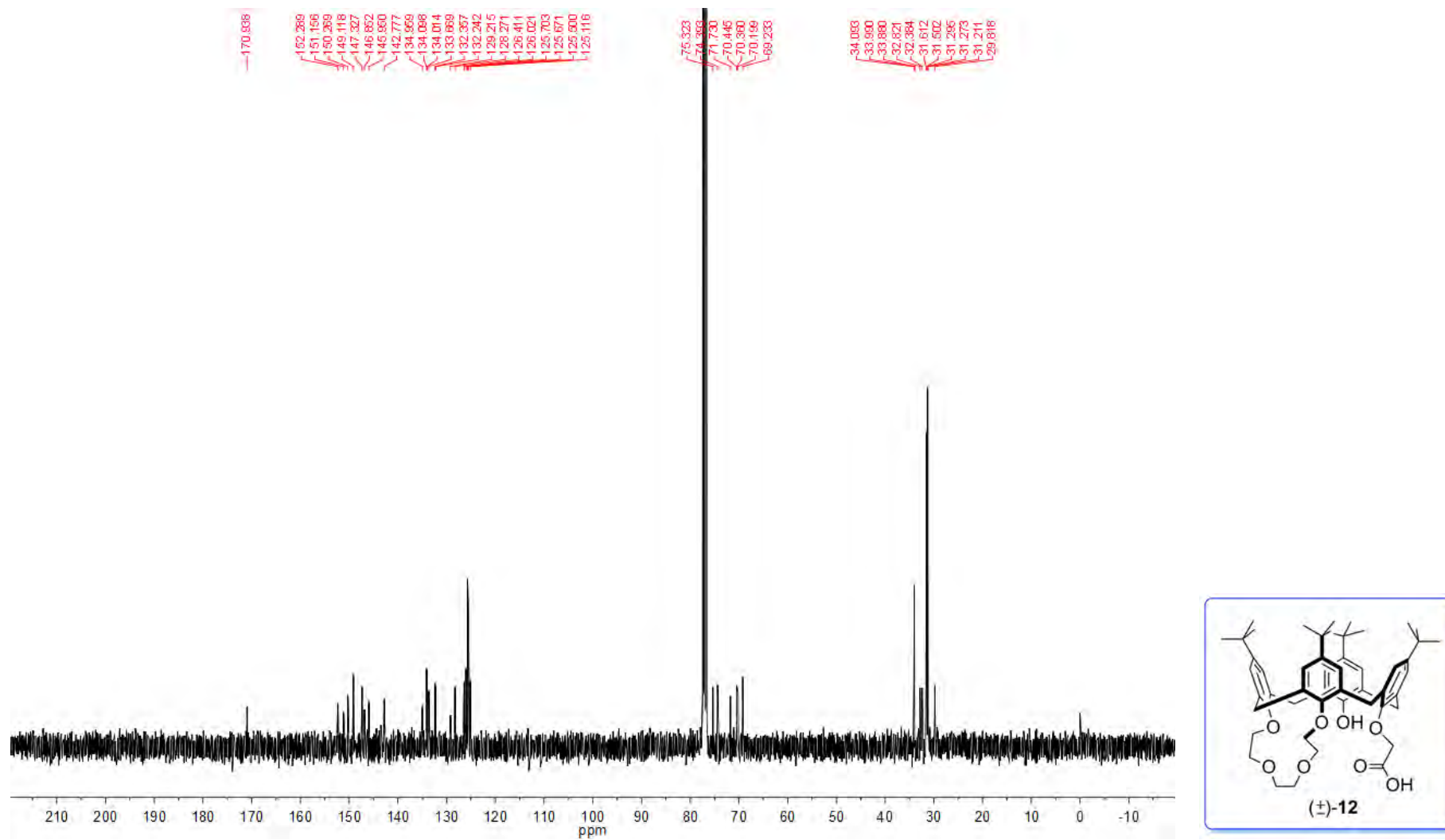


**Fig. S-4**  $^{13}\text{C}$  NMR spectrum of (±)-12 ( $\text{CDCl}_3$ , 100 MHz, 25 °C).

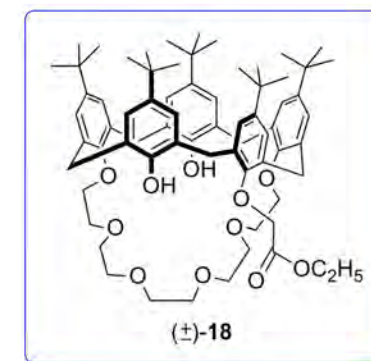
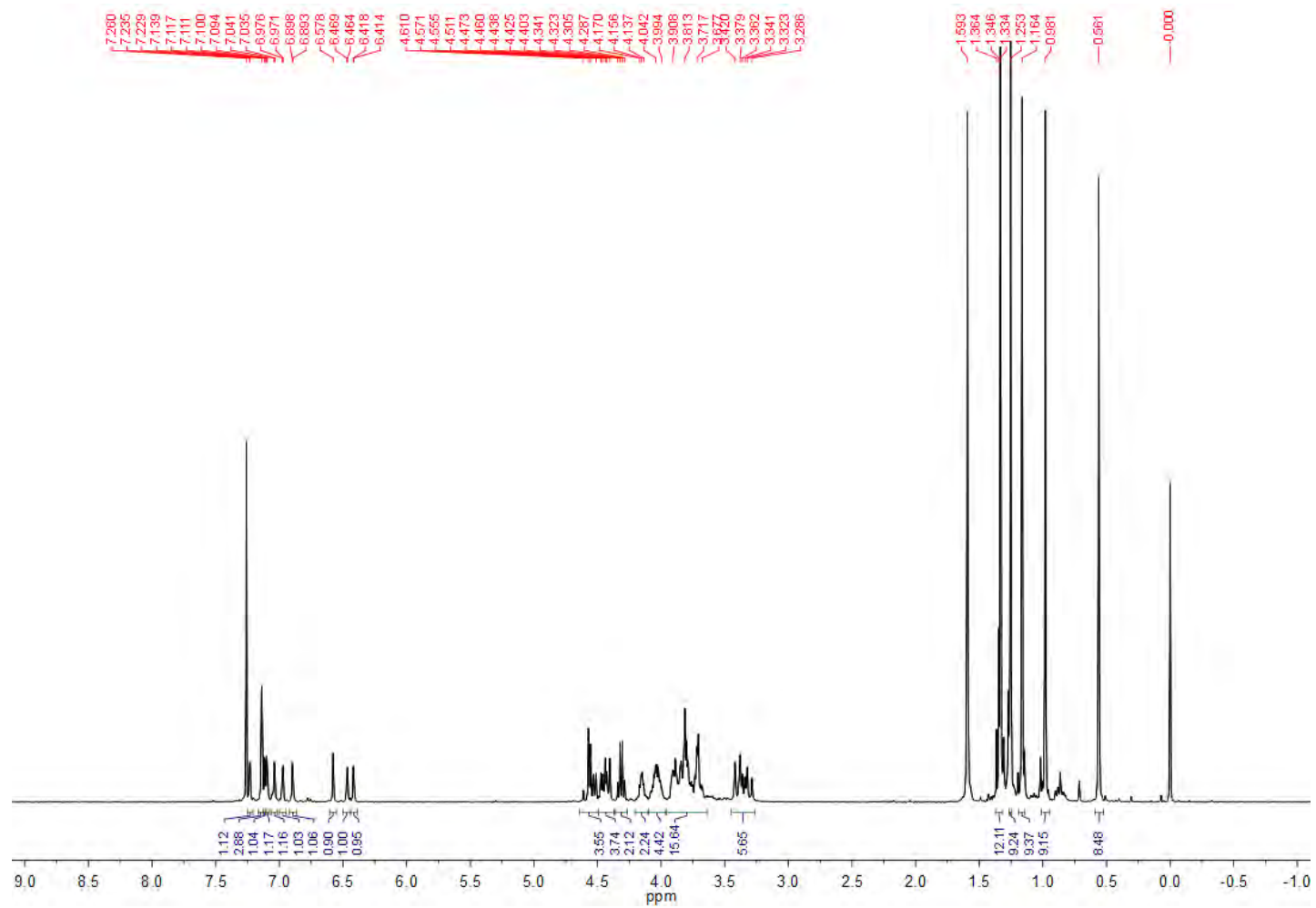
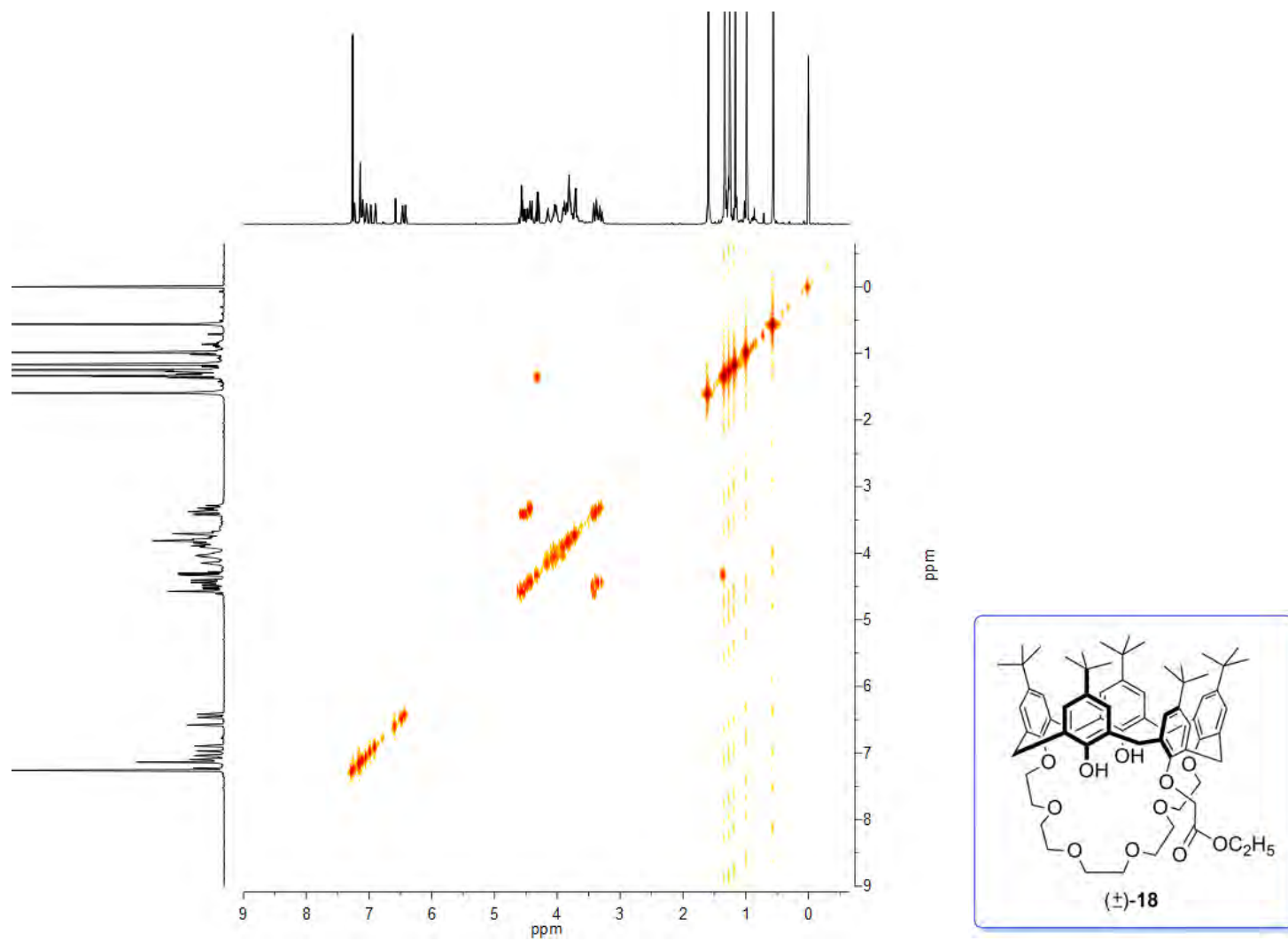
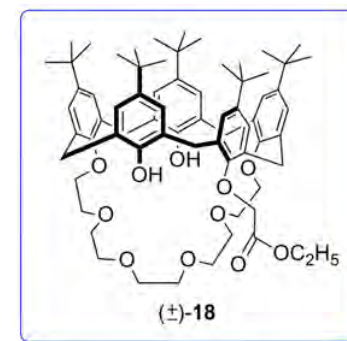
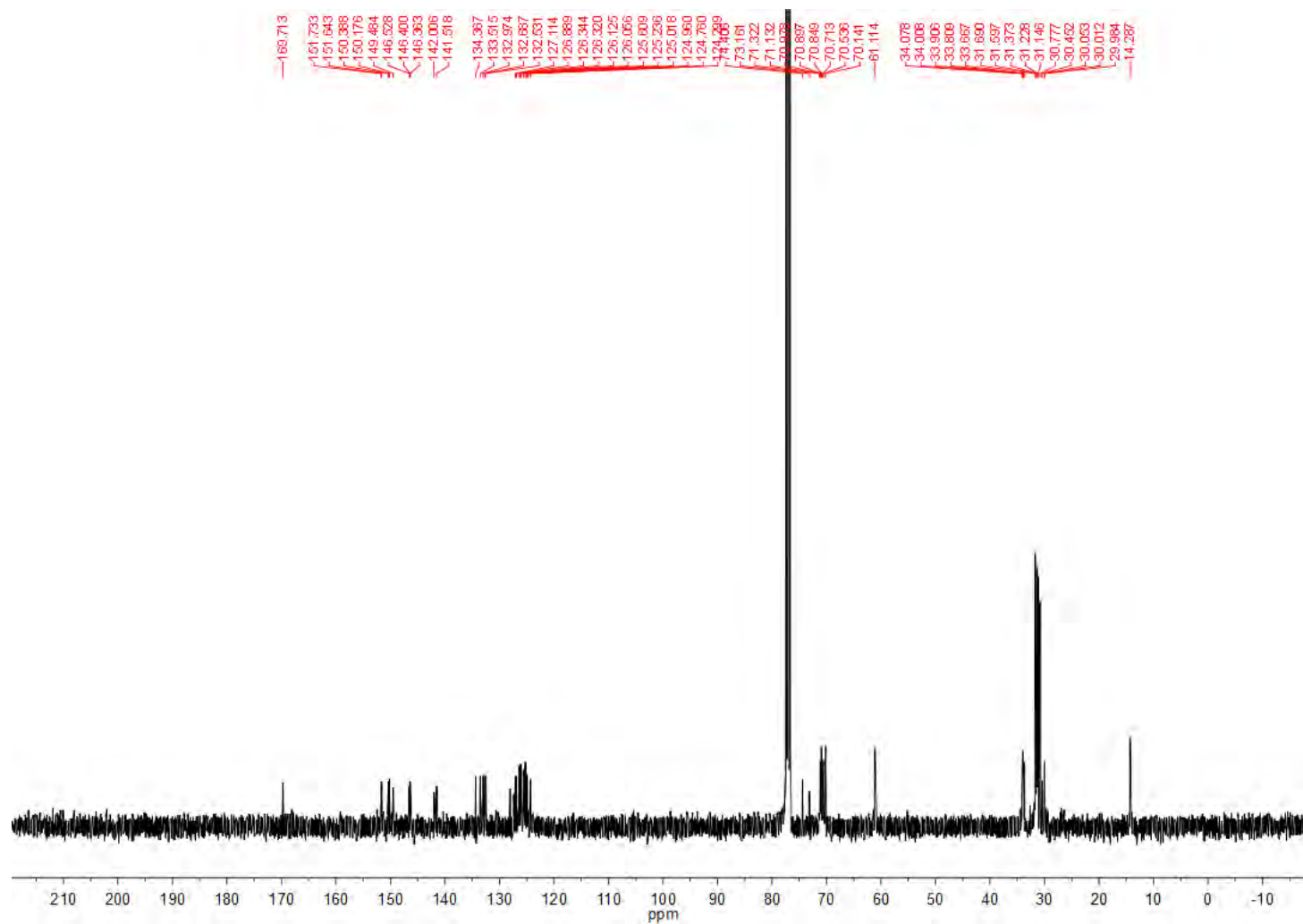


Fig. S-5  $^1\text{H}$  NMR spectrum of (±)-18 ( $\text{CDCl}_3$ , 400 MHz, 25 °C).



**Fig. S-6**  $^1\text{H}$  COSY spectrum of ( $\pm$ )-**18** ( $\text{CDCl}_3$ , 400 MHz, 25 °C)



**Fig. S-7**  $^{13}\text{C}$  NMR spectrum of (±)-**18** ( $\text{CDCl}_3$ , 100 MHz, 25 °C).

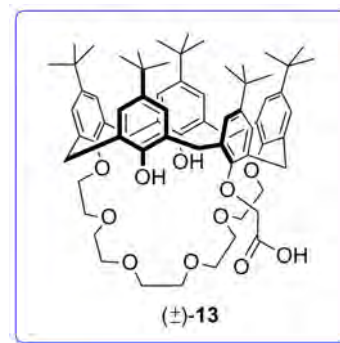
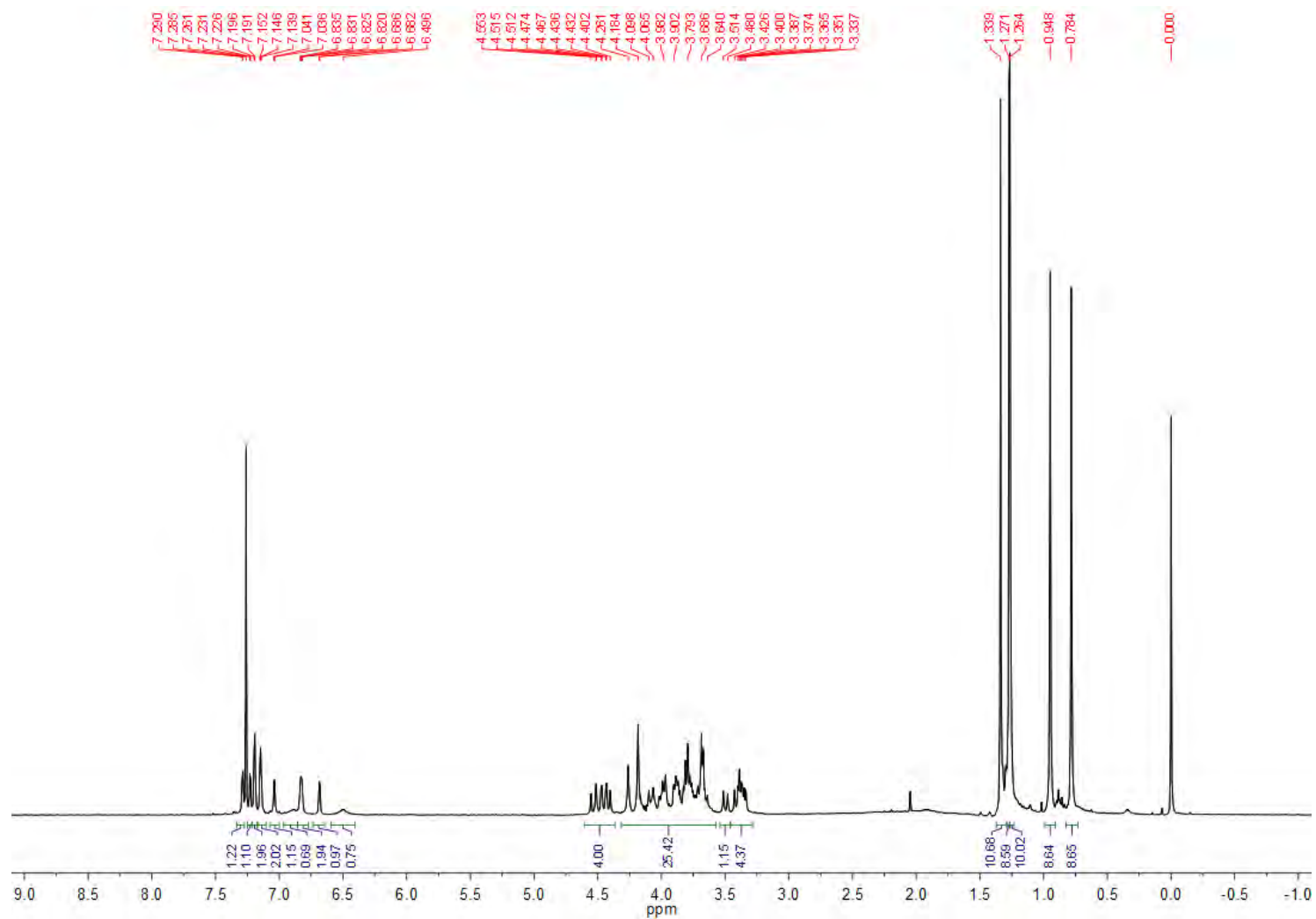


**Fig. S-8**  $^1\text{H}$  NMR spectrum of (±)-13 ( $\text{CDCl}_3$ , 400 MHz, 25 °C).

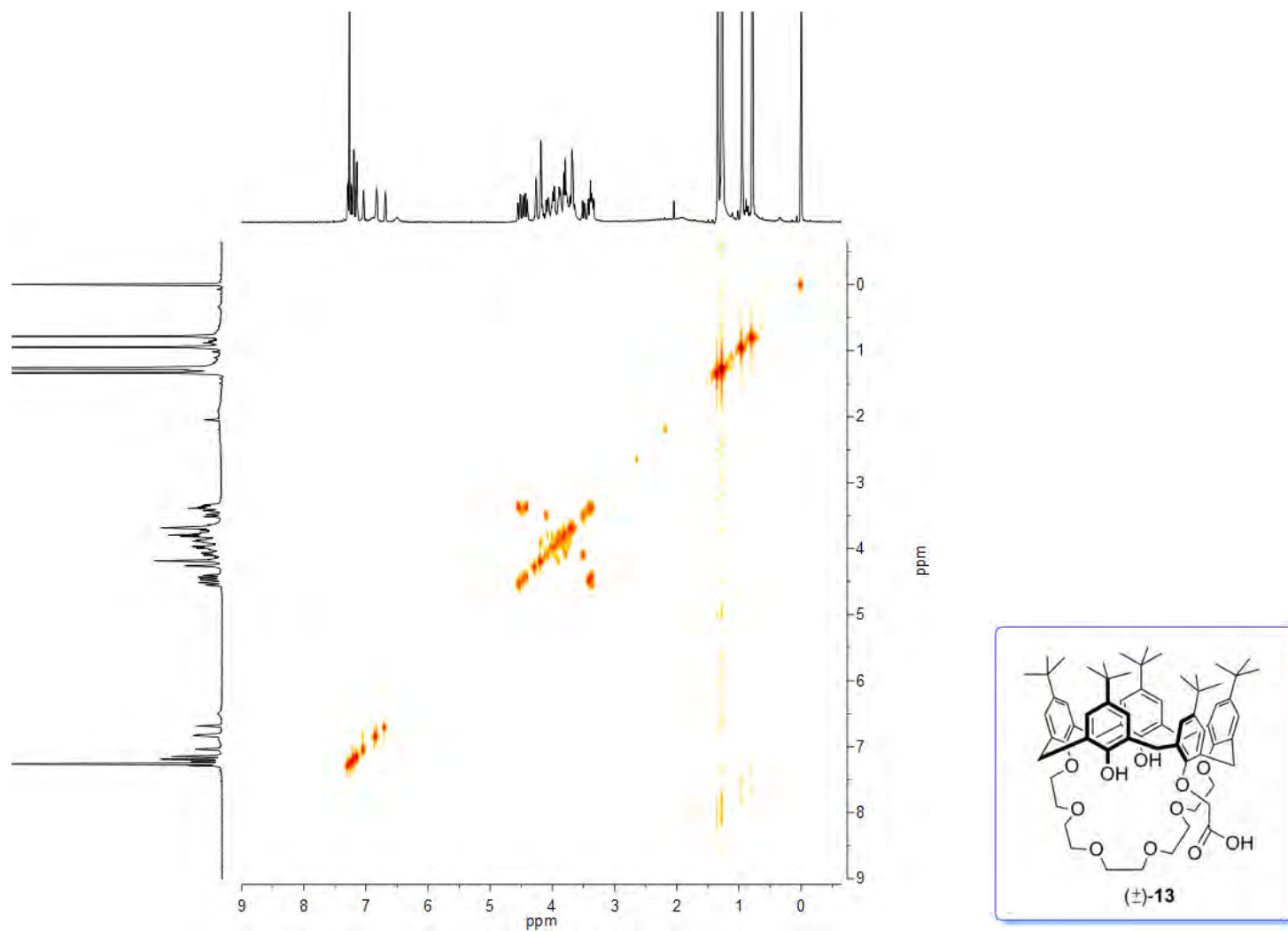


**Fig. S-9**  $^1\text{H}$ - $^1\text{H}$  COSY spectrum of ( $\pm$ )-13 ( $\text{CDCl}_3$ , 400 MHz, 25 °C).

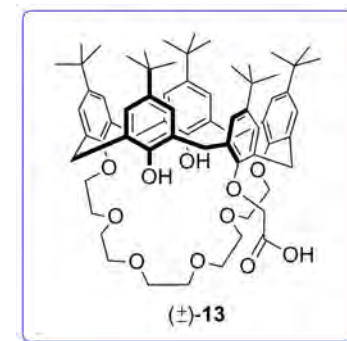
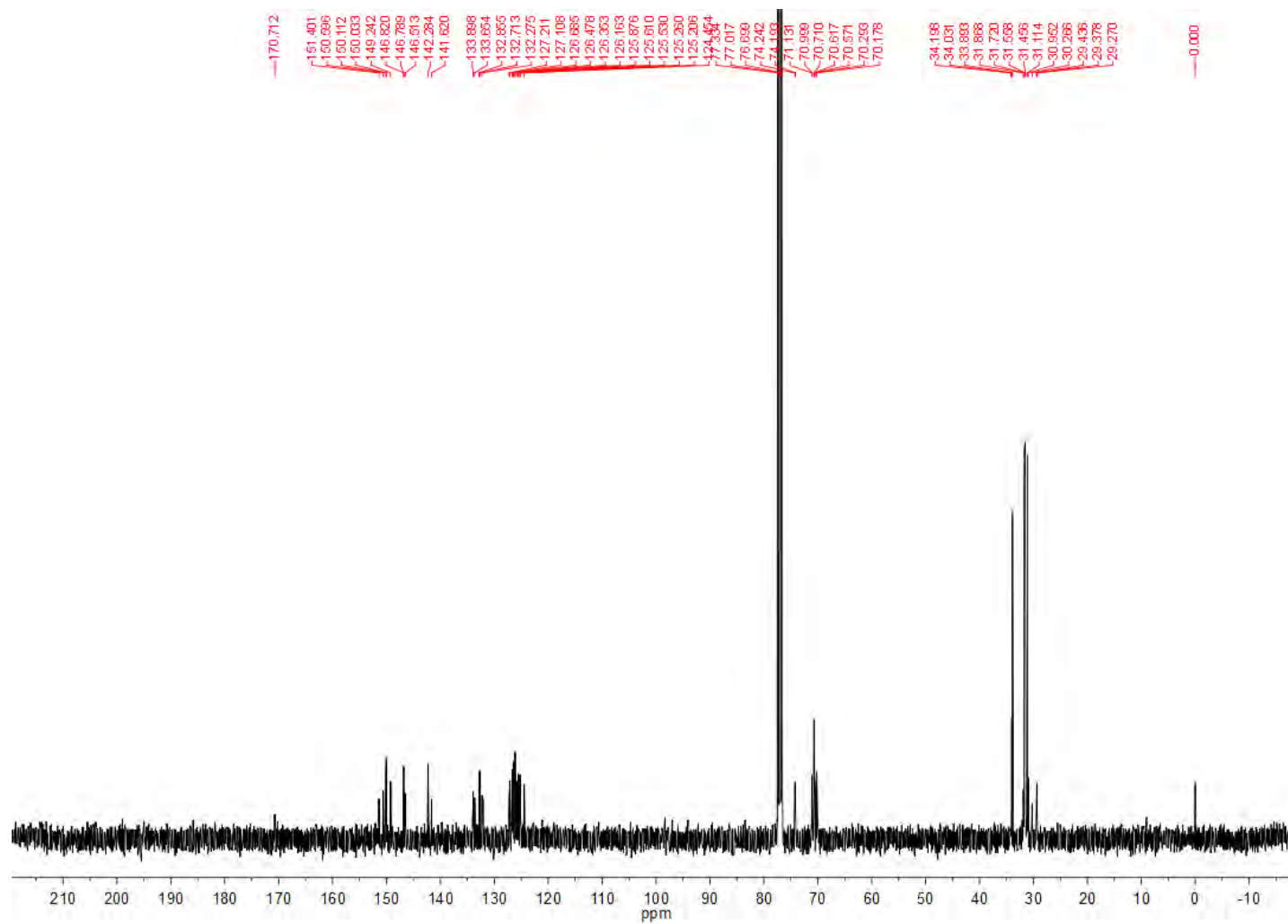
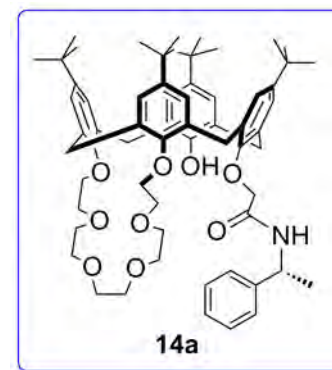
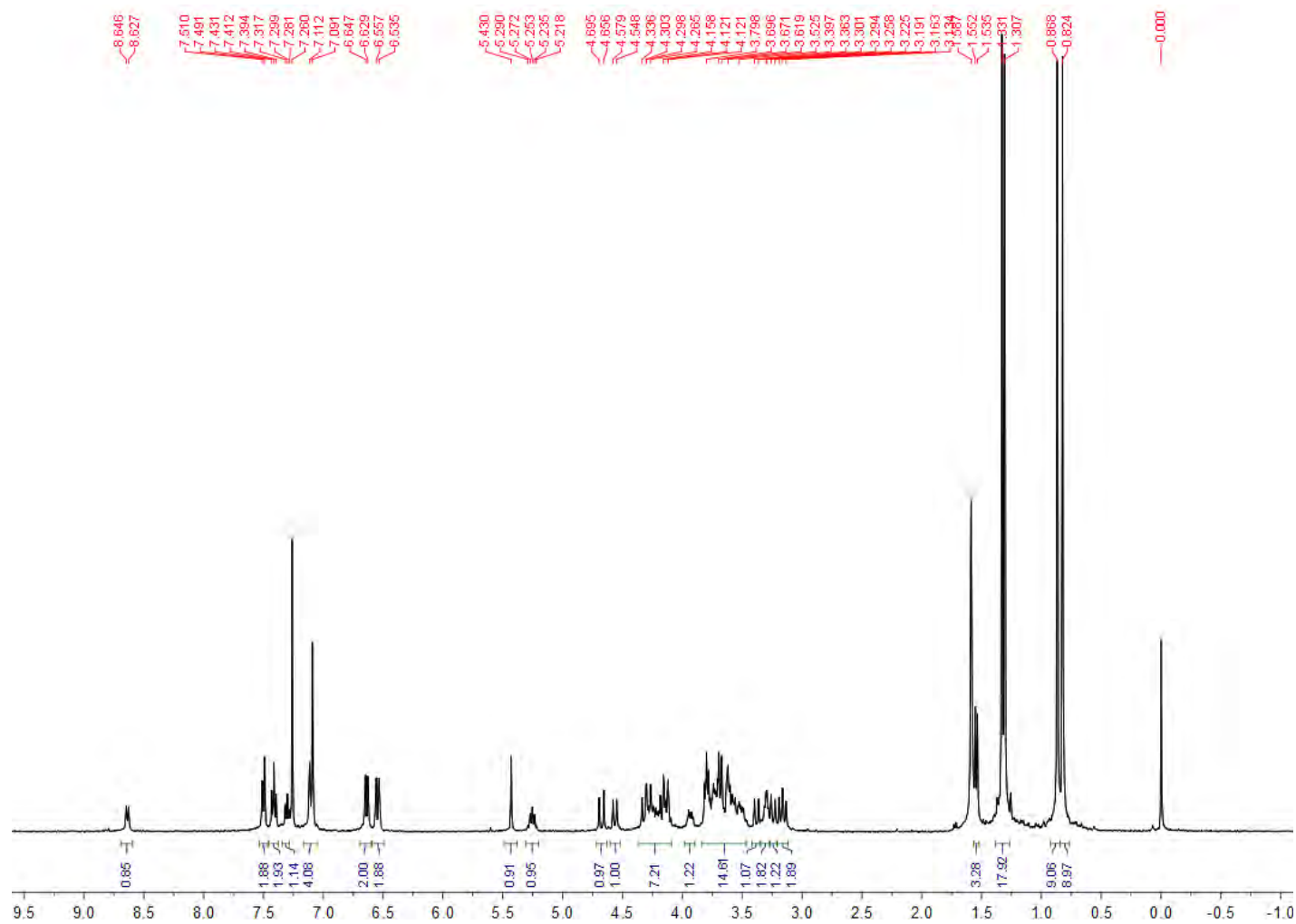
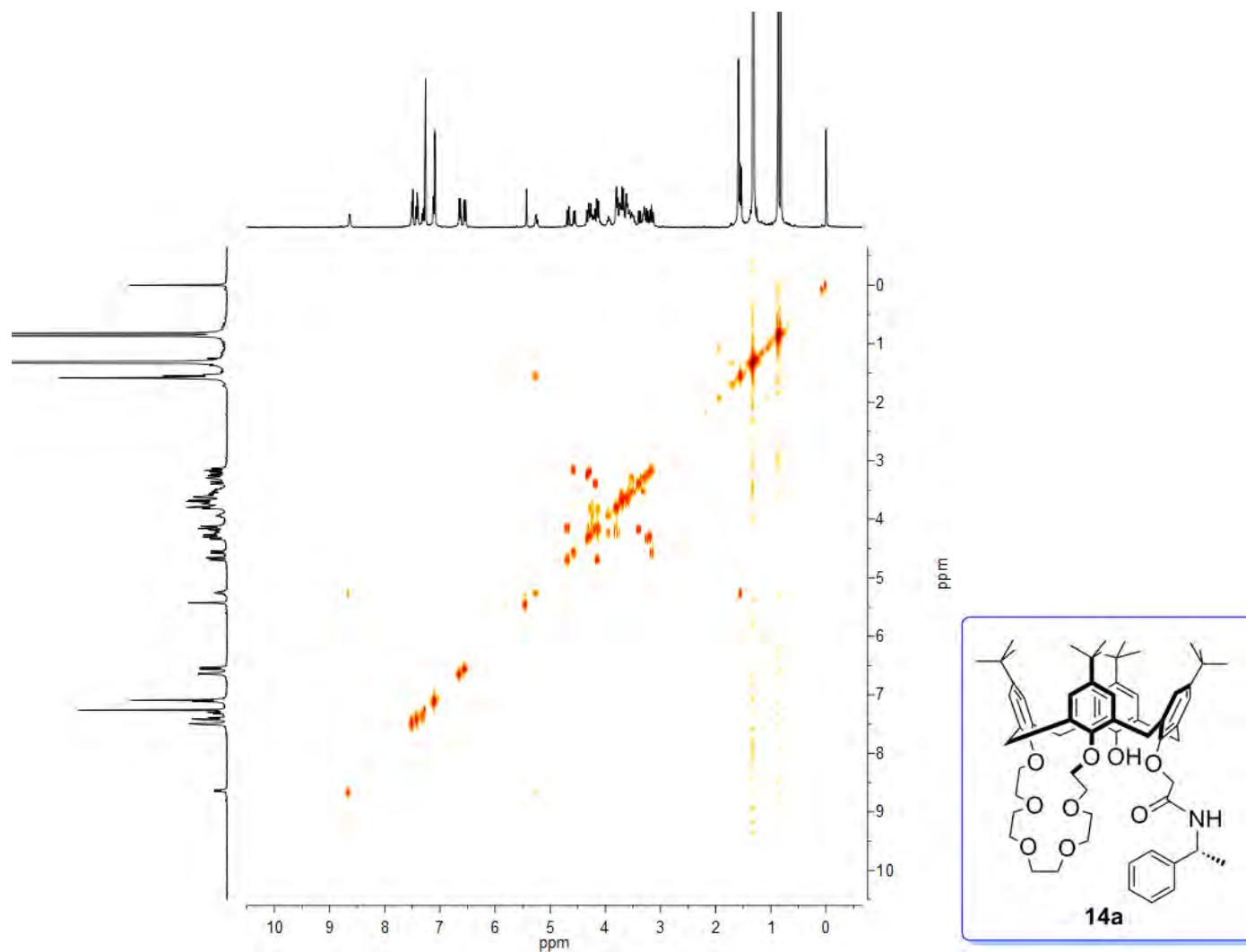


Fig. S-10  $^{13}\text{C}$  NMR spectrum of (±)-13 ( $\text{CDCl}_3$ , 100 MHz, 25 °C).





**Fig. S-11**  $^1\text{H}$  NMR spectrum of **14a** ( $\text{CDCl}_3$ , 400 MHz, 25 °C).



**Fig. S-12**  $^1\text{H}^1\text{H}$  COSY spectrum of **14a** ( $\text{CDCl}_3$ , 400 MHz, 25 °C).

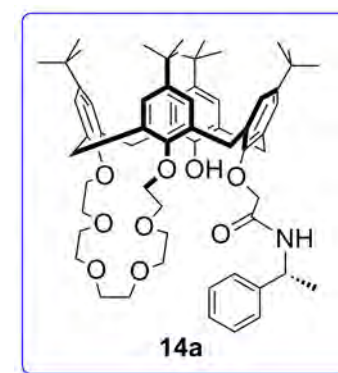
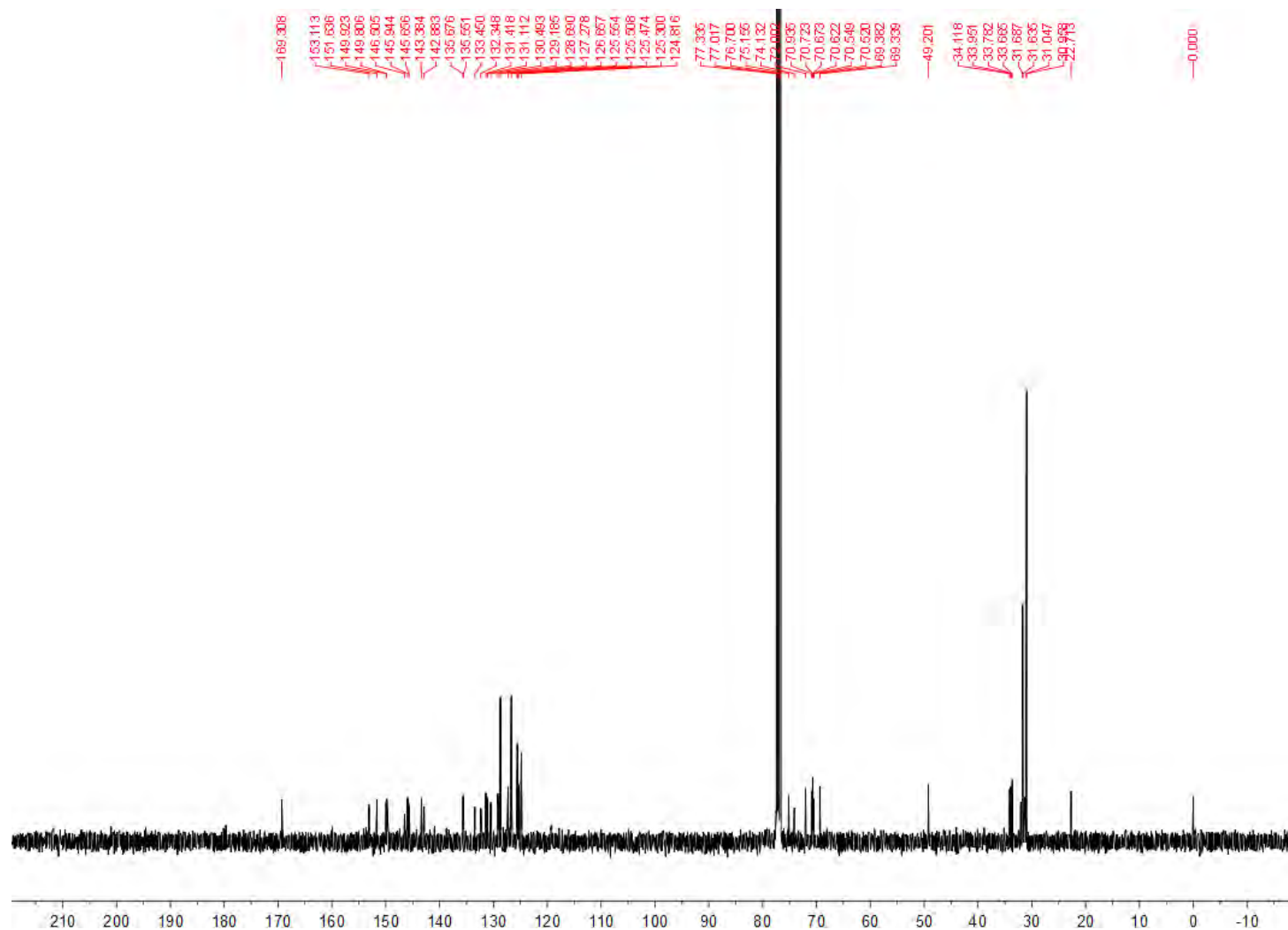


**Fig. S-13**  $^{13}\text{C}$  NMR spectrum of **14a** ( $\text{CDCl}_3$ , 100 MHz, 25 °C).

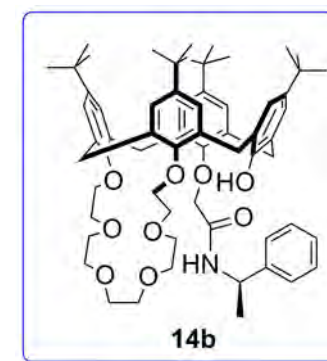
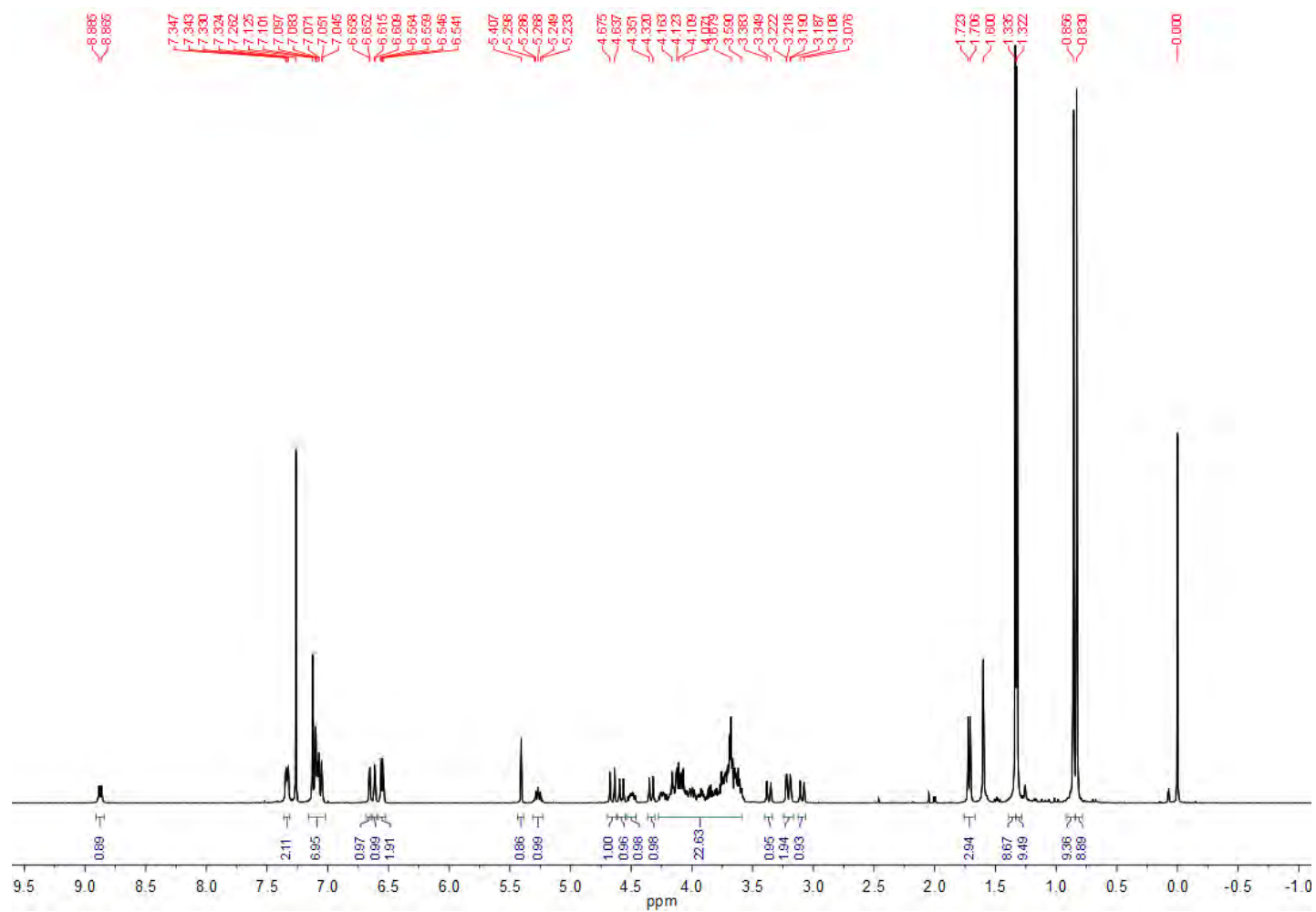


**Fig. S-14**  $^1\text{H}$  NMR spectrum of **14b** ( $\text{CDCl}_3$ , 400 MHz, 25 °C).

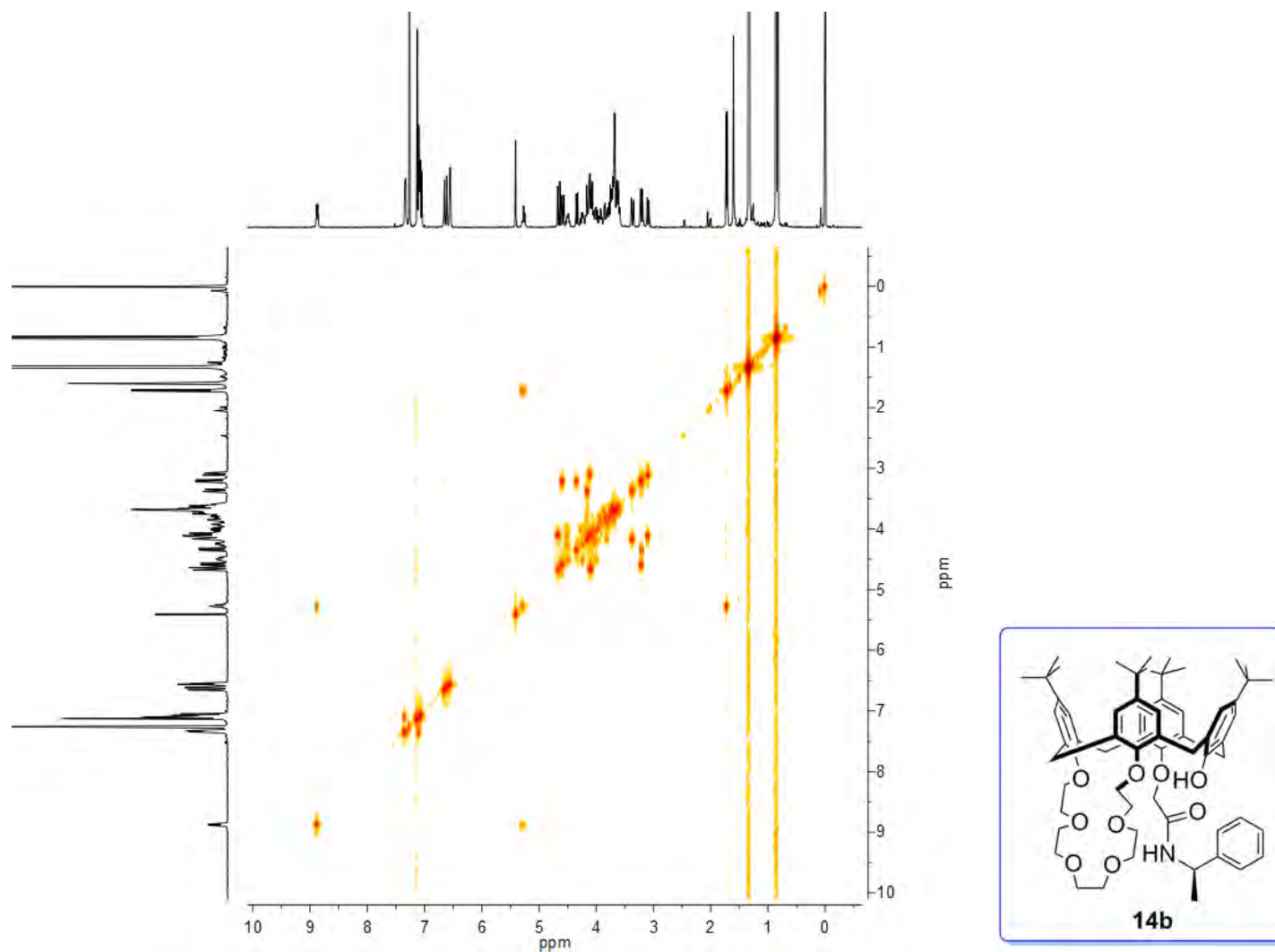


**Fig. S-15**  $^1\text{H}$  COSY spectrum of **14b** ( $\text{CDCl}_3$ , 400 MHz, 25 °C).

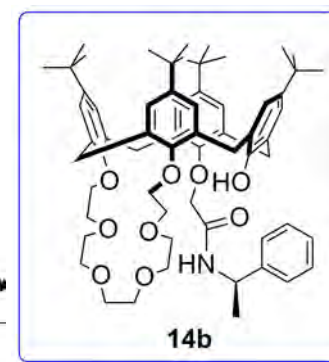
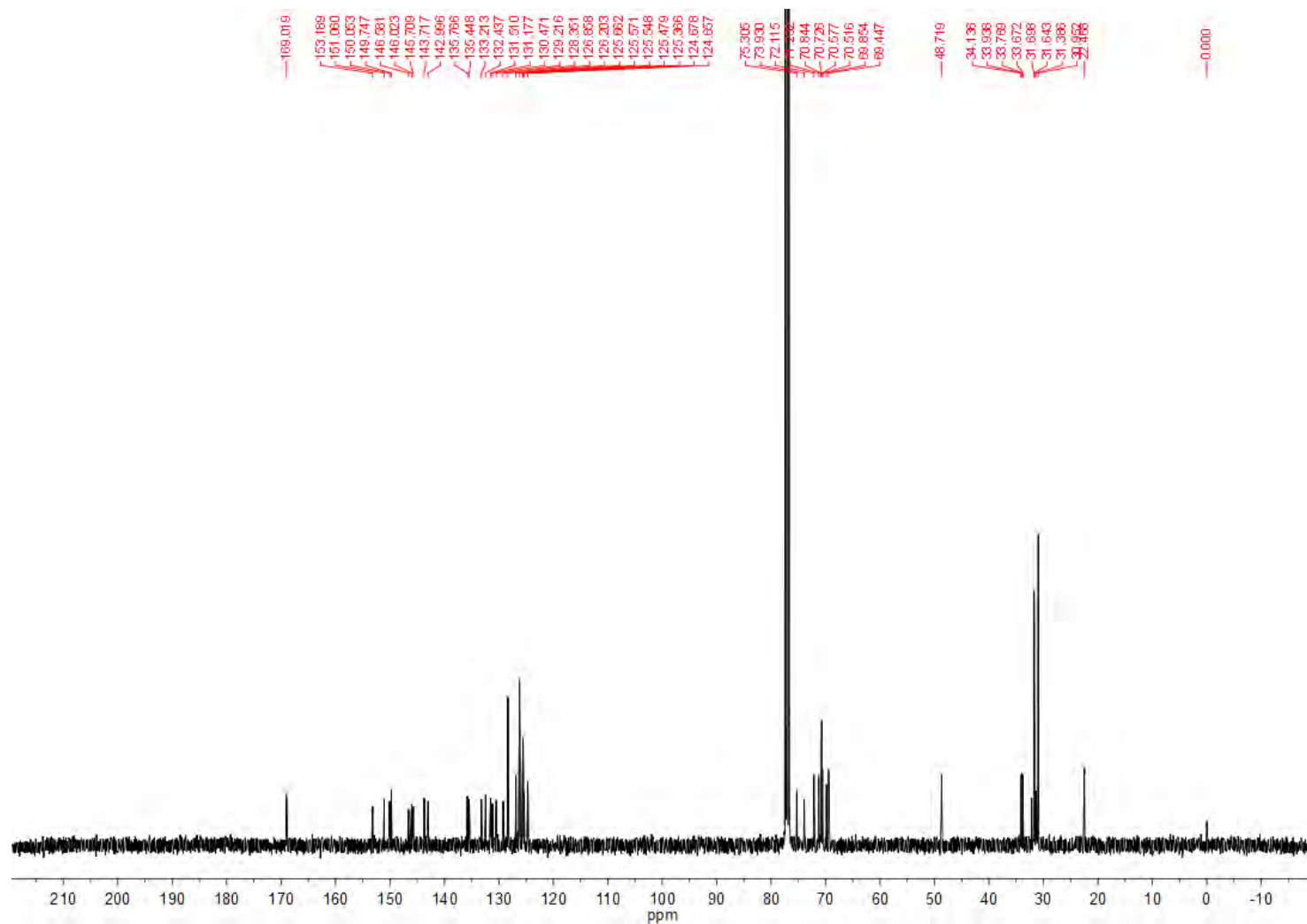


**Fig. S-16**  $^{13}\text{C}$  NMR spectrum of **14b** ( $\text{CDCl}_3$ , 100 MHz, 25 °C).

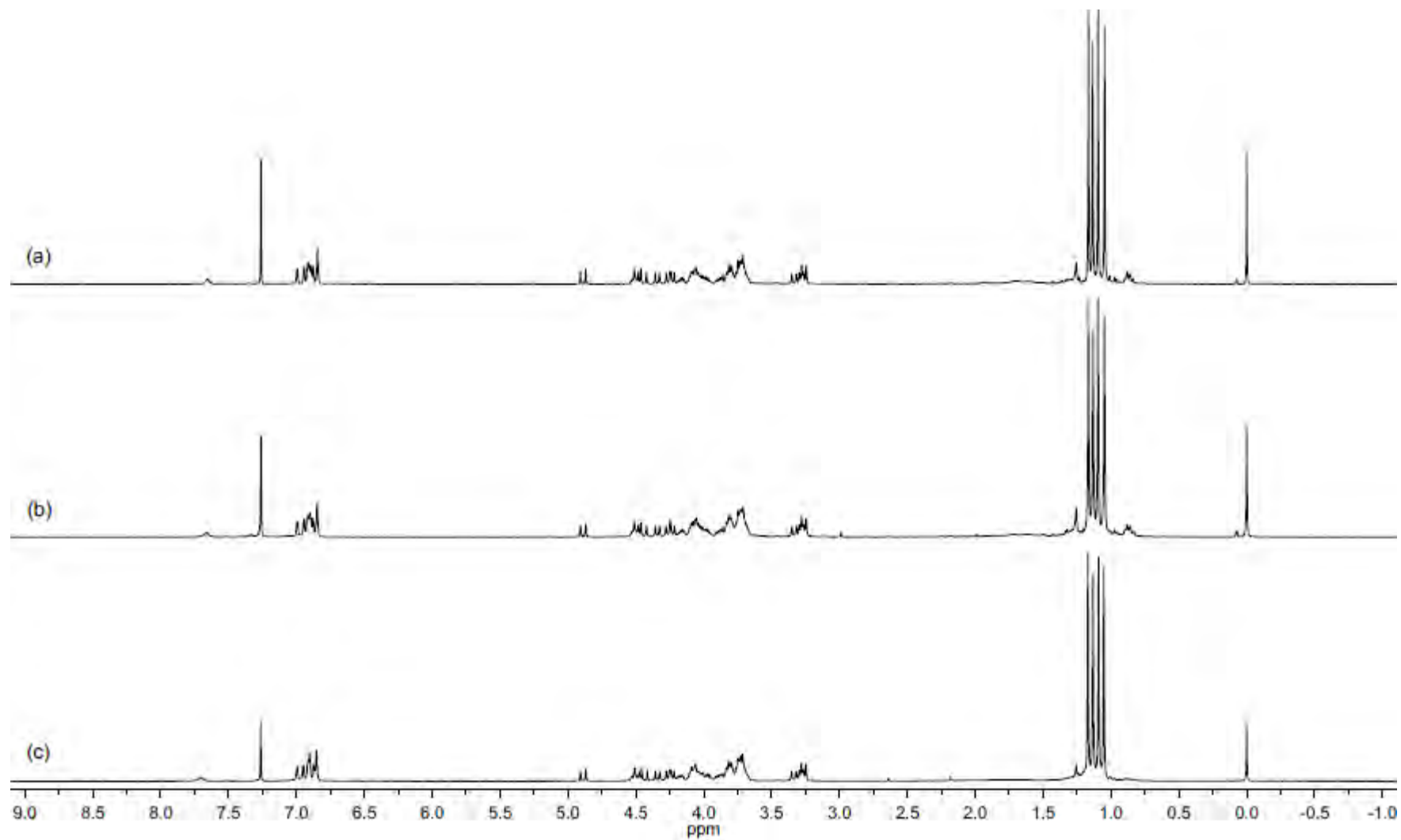


**Fig. S-17** A comparison of the  $^1\text{H}$  NMR spectrum of racemic and enantiopure **10** ( $\text{CDCl}_3$ , 400 MHz, 25  $^\circ\text{C}$ ): (a) racemic; (b) (-)-**10**; (c) (+)-**10**.

## Part C. Preliminary sift of the host

### C-1. $^1\text{H}$ NMR titration of ( $\pm$ )-**8** with G1–G7:

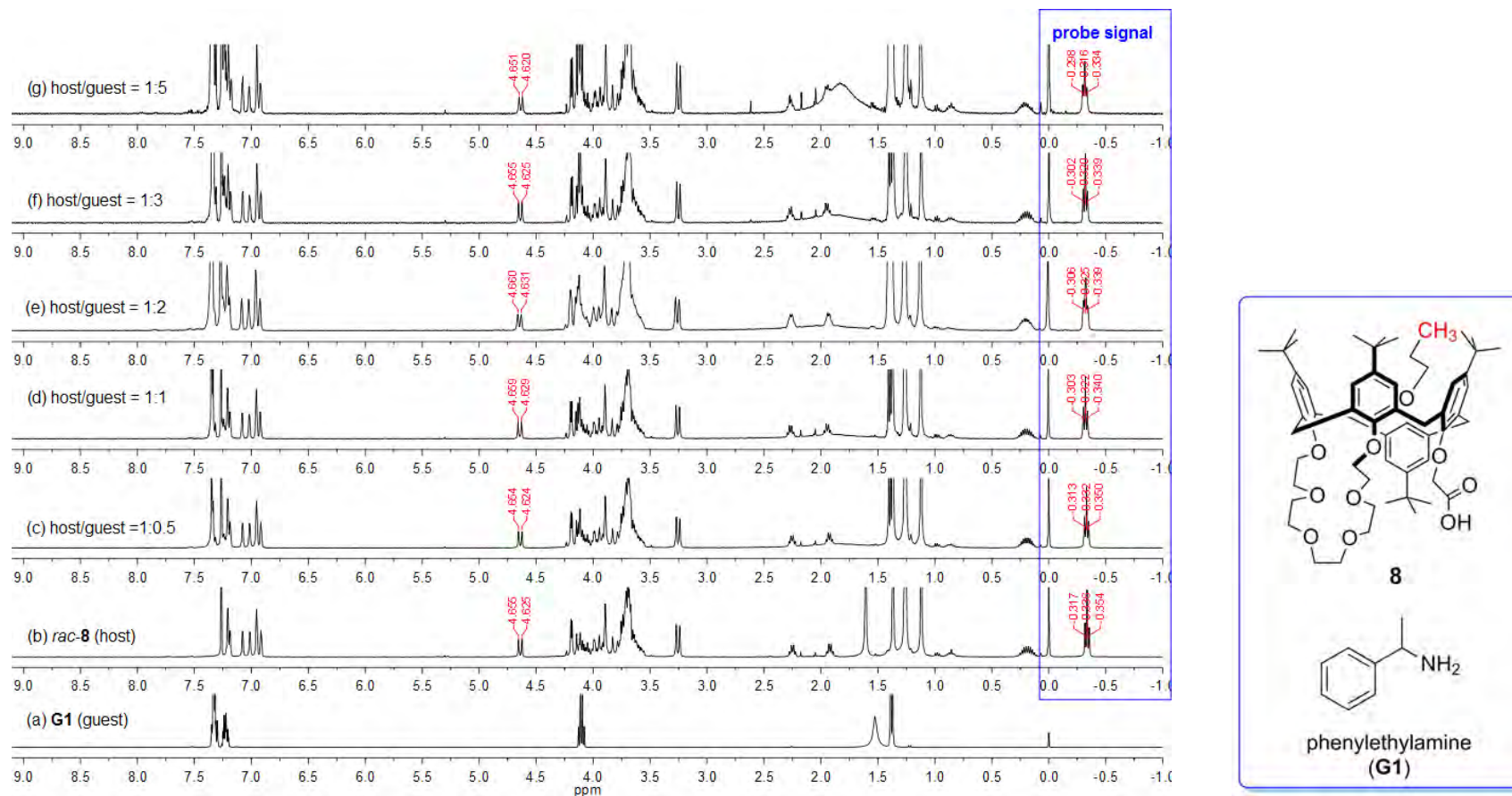


**Fig. S-18**  $^1\text{H}$  NMR spectra (CDCl<sub>3</sub>, 400 MHz, 25 °C) of ( $\pm$ )-**8** (host, 10 mM) in the presence of increasing equivalents of (*R*)-**G1** (guest): (a) (*R*)-**G1**; (b) ( $\pm$ )-**8**; (c) host/guest = 1:0.5; (d) host/guest = 1:1; (e) host/guest = 1:2; (f) host/guest = 1:3; (g) host/guest = 1:5.



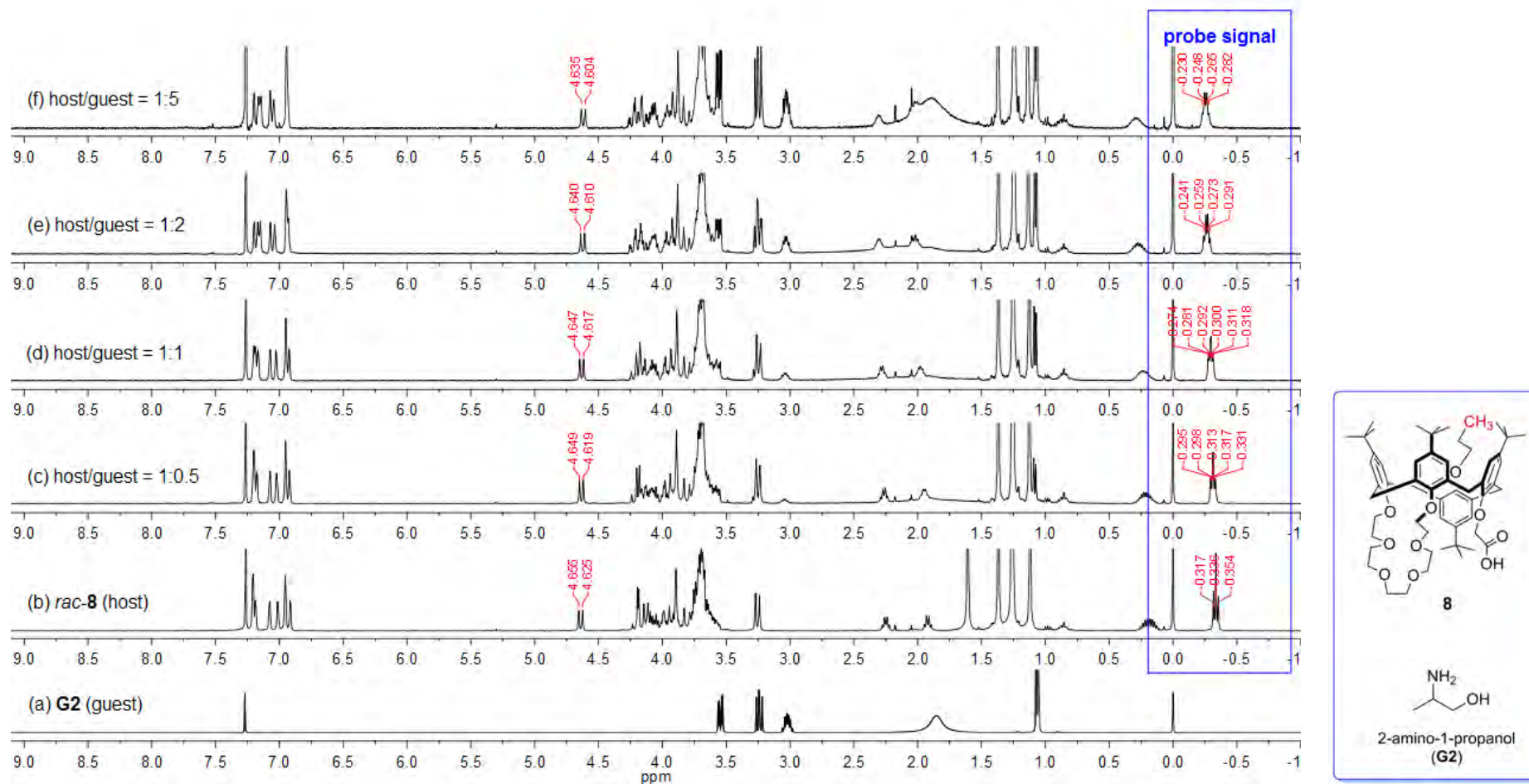


**Fig. S-19** <sup>1</sup>H NMR spectra (CDCl<sub>3</sub>, 400 MHz, 25 °C) of (±)-**8** (host, 10 mM) in the presence of increasing equivalents of (*S*)-**G2** (guest): (a) (*S*)-**G2**; (b) (±)-**8**; (c) host/guest = 1:0.5; (d) host/guest = 1:1; (e) host/guest = 1:2; (f) host/guest = 1:3; (g) host/guest = 1:5.

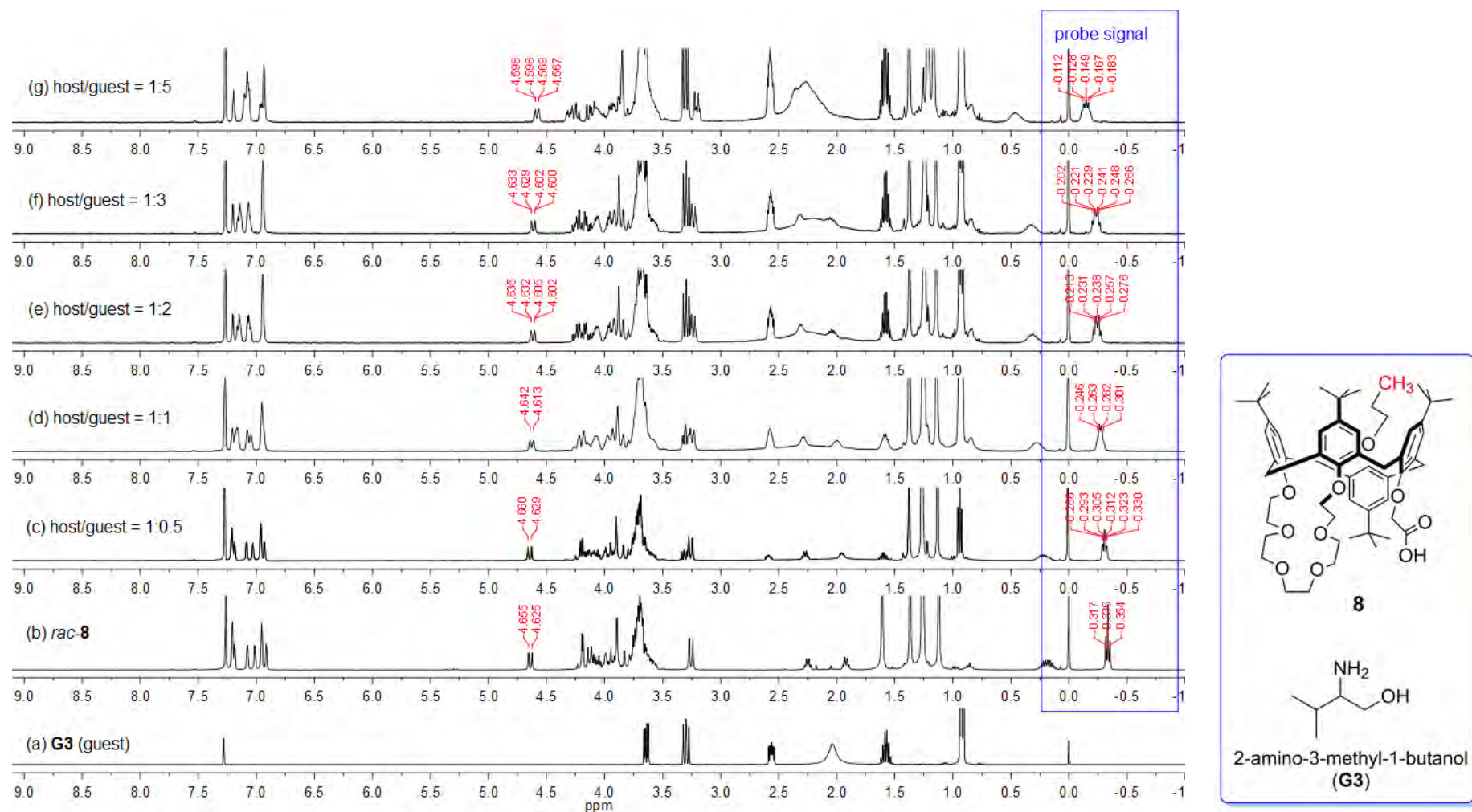


**Fig. S-20** <sup>1</sup>H NMR spectra (CDCl<sub>3</sub>, 400 MHz, 25 °C) of (±)-**8** (host, 10 mM) in the presence of increasing equivalents of (S)-**G3** (guest): (a) (S)-**G3**; (b) (±)-**8**; (c) host/guest = 1:0.5; (d) host/guest = 1:1; (e) host/guest = 1:2; (f) host/guest = 1:3; (g) host/guest = 1:5.

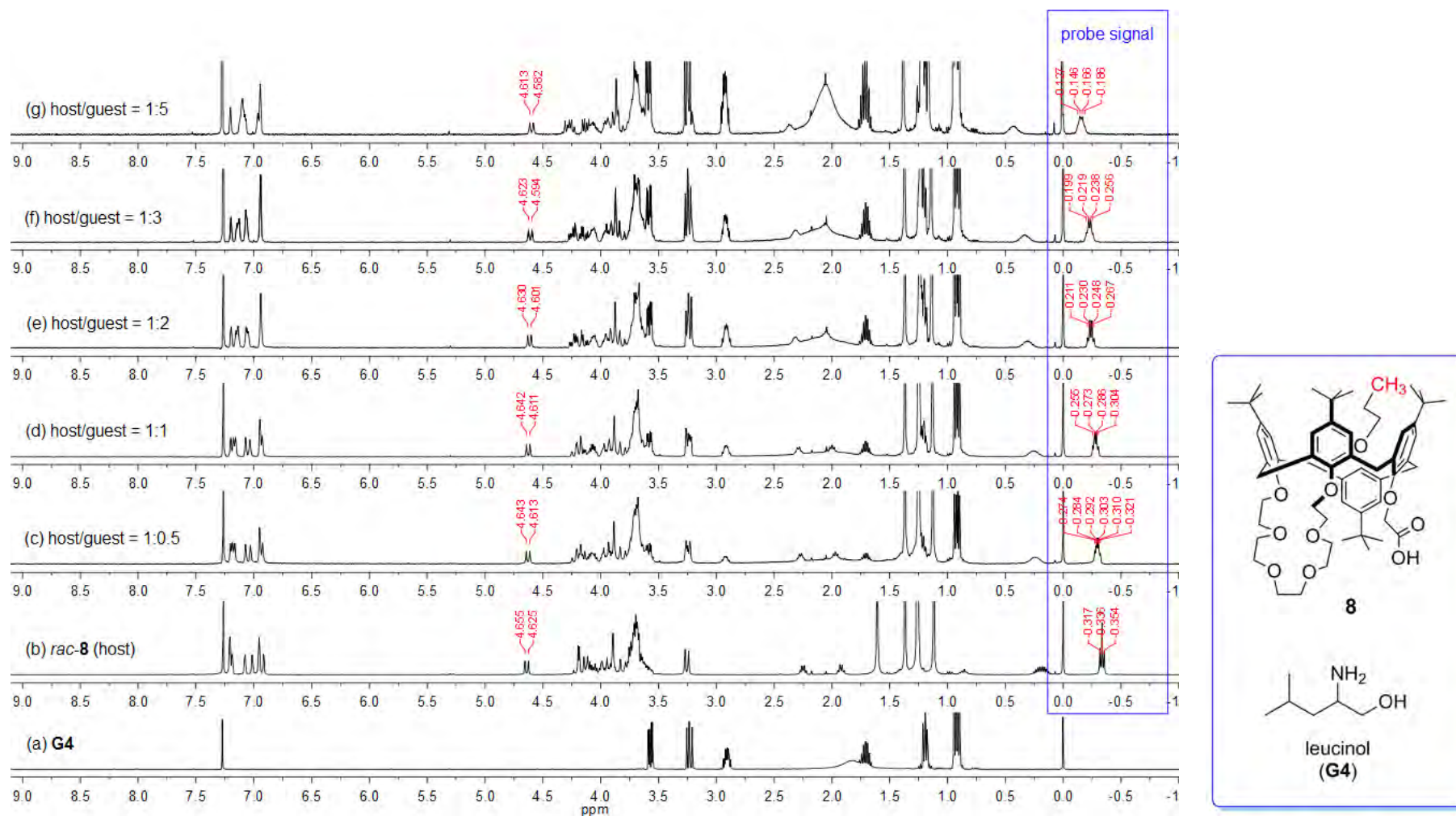


**Fig. S-21** <sup>1</sup>H NMR spectra (CDCl<sub>3</sub>, 400 MHz, 25 °C) of (±)-**8** (host, 10 mM) in the presence of increasing equivalents of (S)-**G4** (guest): (a) (S)-**G4**; (b) (±)-**8**; (c) host/guest = 1:0.5; (d) host/guest = 1:1; (e) host/guest = 1:2; (f) host/guest = 1:3; (g) host/guest = 1:5.

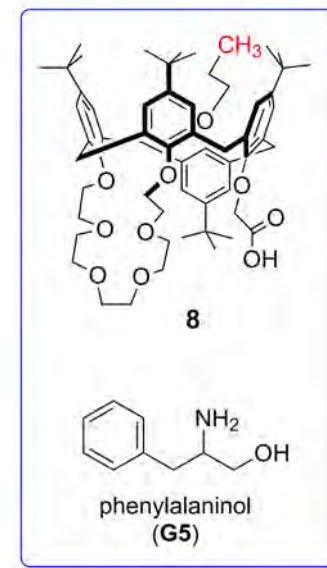
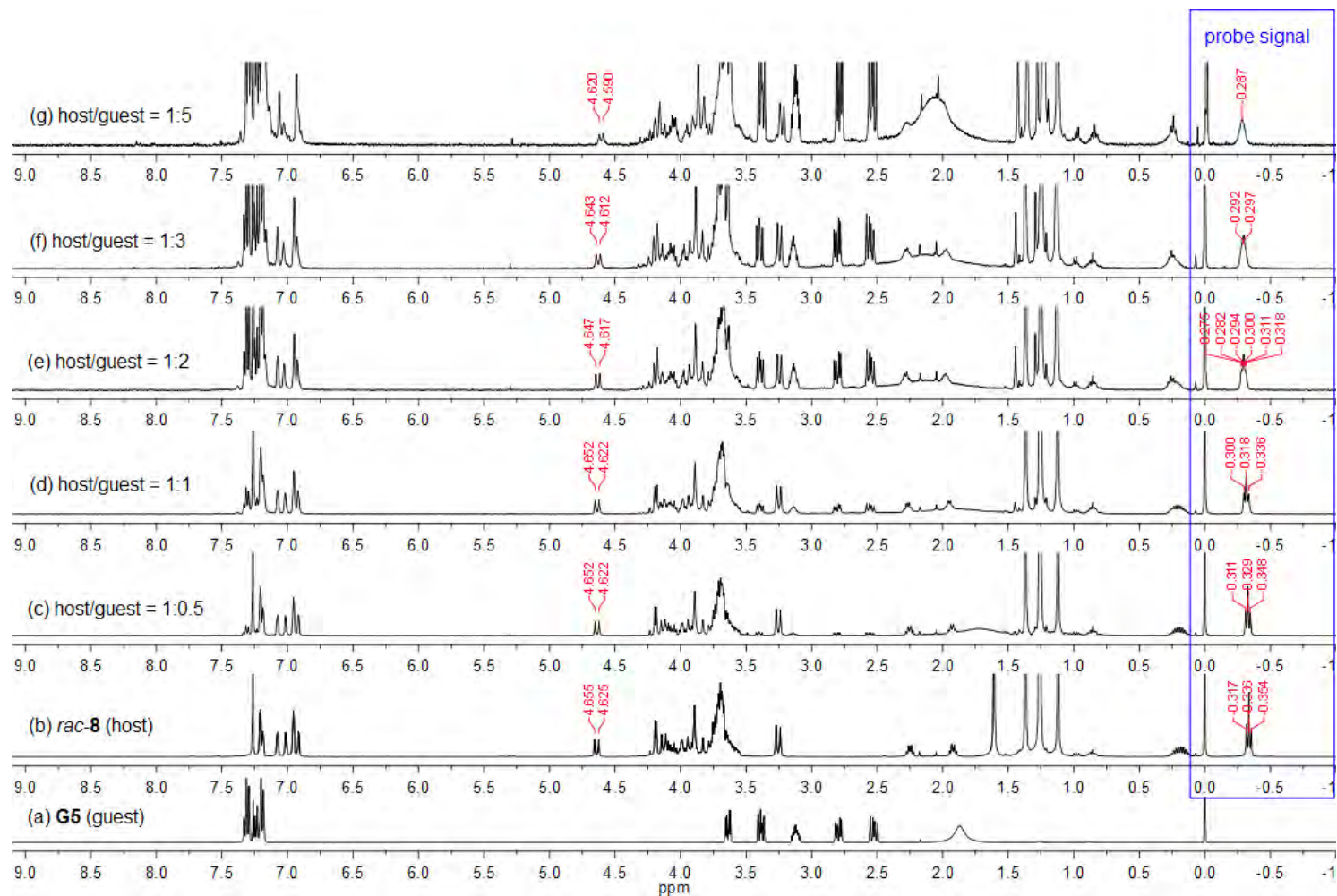


**Fig. S-22** <sup>1</sup>H NMR spectra (CDCl<sub>3</sub>, 400 MHz, 25 °C) of (±)-8 (host, 10 mM) in the presence of increasing equivalents of (*S*)-G5 (guest): (a) (*S*)-G5; (b) (±)-8; (c) host/guest = 1:0.5; (d) host/guest = 1:1; (e) host/guest = 1:2; (f) host/guest = 1:3; (g) host/guest = 1:5.

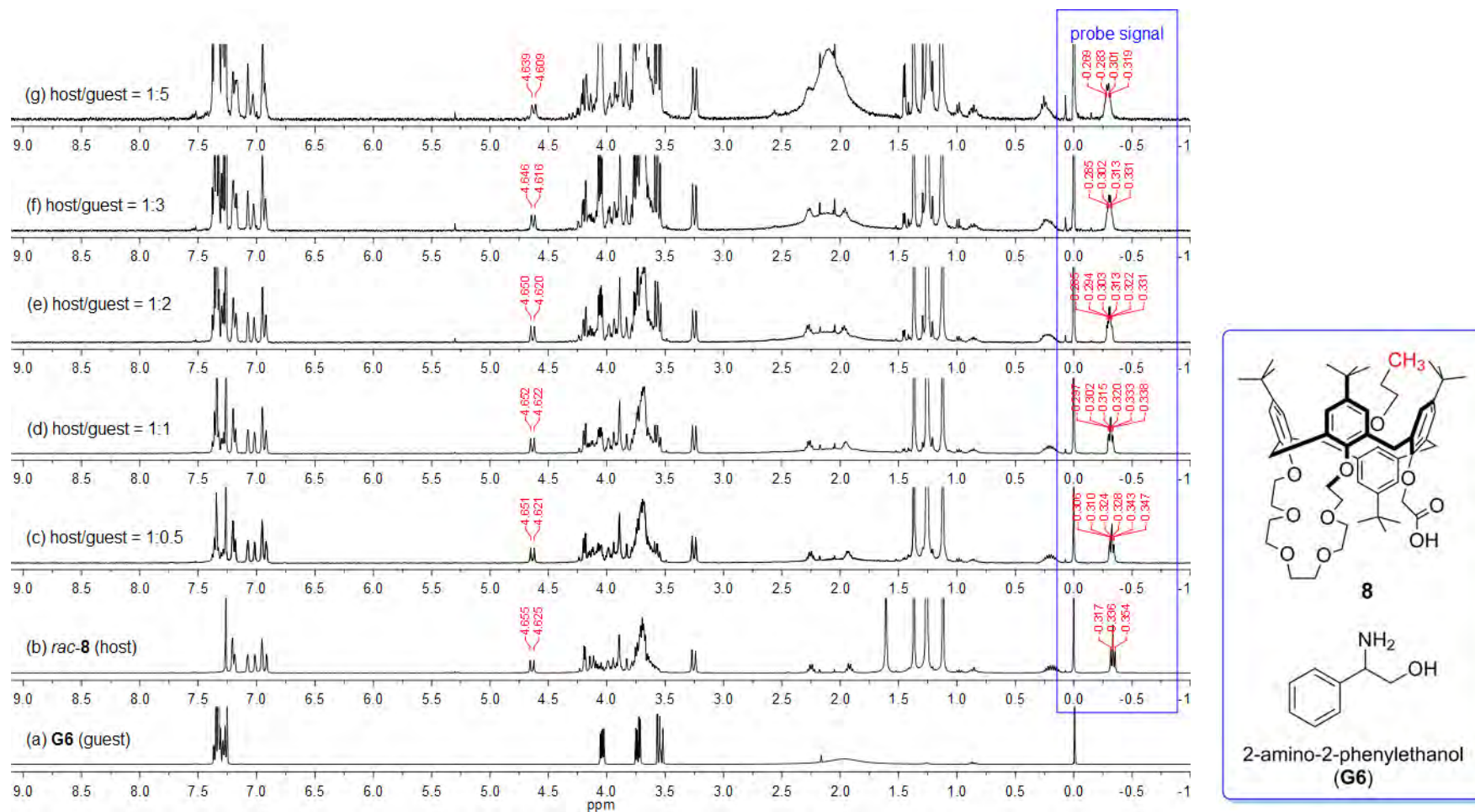


**Fig. S-23** <sup>1</sup>H NMR spectra (CDCl<sub>3</sub>, 400 MHz, 25 °C) of (±)-**8** (host, 10 mM) in the presence of increasing equivalents of (*S*)-**G6** (guest): (a) (*S*)-**G6**; (b) (±)-**8**; (c) host/guest = 1:0.5; (d) host/guest = 1:1; (e) host/guest = 1:2; (f) host/guest = 1:3; (g) host/guest = 1:5.

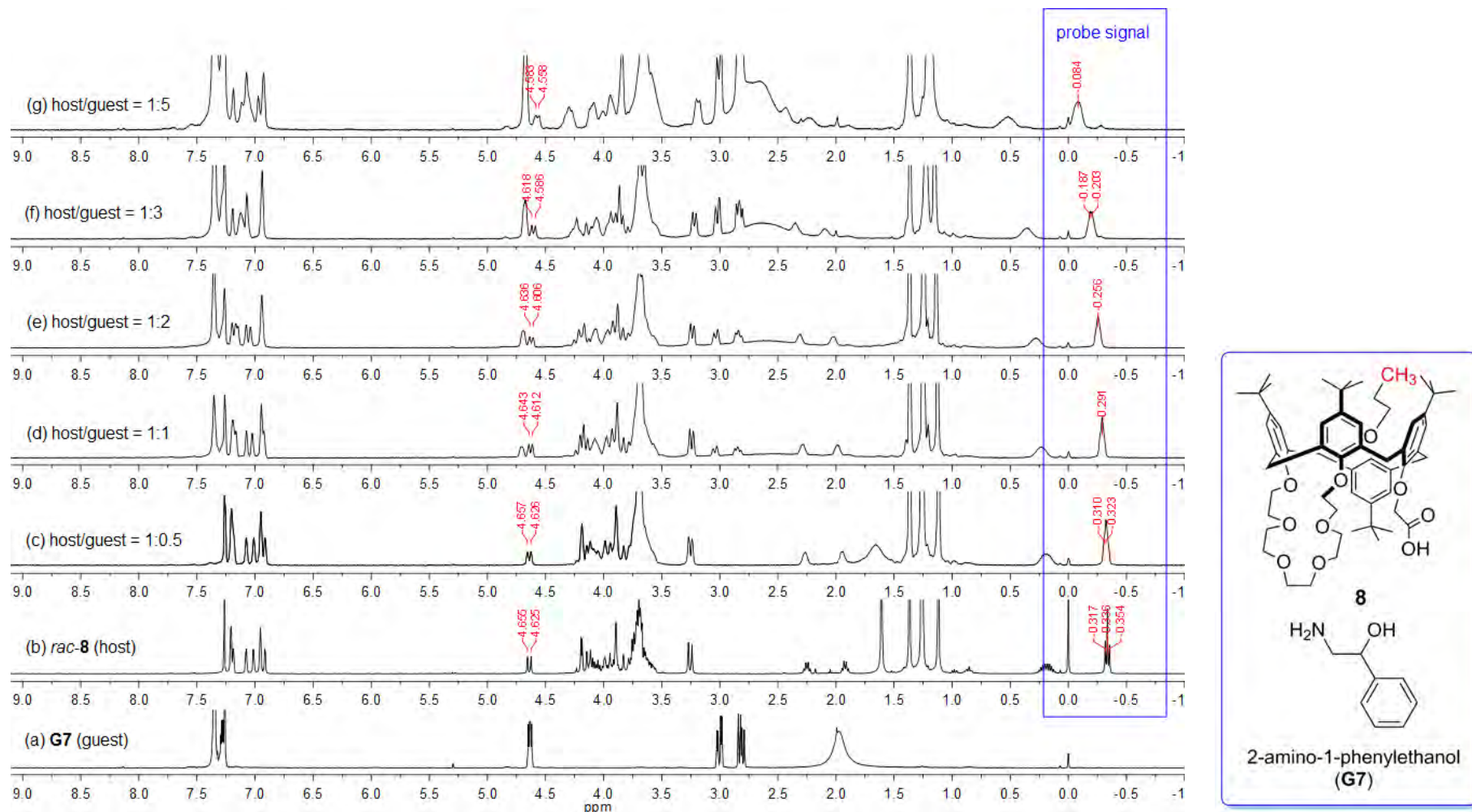


**Fig. S-24** <sup>1</sup>H NMR spectra (CDCl<sub>3</sub>, 400 MHz, 25 °C) of (±)-**8** (host, 10 mM) in the presence of increasing equivalents of (*R*)-**G7** (guest): (a) (*R*)-**G7**; (b) (±)-**8**; (c) host/guest = 1:0.5; (d) host/guest = 1:1; (e) host/guest = 1:2; (f) host/guest = 1:3; (g) host/guest = 1:5.

### C-2. $^1\text{H}$ NMR titration of ( $\pm$ )-**9** with **G1**–**G7**:

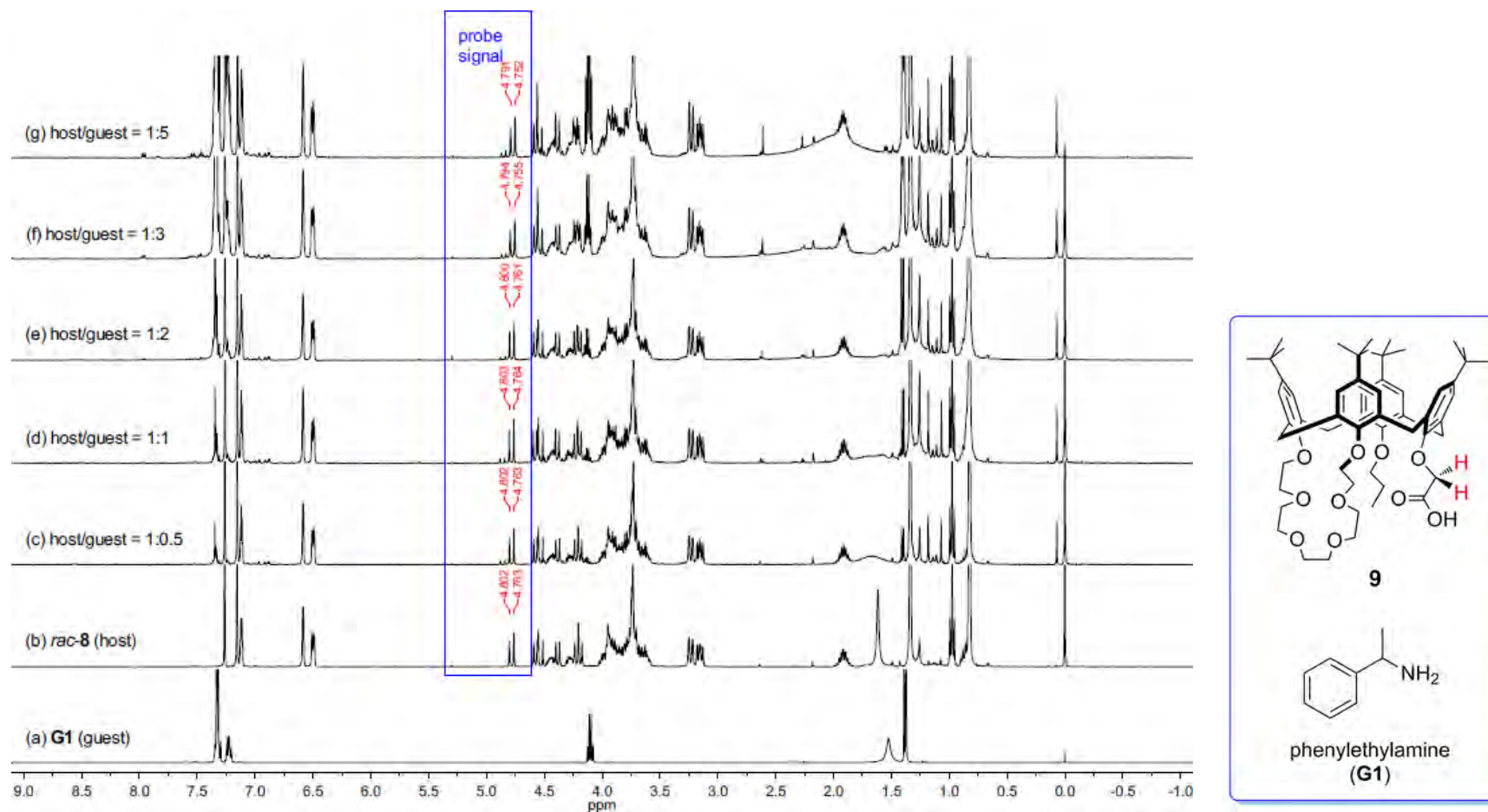


**Fig. S-25**  $^1\text{H}$  NMR spectra ( $\text{CDCl}_3$ , 400 MHz, 25 °C) of ( $\pm$ )-**9** (host, 10 mM) in the presence of increasing equivalents of (*R*)-**G1** (guest): (a) (*R*)-**G1**; (b) ( $\pm$ )-**9**; (c) host/guest = 1:0.5; (d) host/guest = 1:1; (e) host/guest = 1:2; (f) host/guest = 1:3; (g) host/guest = 1:5.

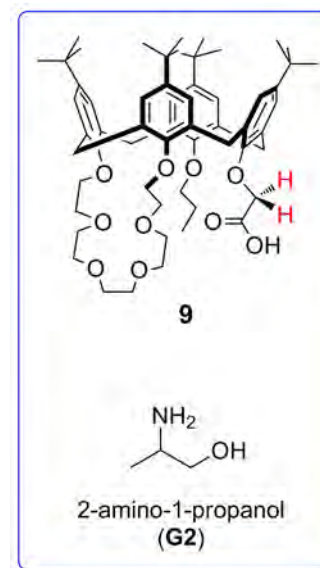
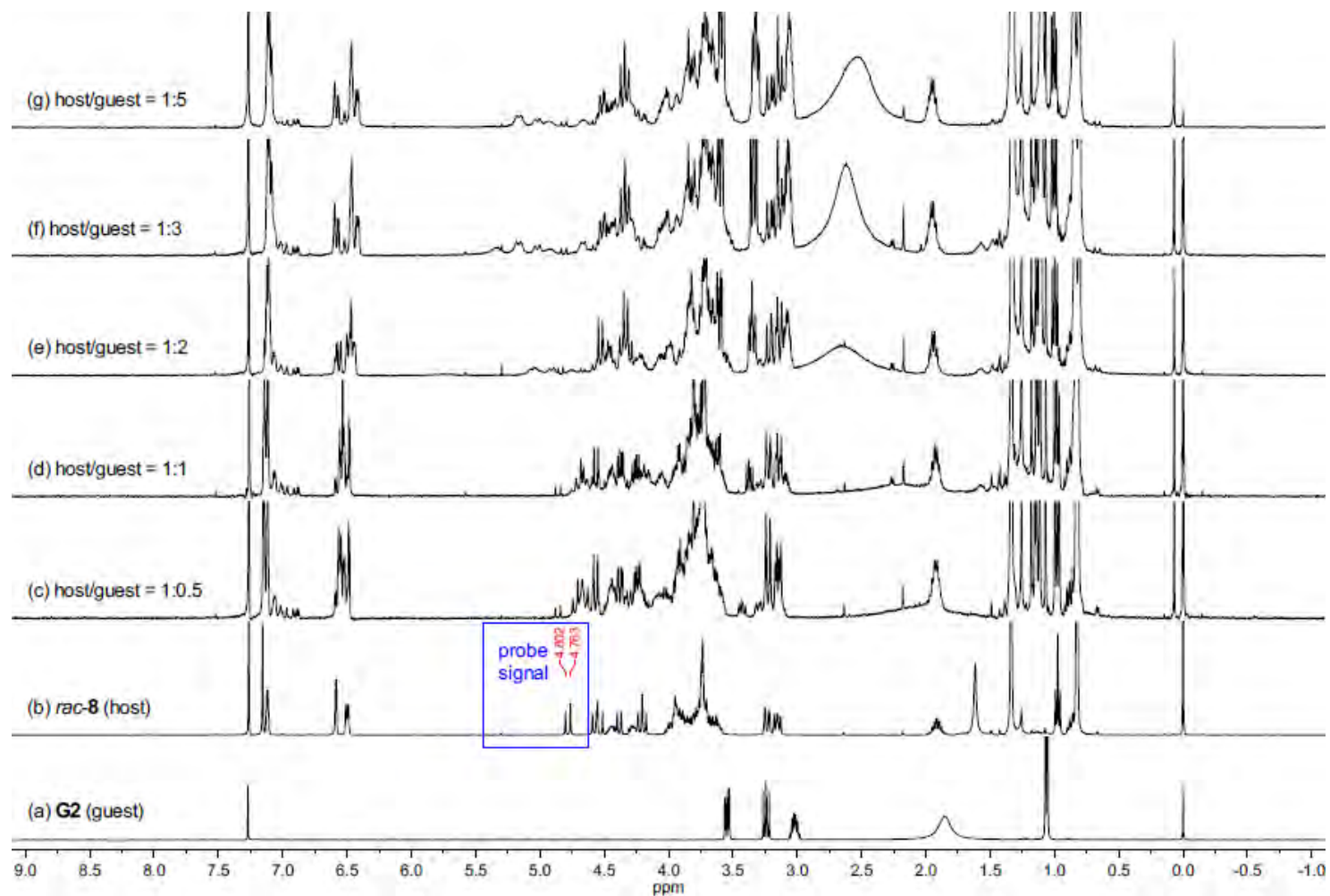


**Fig. S-26** <sup>1</sup>H NMR spectra (CDCl<sub>3</sub>, 400 MHz, 25 °C) of (±)-**9** (host, 10 mM) in the presence of increasing equivalents of (*S*)-**G2** (guest): (a) (*S*)-**G2**; (b) (±)-**9**; (c) host/guest = 1:0.5; (d) host/guest = 1:1; (e) host/guest = 1:2; (f) host/guest = 1:3; (g) host/guest = 1:5.



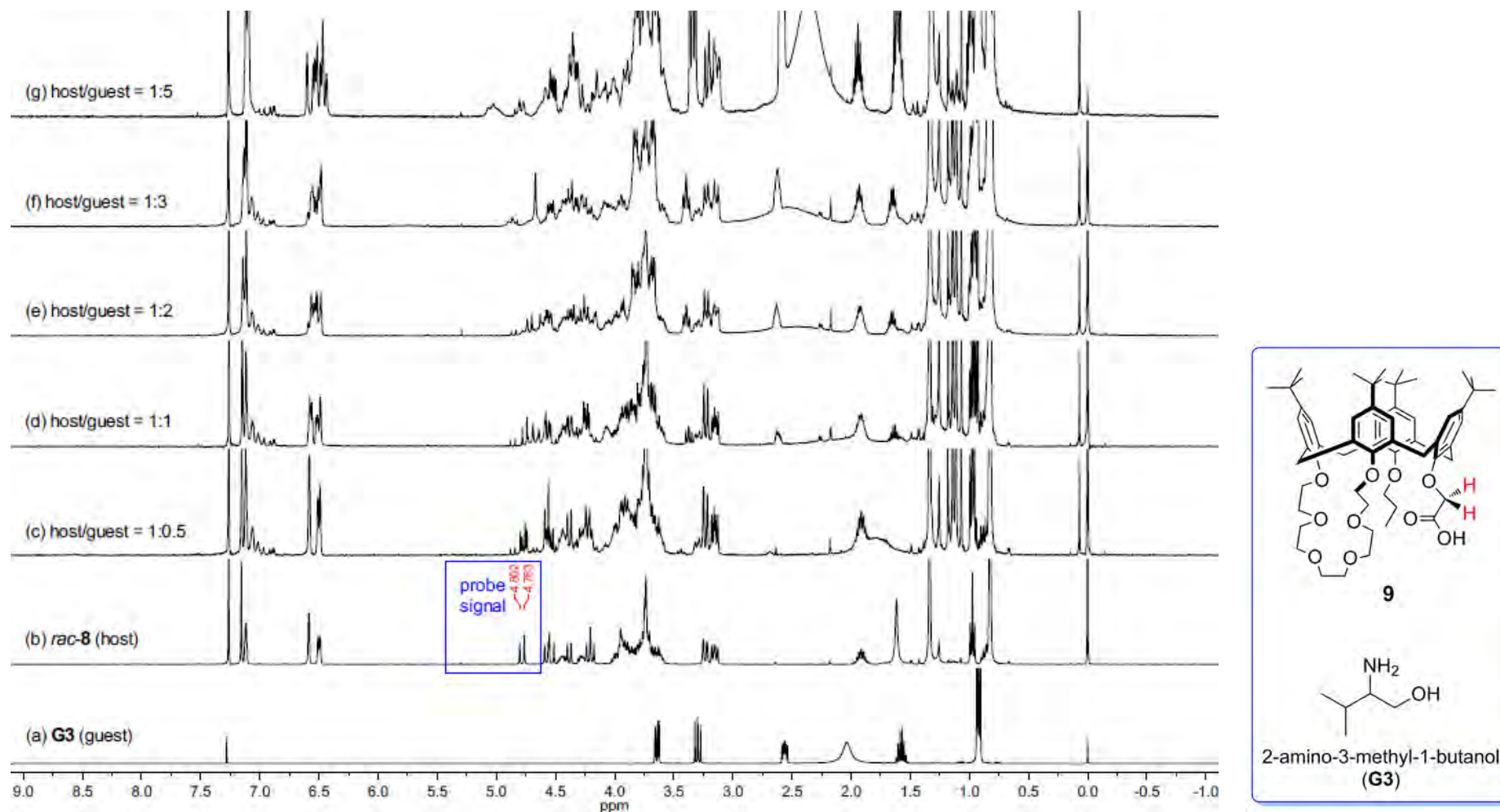


**Fig. S-27** <sup>1</sup>H NMR spectra (CDCl<sub>3</sub>, 400 MHz, 25 °C) of (±)-**9** (host, 10 mM) in the presence of increasing equivalents of (*S*)-**G3** (guest): (a) (*S*)-**G3**; (b) (±)-**9**; (c) host/guest = 1:0.5; (d) host/guest = 1:1; (e) host/guest = 1:2; (f) host/guest = 1:3; (g) host/guest = 1:5.

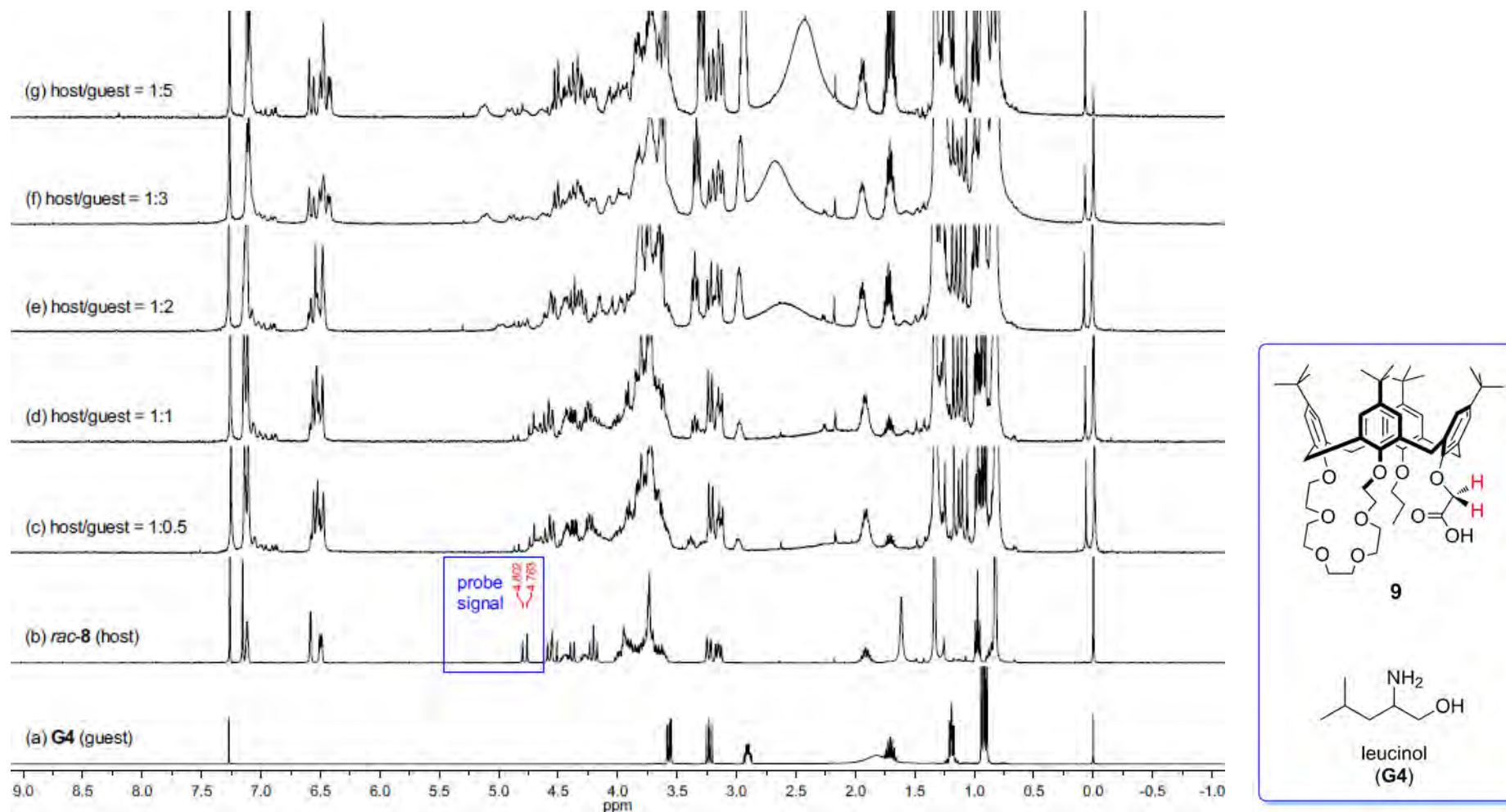


**Fig. S-28** <sup>1</sup>H NMR spectra (CDCl<sub>3</sub>, 400 MHz, 25 °C) of (±)-**9** (host, 10 mM) in the presence of increasing equivalents of (*S*)-**G4** (guest): (a) (*S*)-**G4**; (b) (±)-**9**; (c) host/guest = 1:0.5; (d) host/guest = 1:1; (e) host/guest = 1:2; (f) host/guest = 1:3; (g) host/guest = 1:5.

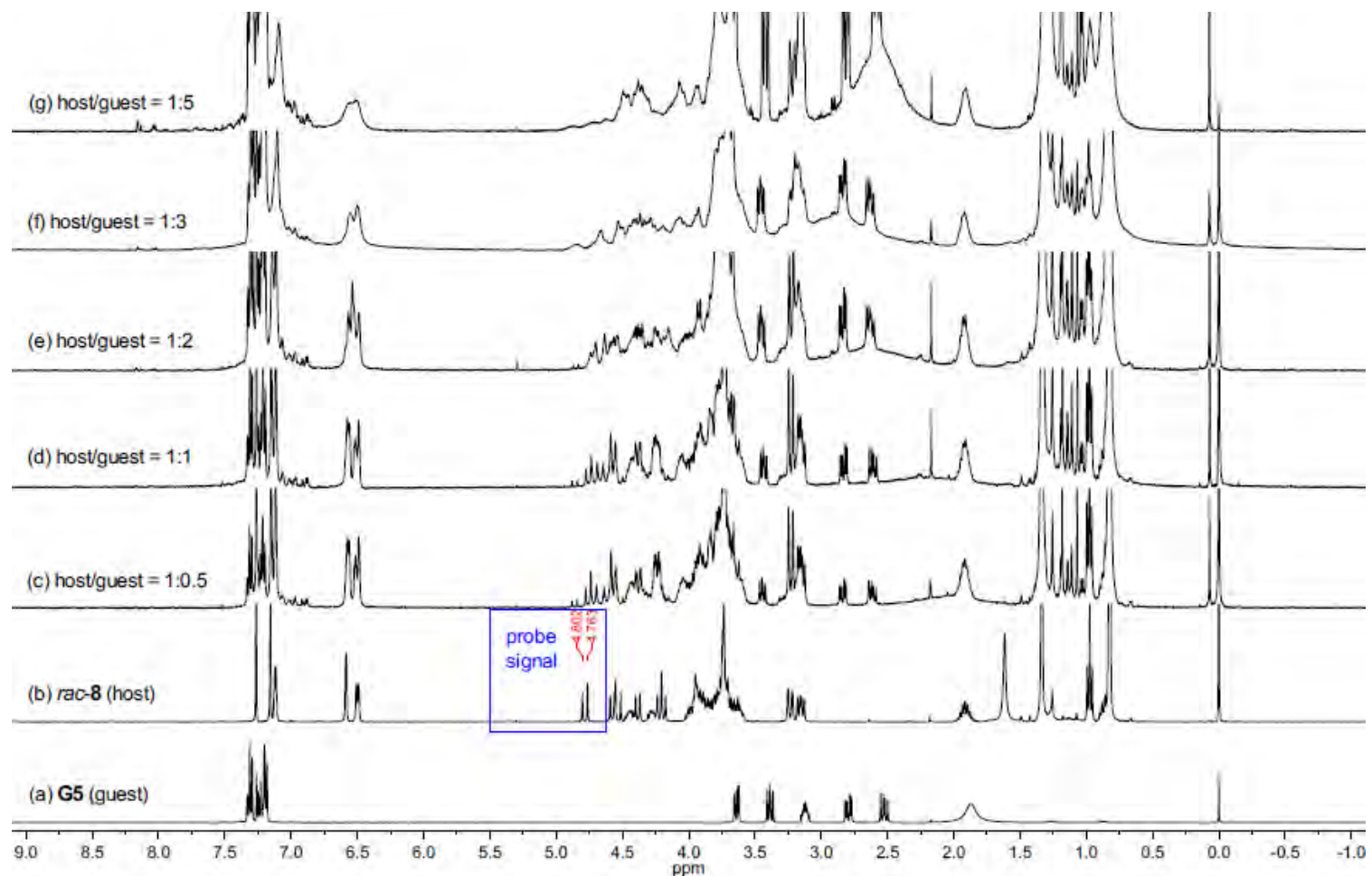


**Fig. S-29** <sup>1</sup>H NMR spectra (CDCl<sub>3</sub>, 400 MHz, 25 °C) of (±)-**9** (host, 10 mM) in the presence of increasing equivalents of (*S*)-**G5** (guest): (a) (*S*)-**G5**; (b) (±)-**9**; (c) host/guest = 1:0.5; (d) host/guest = 1:1; (e) host/guest = 1:2; (f) host/guest = 1:3; (g) host/guest = 1:5.

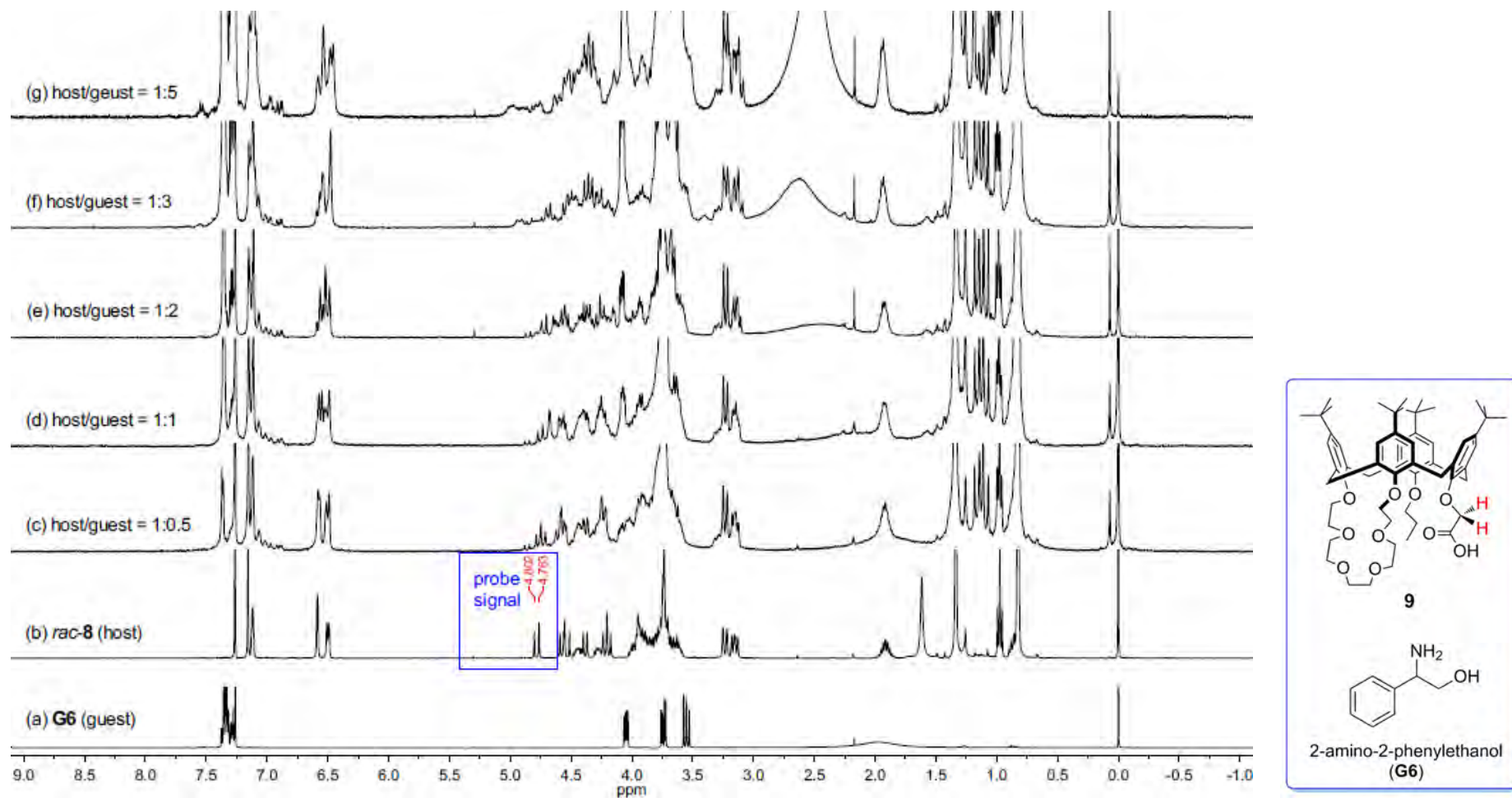


**Fig. S-30** <sup>1</sup>H NMR spectra (CDCl<sub>3</sub>, 400 MHz, 25 °C) of (±)-**9** (host, 10 mM) in the presence of increasing equivalents of (*S*)-**G6** (guest): (a) (*S*)-**G6**; (b) (±)-**9**; (c) host/guest = 1:0.5; (d) host/guest = 1:1; (e) host/guest = 1:2; (f) host/guest = 1:3; (g) host/guest = 1:5.

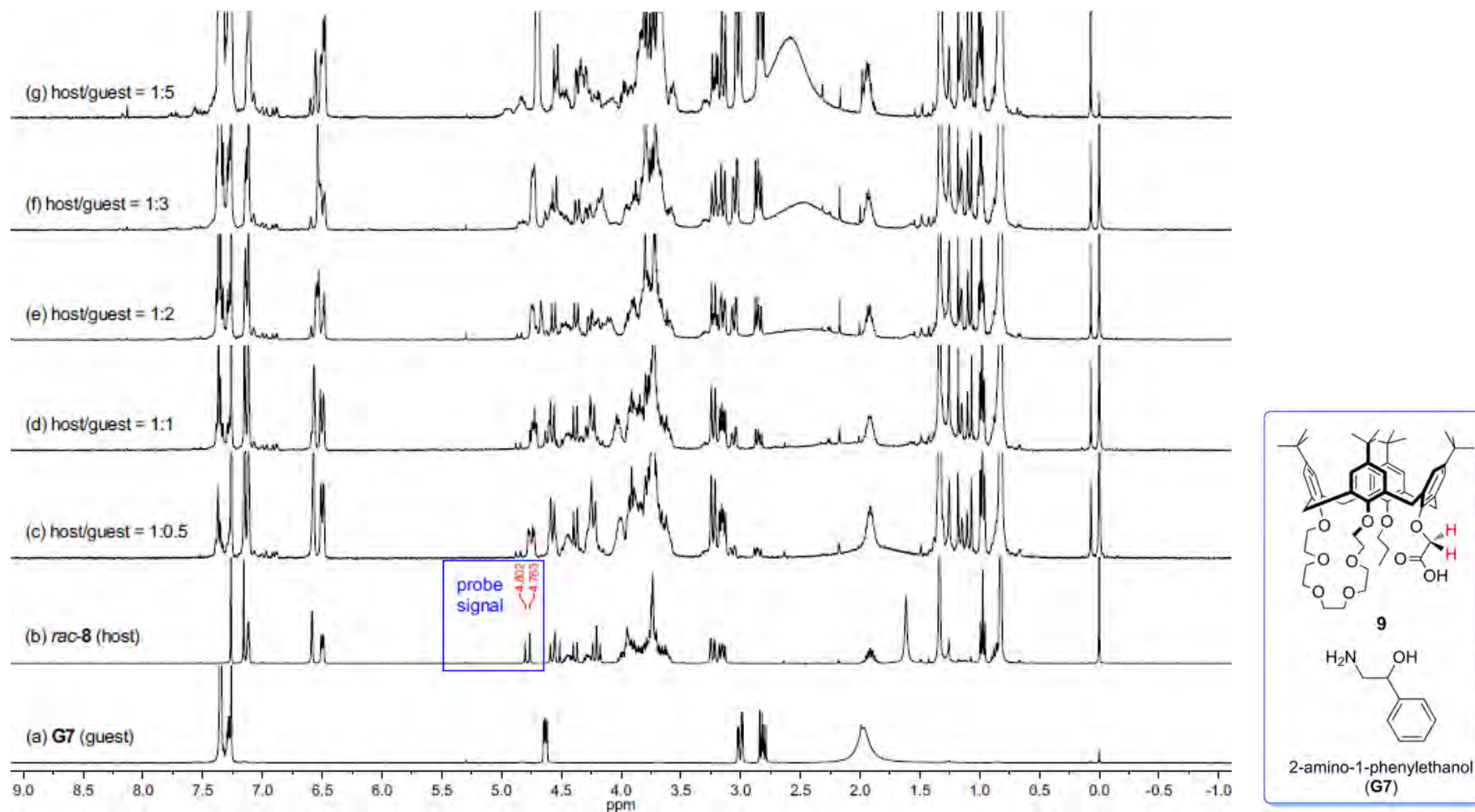


**Fig. S-31** <sup>1</sup>H NMR spectra (CDCl<sub>3</sub>, 400 MHz, 25 °C) of (±)-**9** (host, 10 mM) in the presence of increasing equivalents of (*R*)-**G7** (guest): (a) (*R*)-**G7**; (b) (±)-**9**; (c) host/guest = 1:0.5; (d) host/guest = 1:1; (e) host/guest = 1:2; (f) host/guest = 1:3; (g) host/guest = 1:5.

### C-3. $^1\text{H}$ NMR titration of ( $\pm$ )-**10** with **G1**–**G7**:

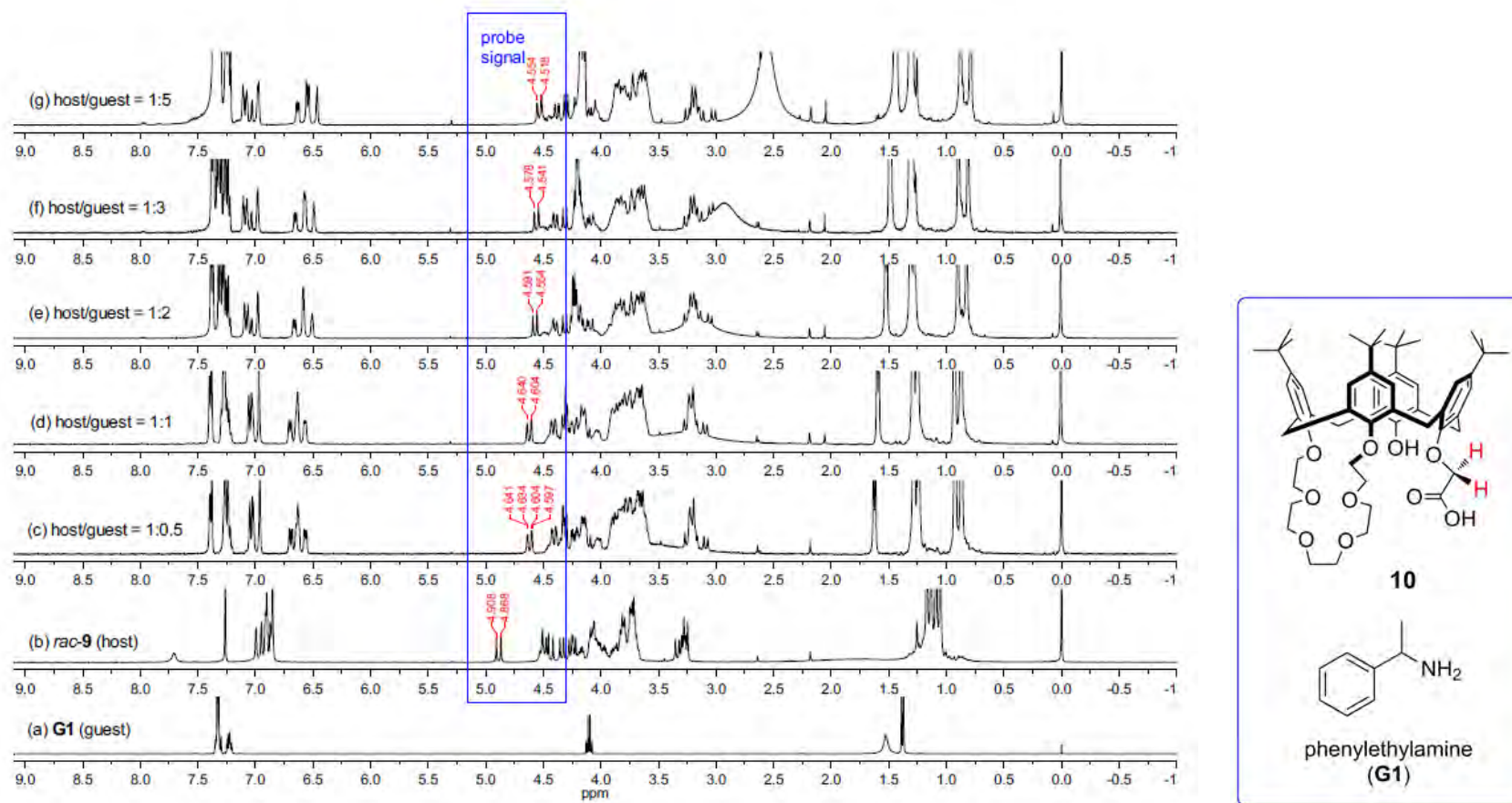


**Fig. S-32**  $^1\text{H}$  NMR spectra ( $\text{CDCl}_3$ , 400 MHz, 25 °C) of ( $\pm$ )-**10** (host, 10 mM) in the presence of increasing equivalents of (*R*)-**G1** (guest): (a) (*R*)-**G1**; (b) ( $\pm$ )-**10**; (c) host/guest = 1:0.5; (d) host/guest = 1:1; (e) host/guest = 1:2; (f) host/guest = 1:3; (g) host/guest = 1:5.

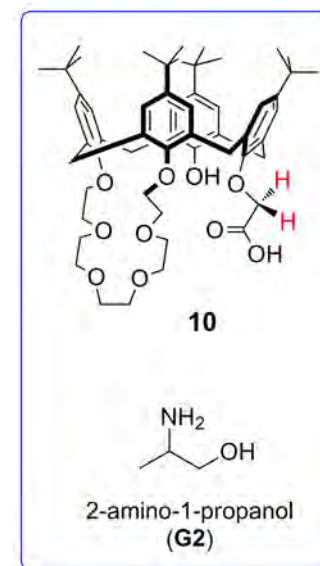
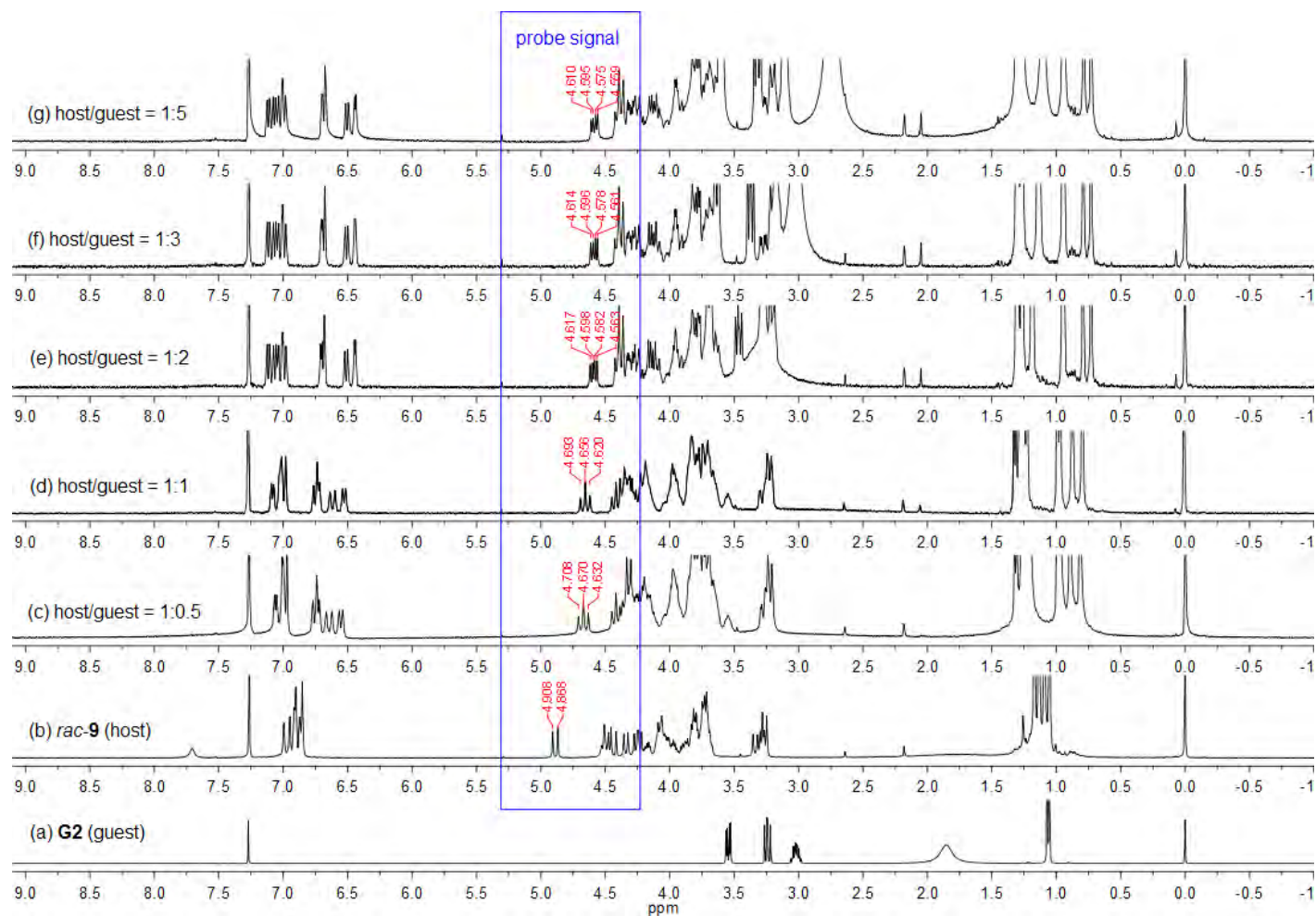


**Fig. S-33** <sup>1</sup>H NMR spectra (CDCl<sub>3</sub>, 400 MHz, 25 °C) of (±)-**10** (host, 10 mM) in the presence of increasing equivalents of (*S*)-**G2** (guest): (a) (*S*)-**G2**; (b) (±)-**10**; (c) host/guest = 1:0.5; (d) host/guest = 1:1; (e) host/guest = 1:2; (f) host/guest = 1:3; (g) host/guest = 1:5.

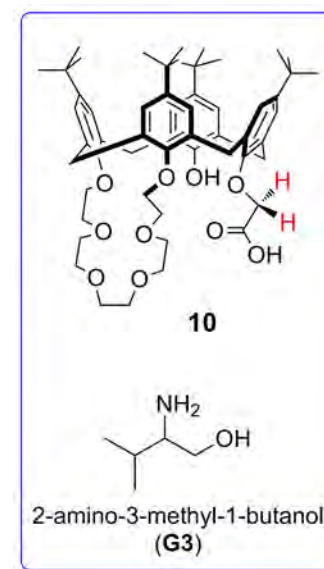
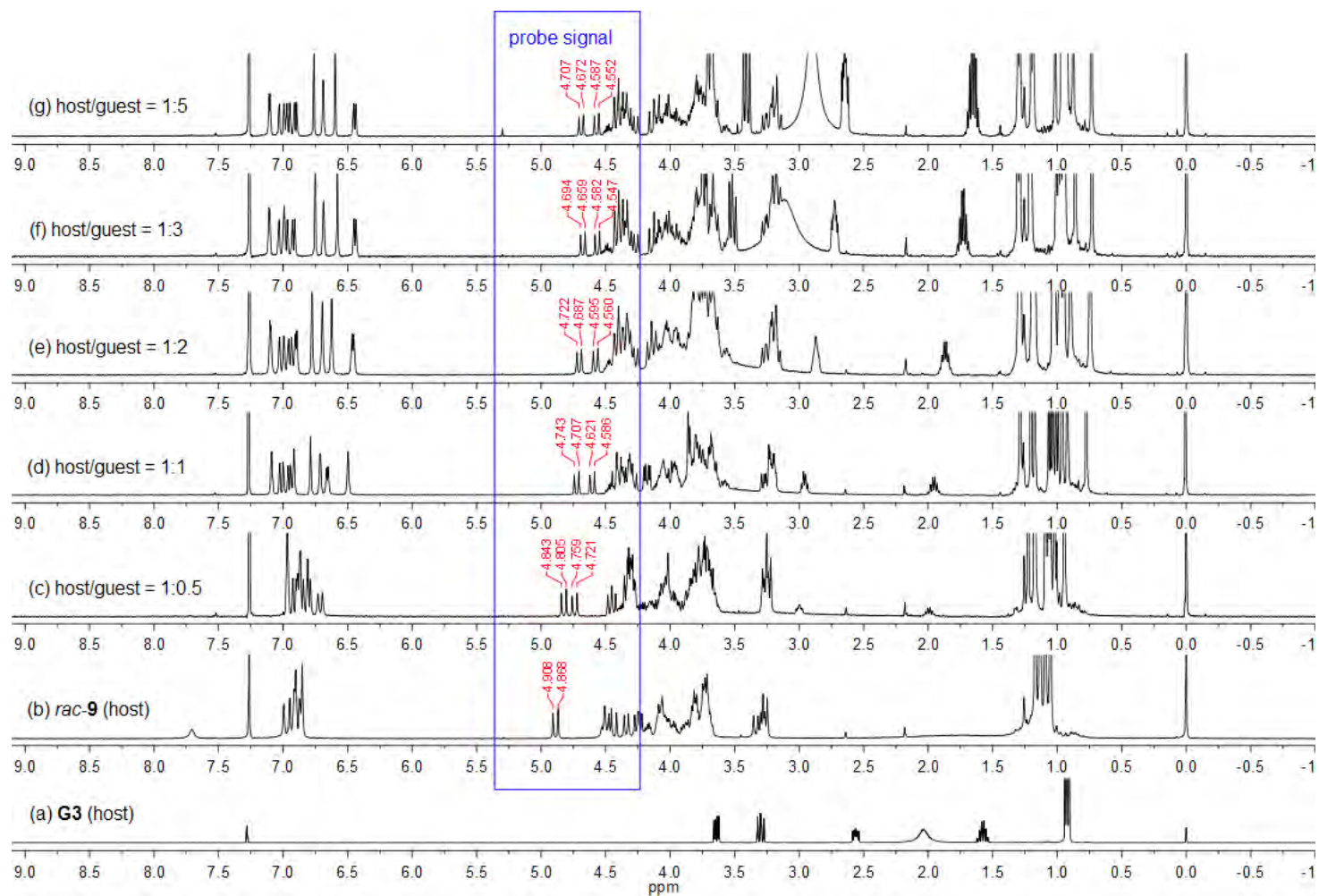


**Fig. S-34** <sup>1</sup>H NMR spectra (CDCl<sub>3</sub>, 400 MHz, 25 °C) of (±)-**10** (host, 10 mM) in the presence of increasing equivalents of (*S*)-**G3** (guest): (a) (*S*)-**G3**; (b) (±)-**10**; (c) host/guest = 1:0.5; (d) host/guest = 1:1; (e) host/guest = 1:2; (f) host/guest = 1:3; (g) host/guest = 1:5.



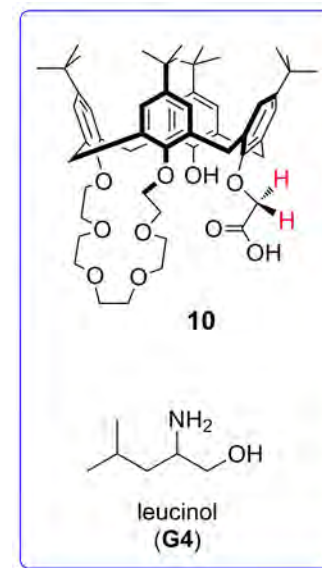
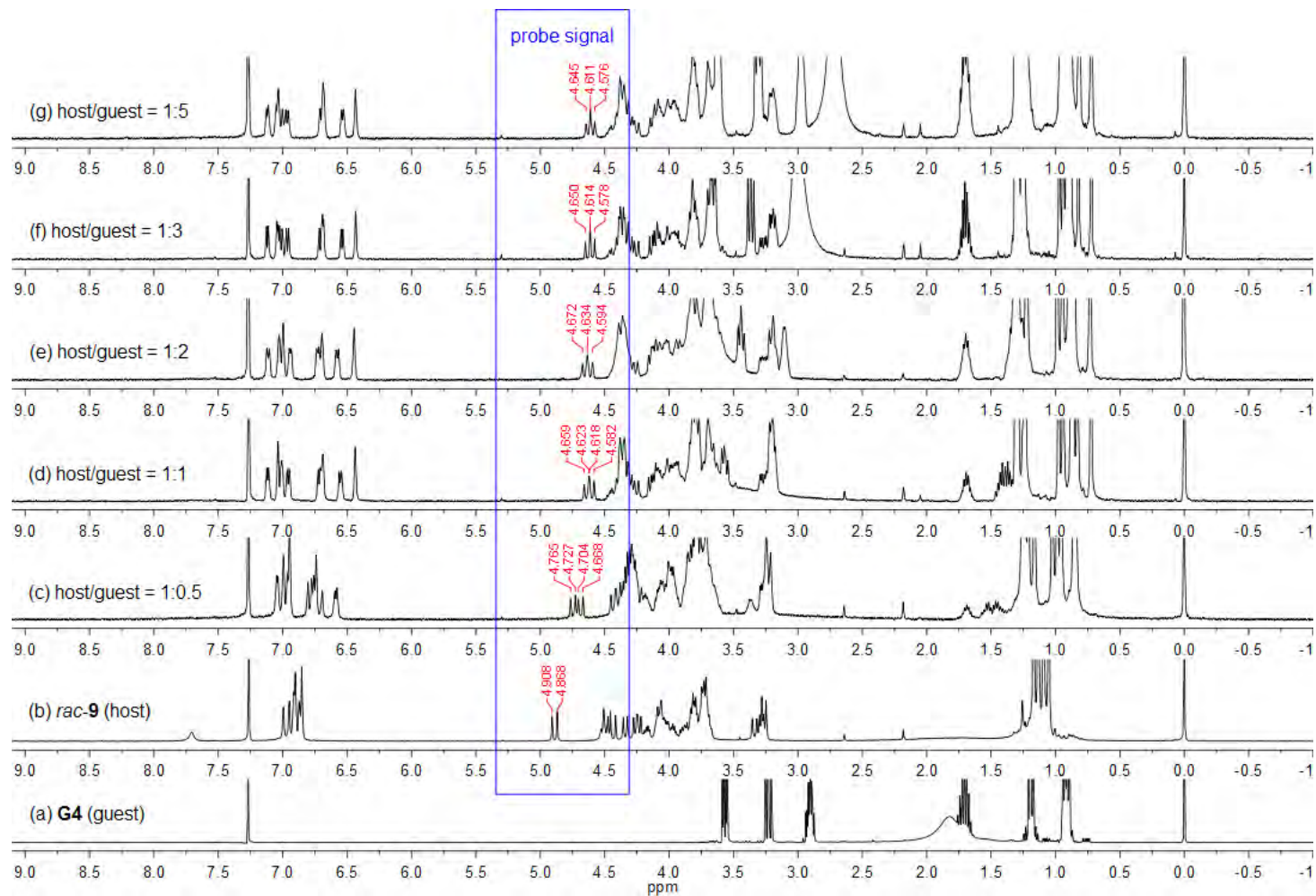


**Fig. S-35** <sup>1</sup>H NMR spectra (CDCl<sub>3</sub>, 400 MHz, 25 °C) of (±)-**10** (host, 10 mM) in the presence of increasing equivalents of (*S*)-**G4** (guest): (a) (*S*)-**G4**; (b) (±)-**10**; (c) host/guest = 1:0.5; (d) host/guest = 1:1; (e) host/guest = 1:2; (f) host/guest = 1:3; (g) host/guest = 1:5.

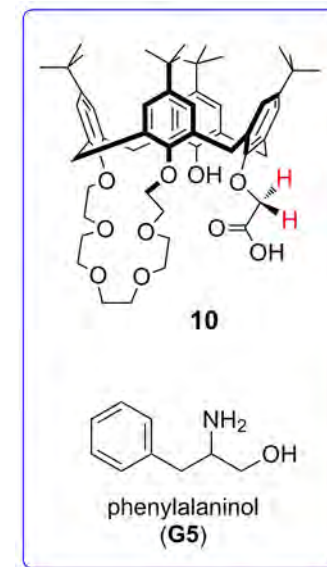
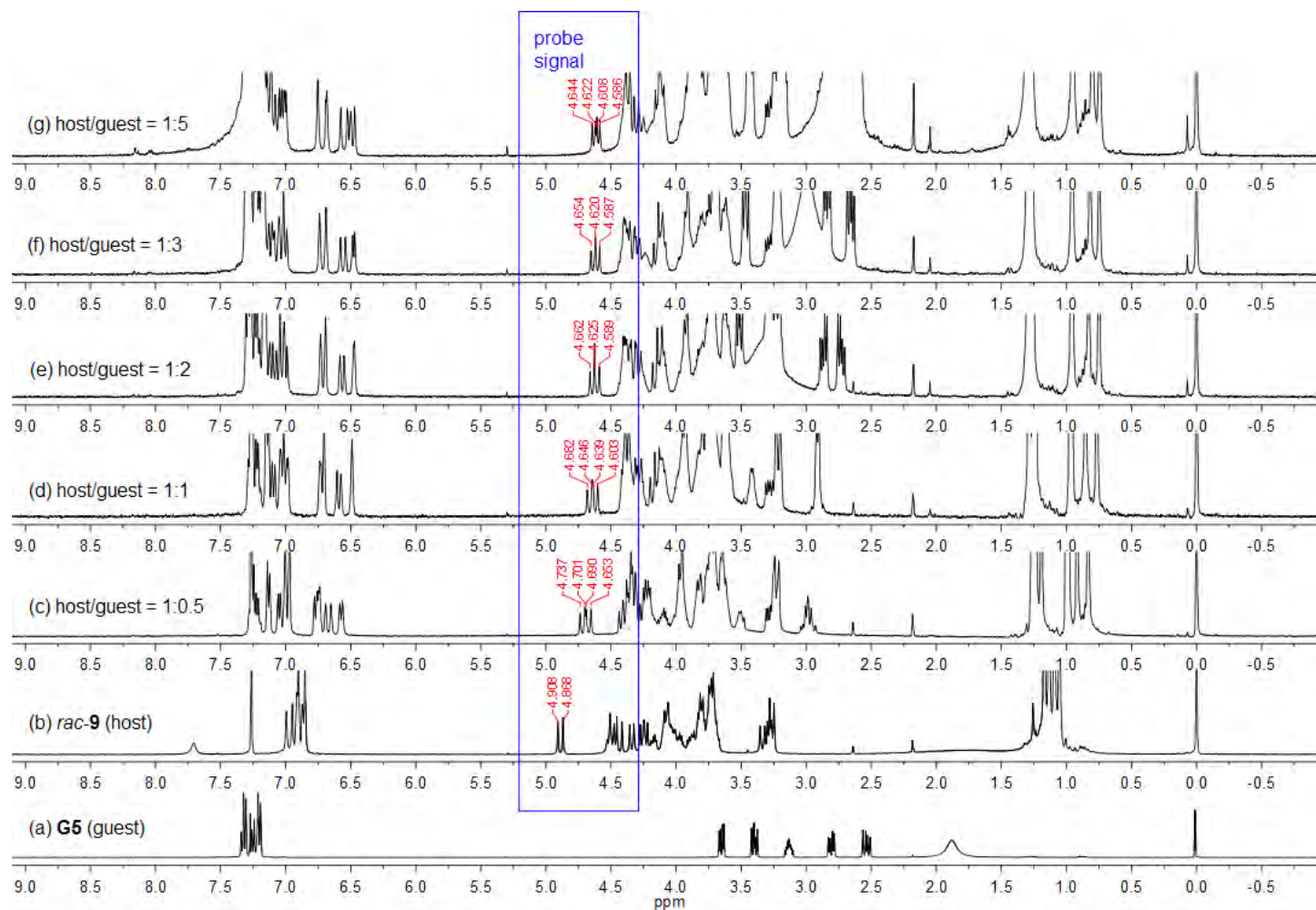


**Fig. S-36** <sup>1</sup>H NMR spectra (CDCl<sub>3</sub>, 400 MHz, 25 °C) of (±)-**10** (host, 10 mM) in the presence of increasing equivalents of (*S*)-**G5** (guest): (a) (*S*)-**G5**; (b) (±)-**10**; (c) host/guest = 1:0.5; (d) host/guest = 1:1; (e) host/guest = 1:2; (f) host/guest = 1:3; (g) host/guest = 1:5.

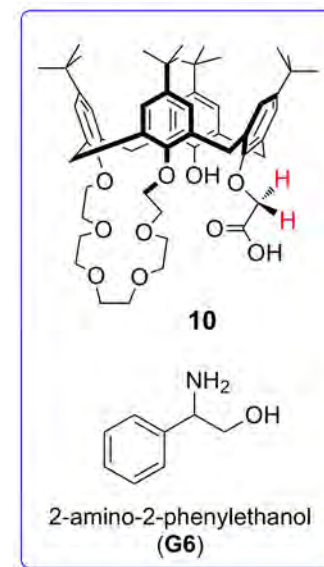
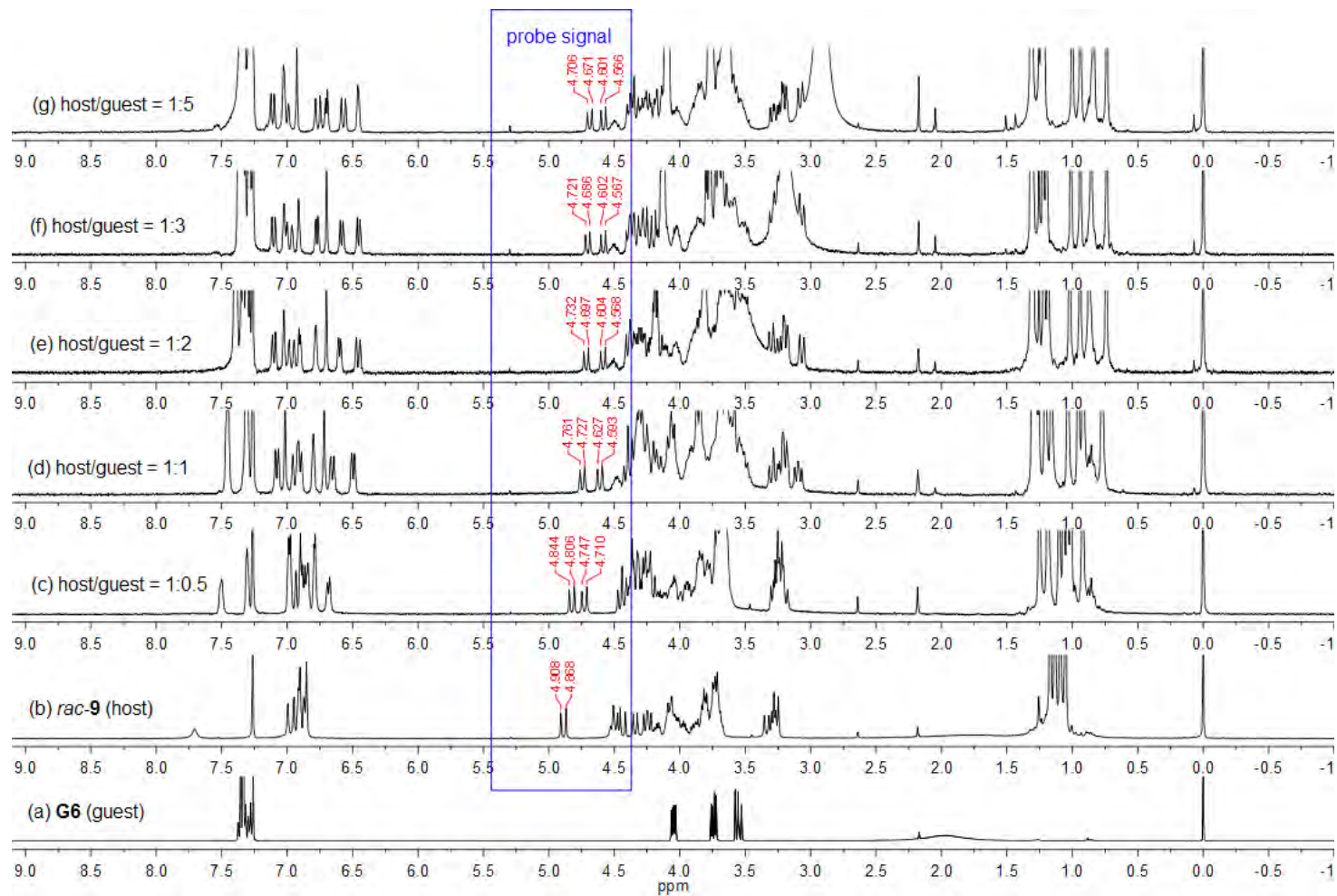


**Fig. S-37** <sup>1</sup>H NMR spectra (CDCl<sub>3</sub>, 400 MHz, 25 °C) of (±)-**10** (host, 10 mM) in the presence of increasing equivalents of (*S*)-**G6** (guest): (a) (*S*)-**G6**; (b) (±)-**10**; (c) host/guest = 1:0.5; (d) host/guest = 1:1; (e) host/guest = 1:2; (f) host/guest = 1:3; (g) host/guest = 1:5.

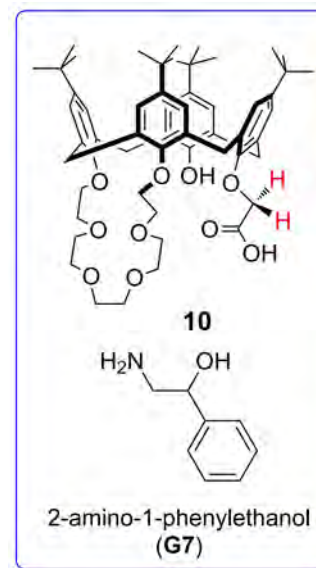
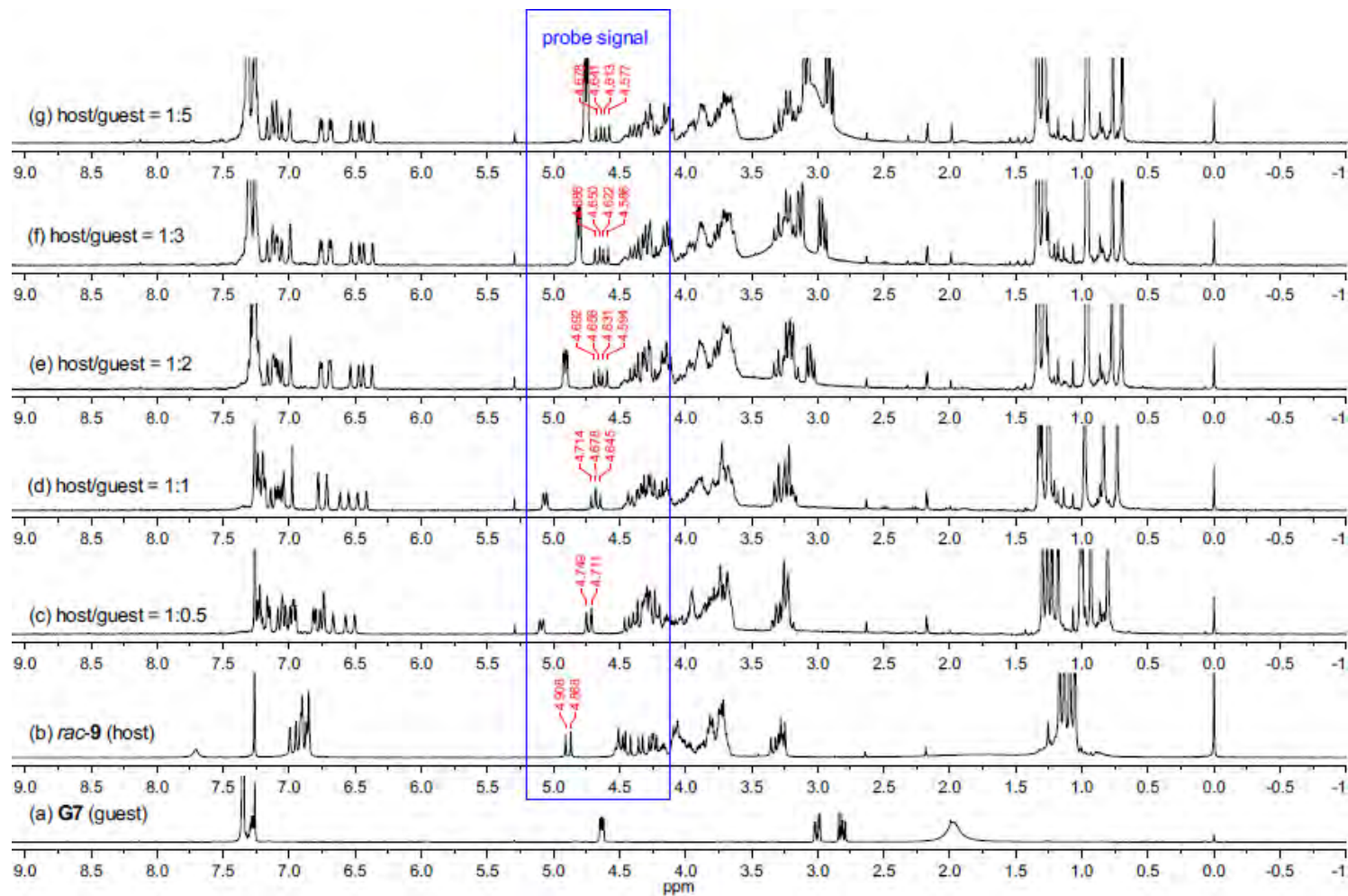


**Fig. S-38** <sup>1</sup>H NMR spectra (CDCl<sub>3</sub>, 400 MHz, 25 °C) of (±)-**10** (host, 10 mM) in the presence of increasing equivalents of (*R*)-**G7** (guest): (a) (*R*)-**G7**; (b) (±)-**10**; (c) host/guest = 1:0.5; (d) host/guest = 1:1; (e) host/guest = 1:2; (f) host/guest = 1:3; (g) host/guest = 1:5.

#### C-4. $^1\text{H}$ NMR titration of ( $\pm$ )-**11** with **G1**–**G7**:

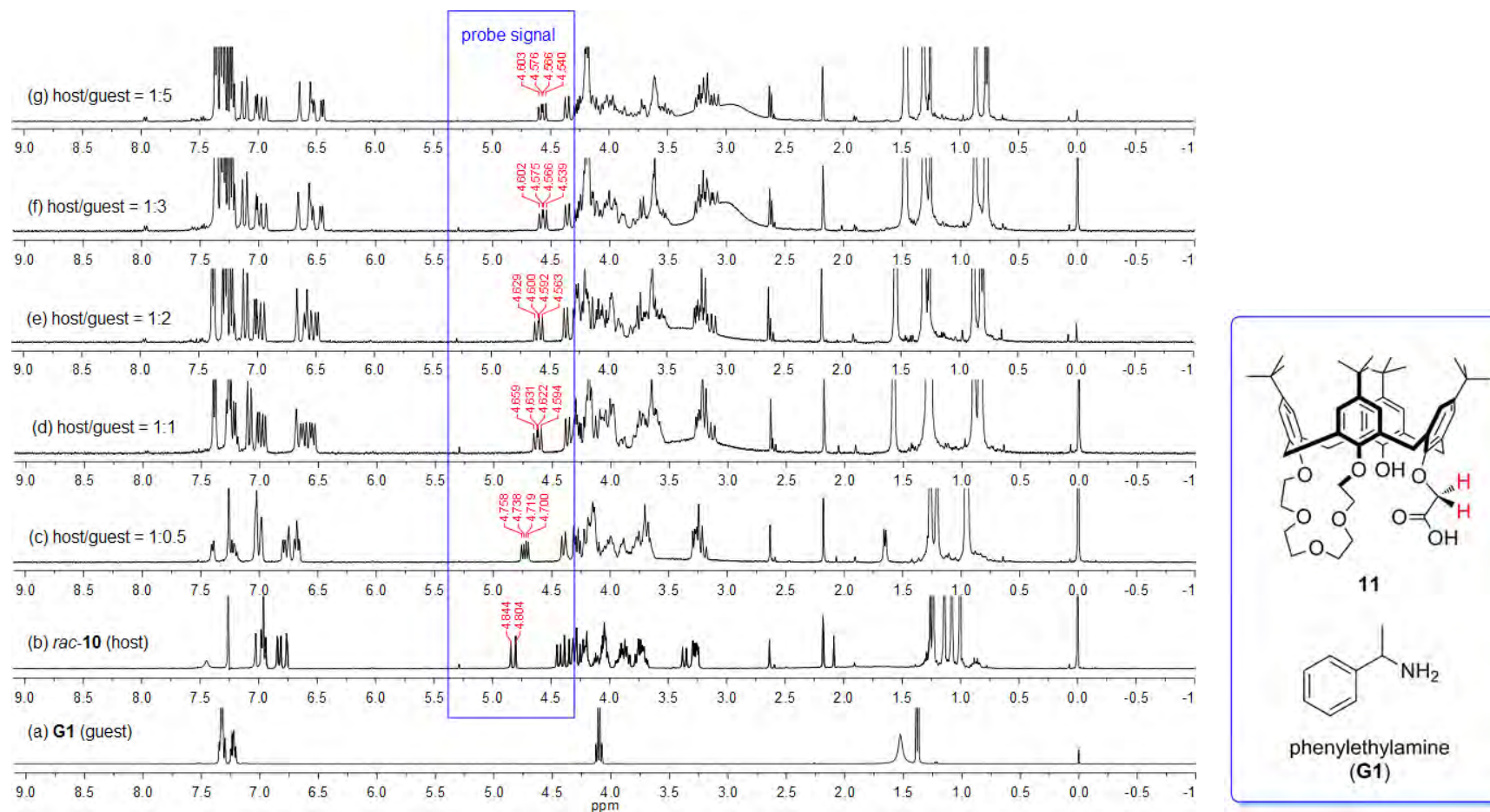


**Fig. S-39**  $^1\text{H}$  NMR spectra (CDCl<sub>3</sub>, 400 MHz, 25 °C) of ( $\pm$ )-**11** (host, 10 mM) in the presence of increasing equivalents of (*R*)-**G1** (guest): (a) (*R*)-**G1**; (b) ( $\pm$ )-**11**; (c) host/guest = 1:0.5; (d) host/guest = 1:1; (e) host/guest = 1:2; (f) host/guest = 1:3; (g) host/guest = 1:5.

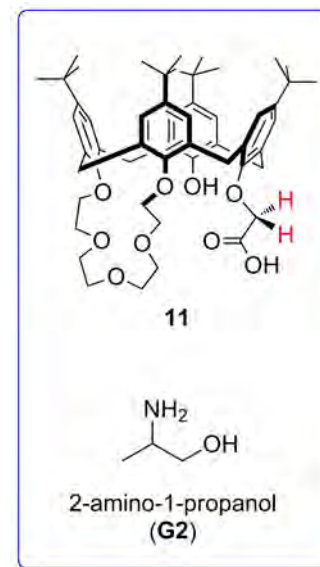
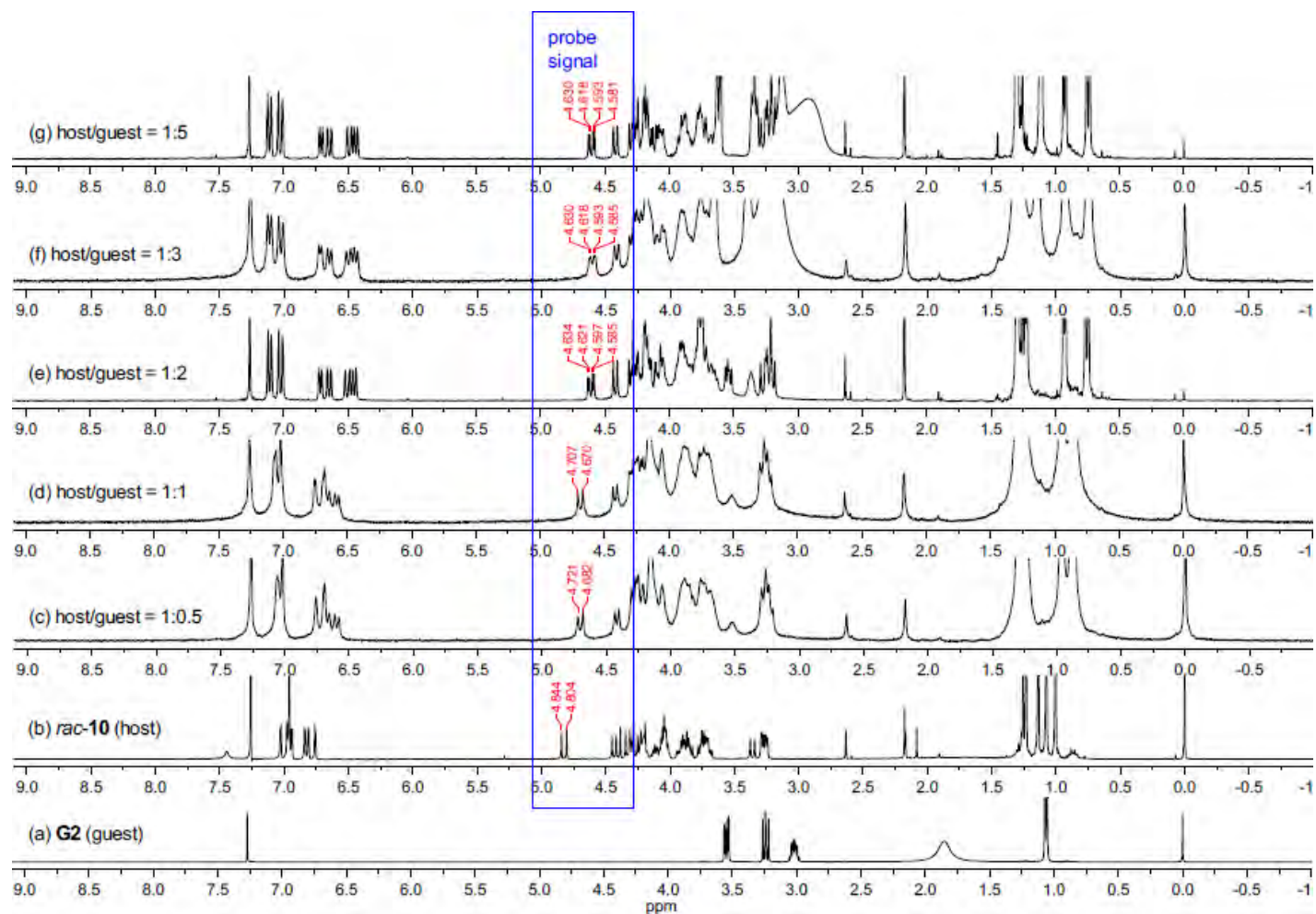


**Fig. S-40** <sup>1</sup>H NMR spectra (CDCl<sub>3</sub>, 400 MHz, 25 °C) of (±)-**11** (host, 10 mM) in the presence of increasing equivalents of (*S*)-**G2** (guest): (a) (*S*)-**G2**; (b) (±)-**11**; (c) host/guest = 1:0.5; (d) host/guest = 1:1; (e) host/guest = 1:2; (f) host/guest = 1:3; (g) host/guest = 1:5.

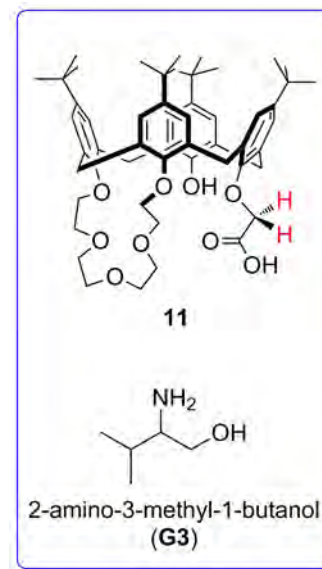
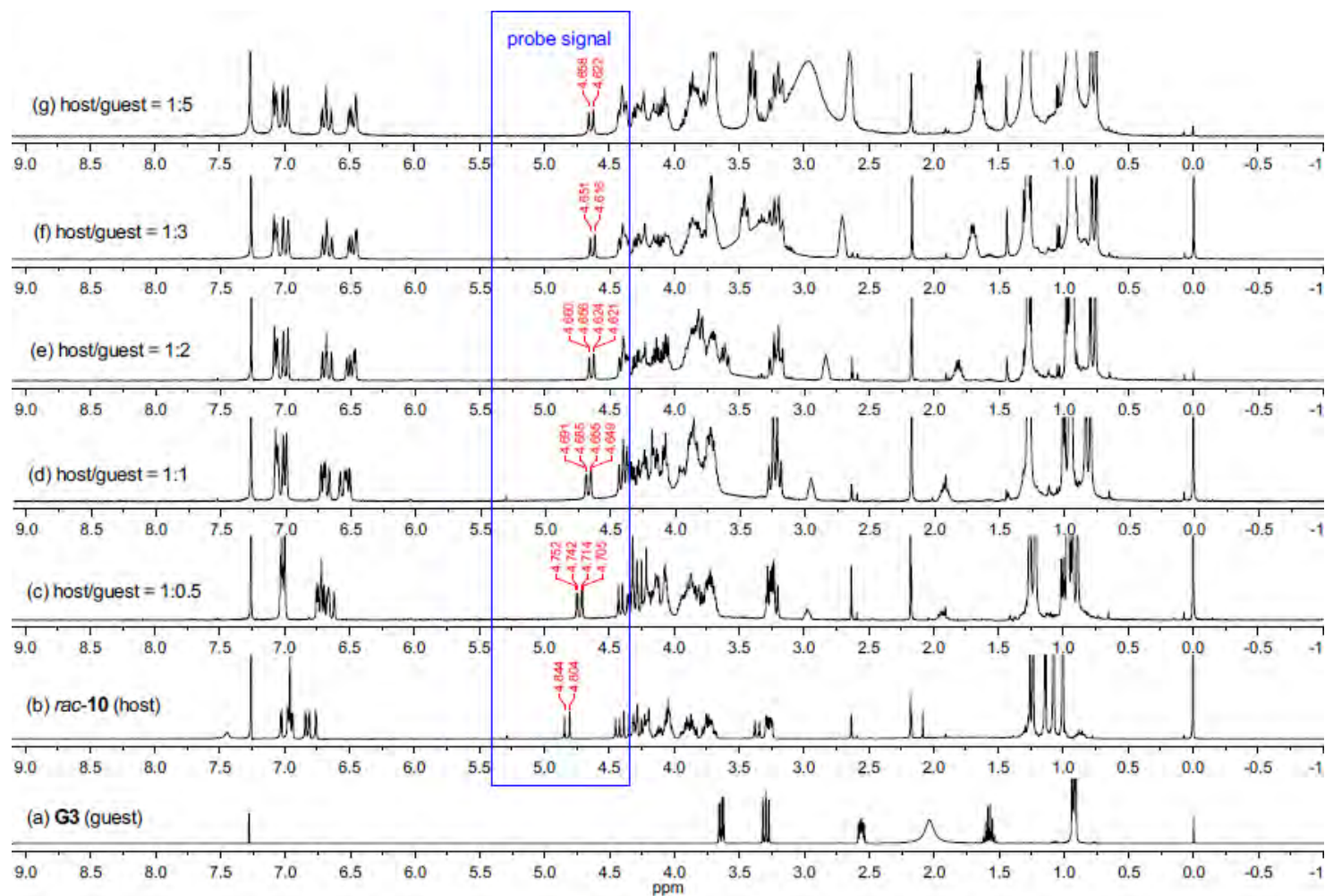


**Fig. S-41** <sup>1</sup>H NMR spectra (CDCl<sub>3</sub>, 400 MHz, 25 °C) of (±)-**11** (host, 10 mM) in the presence of increasing equivalents of (*S*)-**G3** (guest): (a) (*S*)-**G3**; (b) (±)-**11**; (c) host/guest = 1:0.5; (d) host/guest = 1:1; (e) host/guest = 1:2; (f) host/guest = 1:3; (g) host/guest = 1:5.

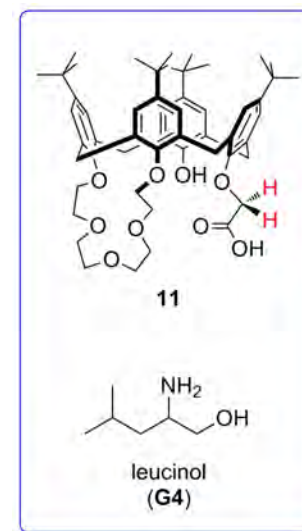
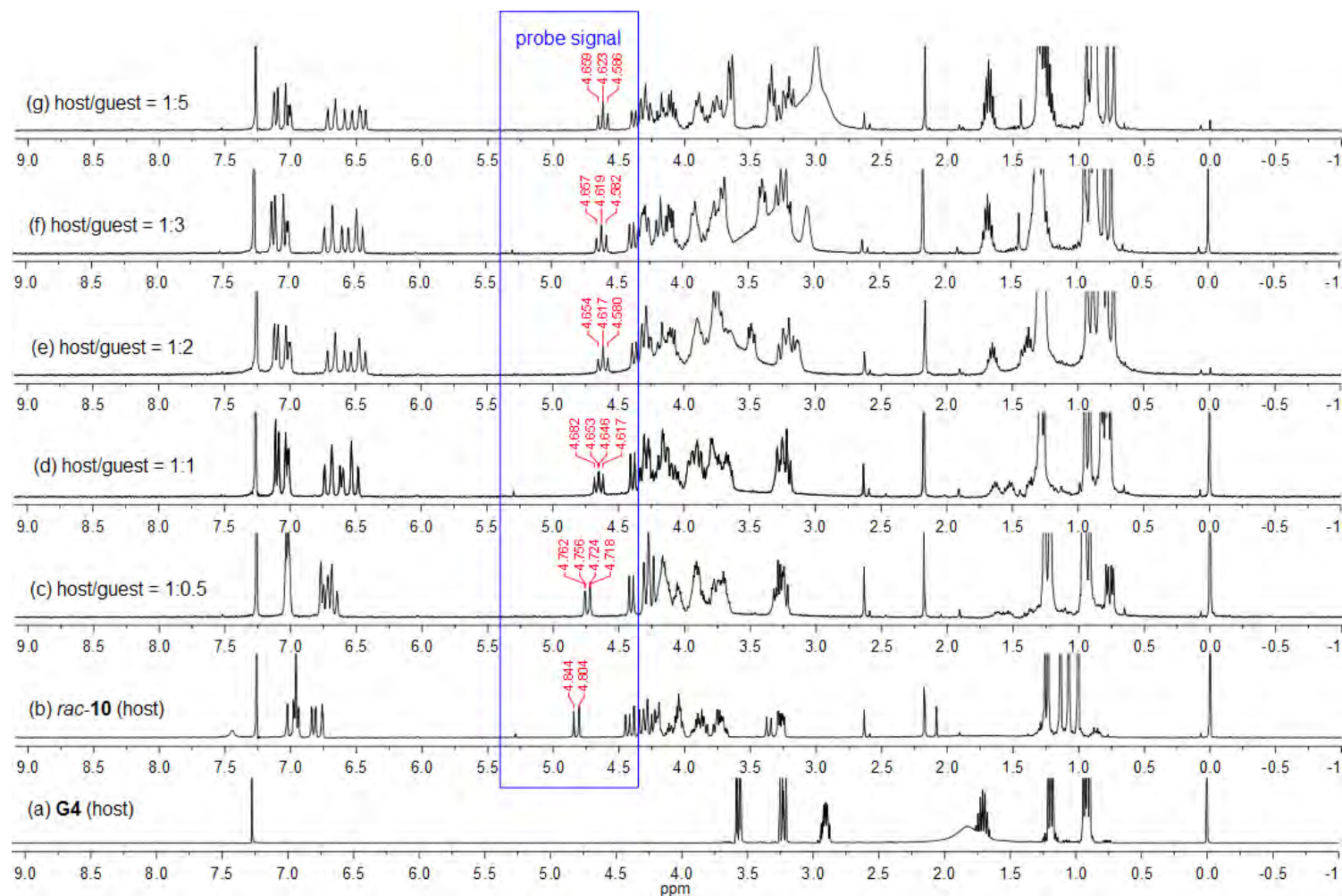


**Fig. S-42** <sup>1</sup>H NMR spectra (CDCl<sub>3</sub>, 400 MHz, 25 °C) of (±)-**11** (host, 10 mM) in the presence of increasing equivalents of (*S*)-**G4** (guest): (a) (*S*)-**G4**; (b) (±)-**11**; (c) host/guest = 1:0.5; (d) host/guest = 1:1; (e) host/guest = 1:2; (f) host/guest = 1:3; (g) host/guest = 1:5.



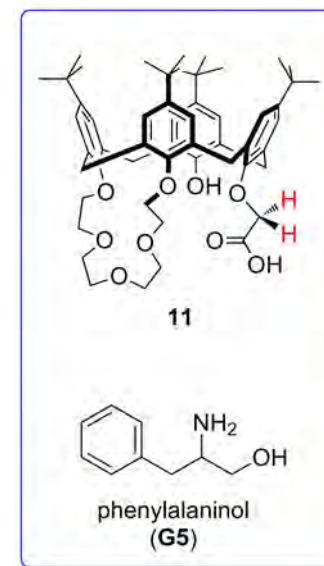
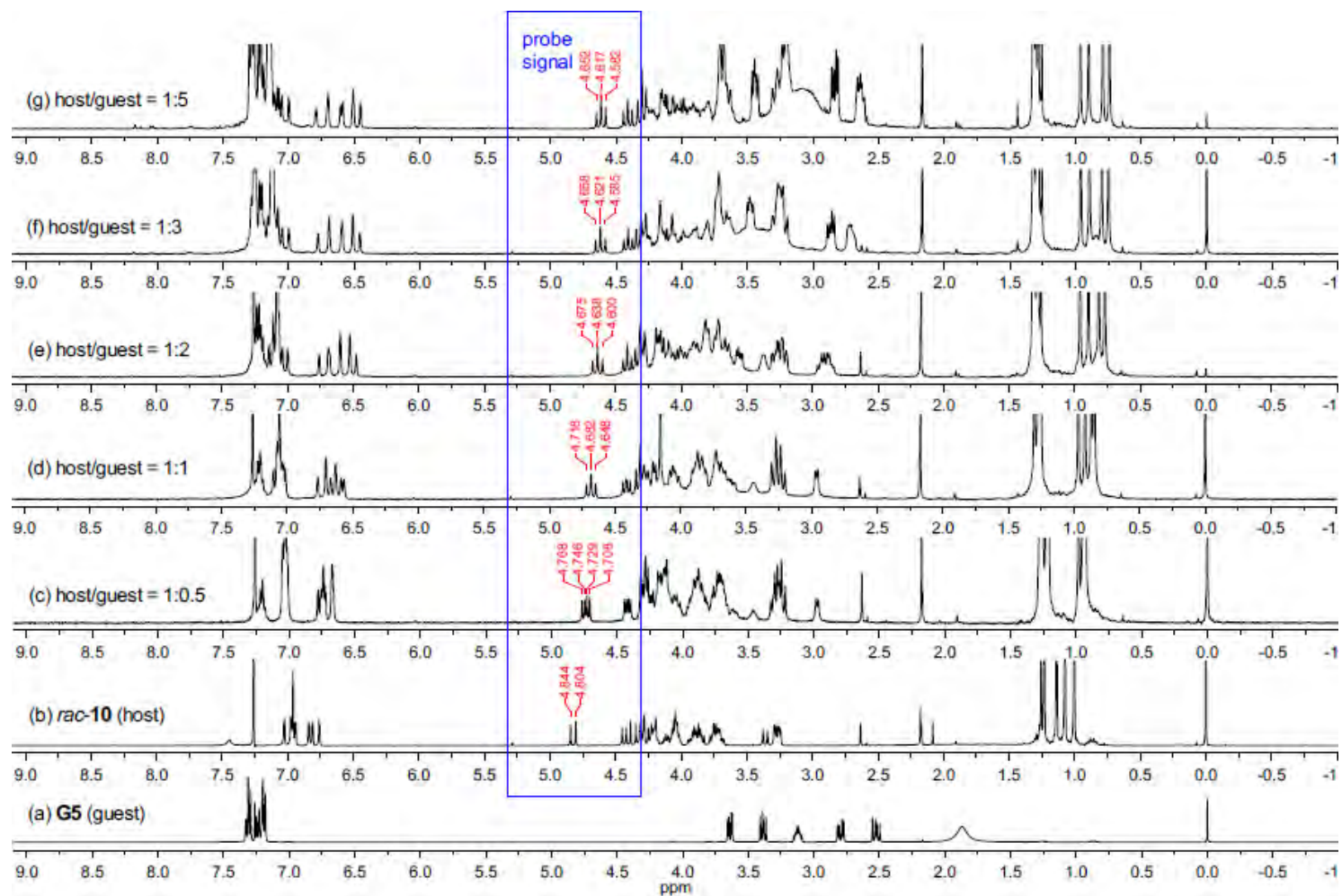


**Fig. S-43** <sup>1</sup>H NMR spectra (CDCl<sub>3</sub>, 400 MHz, 25 °C) of (±)-11 (host, 10 mM) in the presence of increasing equivalents of (S)-G5 (guest): (a) (S)-G5; (b) (±)-11; (c) host/guest = 1:0.5; (d) host/guest = 1:1; (e) host/guest = 1:2; (f) host/guest = 1:3; (g) host/guest = 1:5.

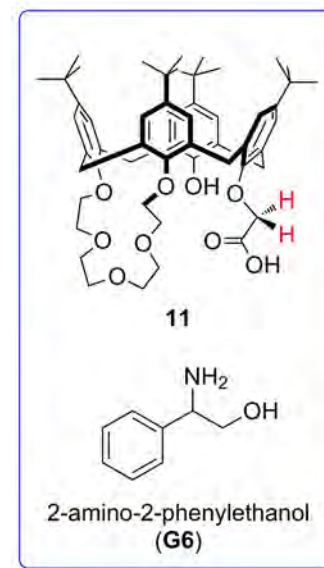
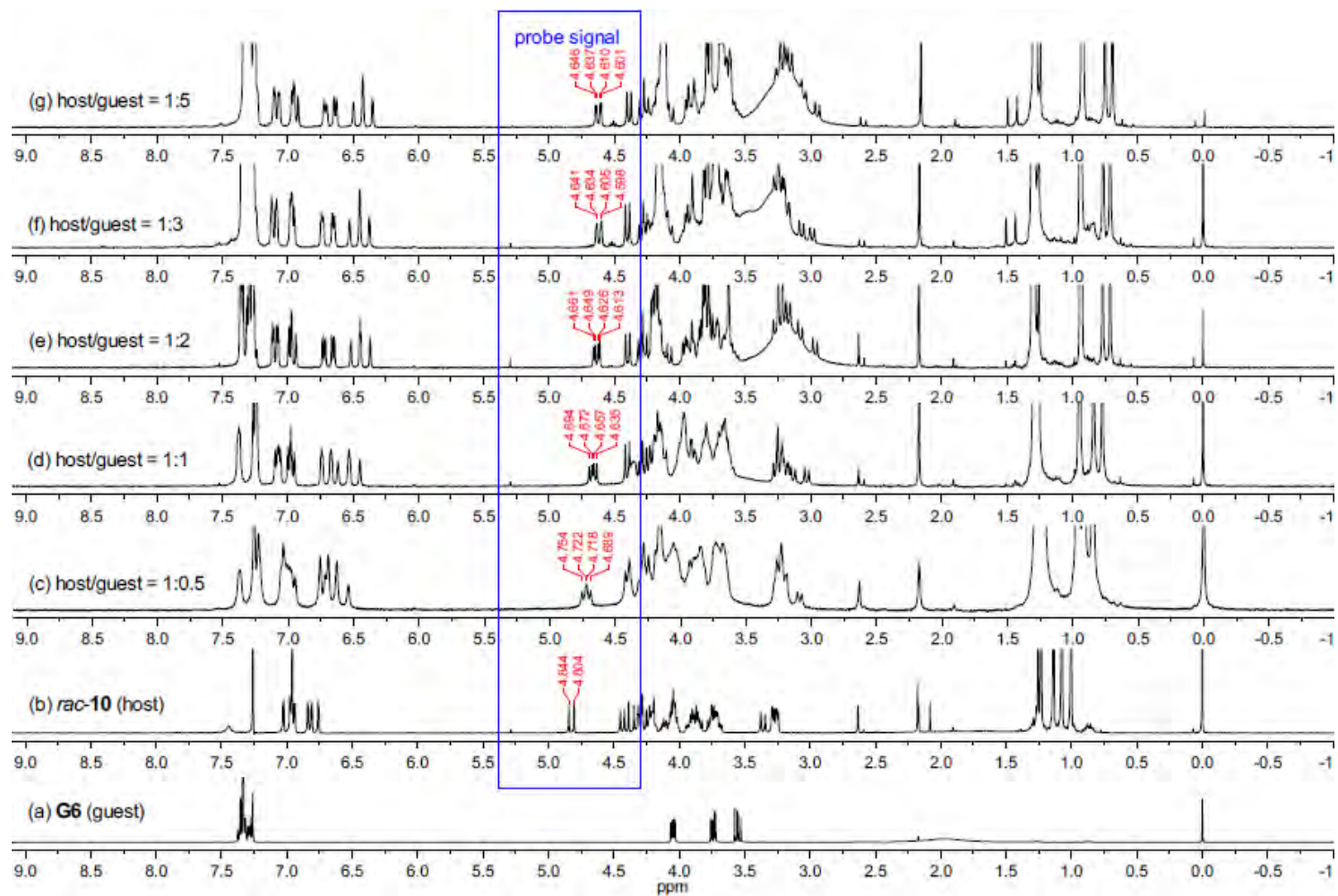


**Fig. S-44** <sup>1</sup>H NMR spectra (CDCl<sub>3</sub>, 400 MHz, 25 °C) of (±)-**11** (host, 10 mM) in the presence of increasing equivalents of (*S*)-**G6** (guest): (a) (*S*)-**G6**; (b) (±)-**11**; (c) host/guest = 1:0.5; (d) host/guest = 1:1; (e) host/guest = 1:2; (f) host/guest = 1:3; (g) host/guest = 1:5.

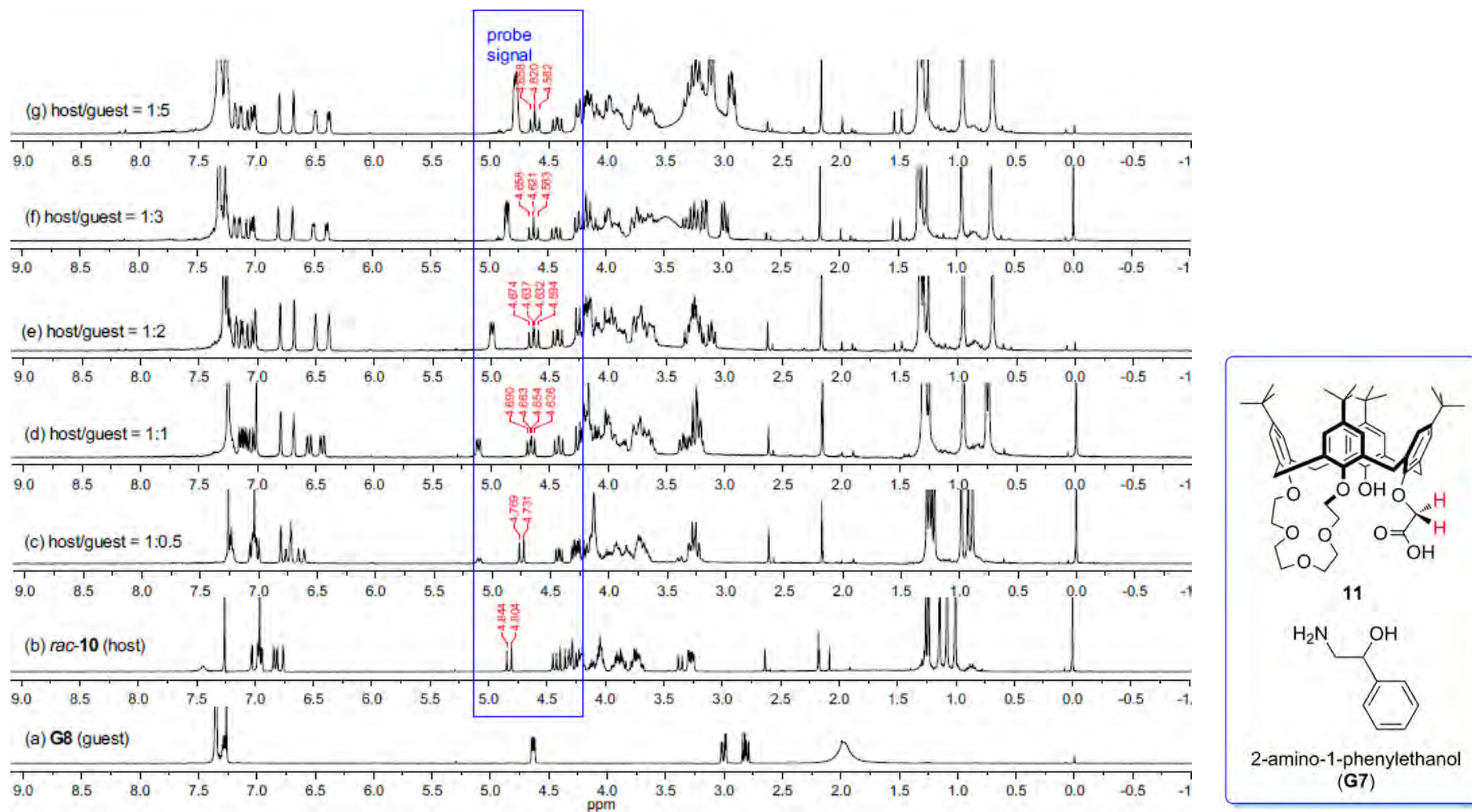


**Fig. S-45** <sup>1</sup>H NMR spectra (CDCl<sub>3</sub>, 400 MHz, 25 °C) of (±)-**11** (host, 10 mM) in the presence of increasing equivalents of (*R*)-**G7** (guest): (a) (*R*)-**G7**; (b) (±)-**11**; (c) host/guest = 1:0.5; (d) host/guest = 1:1; (e) host/guest = 1:2; (f) host/guest = 1:3; (g) host/guest = 1:5.

### C-5. $^1\text{H}$ NMR titration of ( $\pm$ )-**12** with **G1**–**G7**:

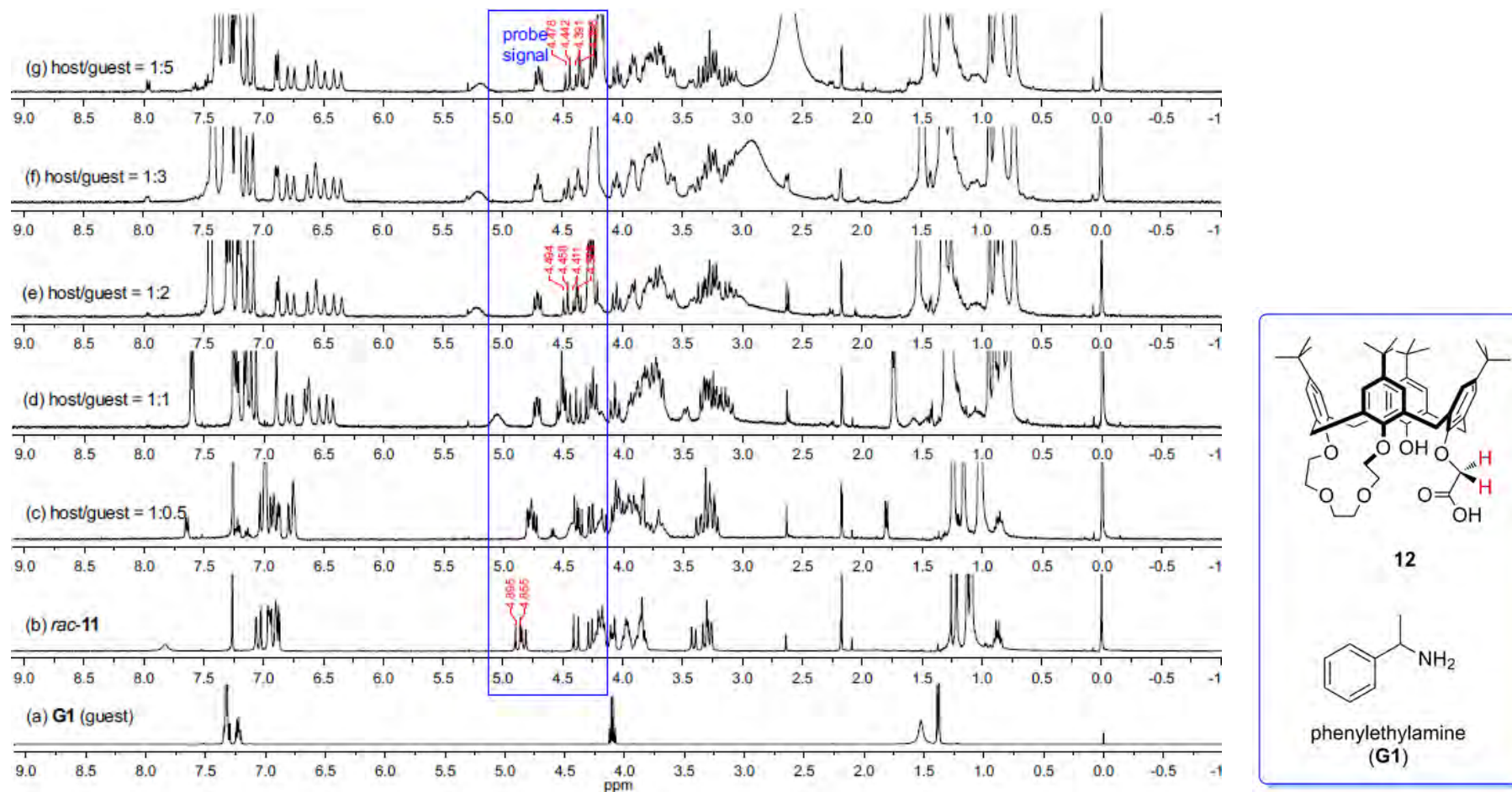


**Fig. S-46**  $^1\text{H}$  NMR spectra ( $\text{CDCl}_3$ , 400 MHz, 25 °C) of ( $\pm$ )-**12** (host, 10 mM) in the presence of increasing equivalents of (*R*)-**G1** (guest): (a) (*R*)-**G1**; (b) ( $\pm$ )-**12**; (c) host/guest = 1:0.5; (d) host/guest = 1:1; (e) host/guest = 1:2; (f) host/guest = 1:3; (g) host/guest = 1:5.

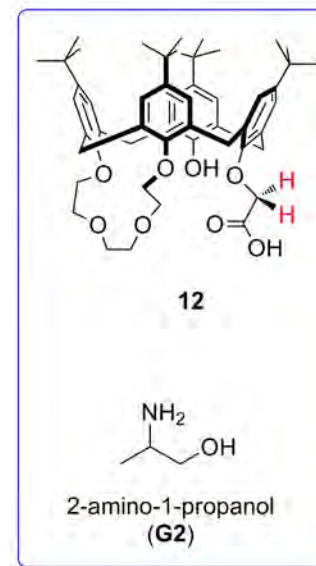
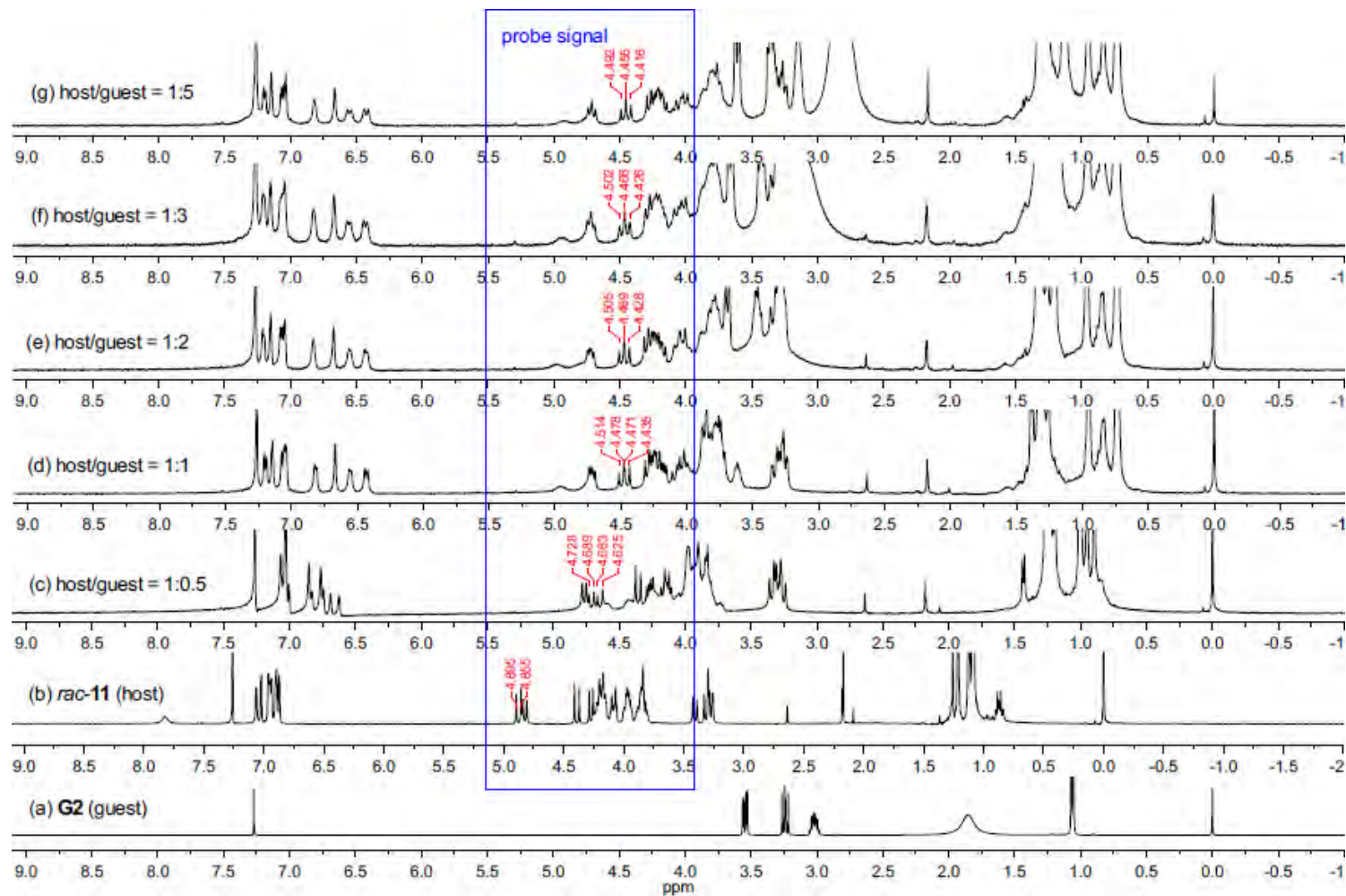


**Fig. S-47** <sup>1</sup>H NMR spectra (CDCl<sub>3</sub>, 400 MHz, 25 °C) of (±)-**12** (host, 10 mM) in the presence of increasing equivalents of (*S*)-**G2** (guest): (a) (*S*)-**G2**; (b) (±)-**12**; (c) host/guest = 1:0.5; (d) host/guest = 1:1; (e) host/guest = 1:2; (f) host/guest = 1:3; (g) host/guest = 1:5.

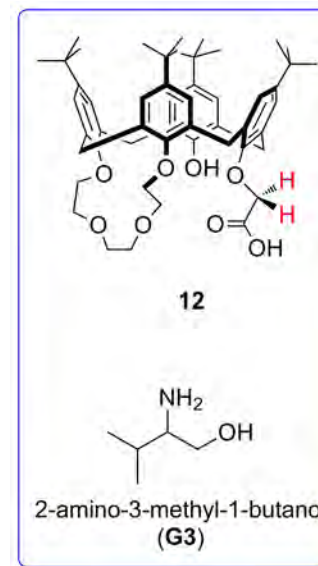
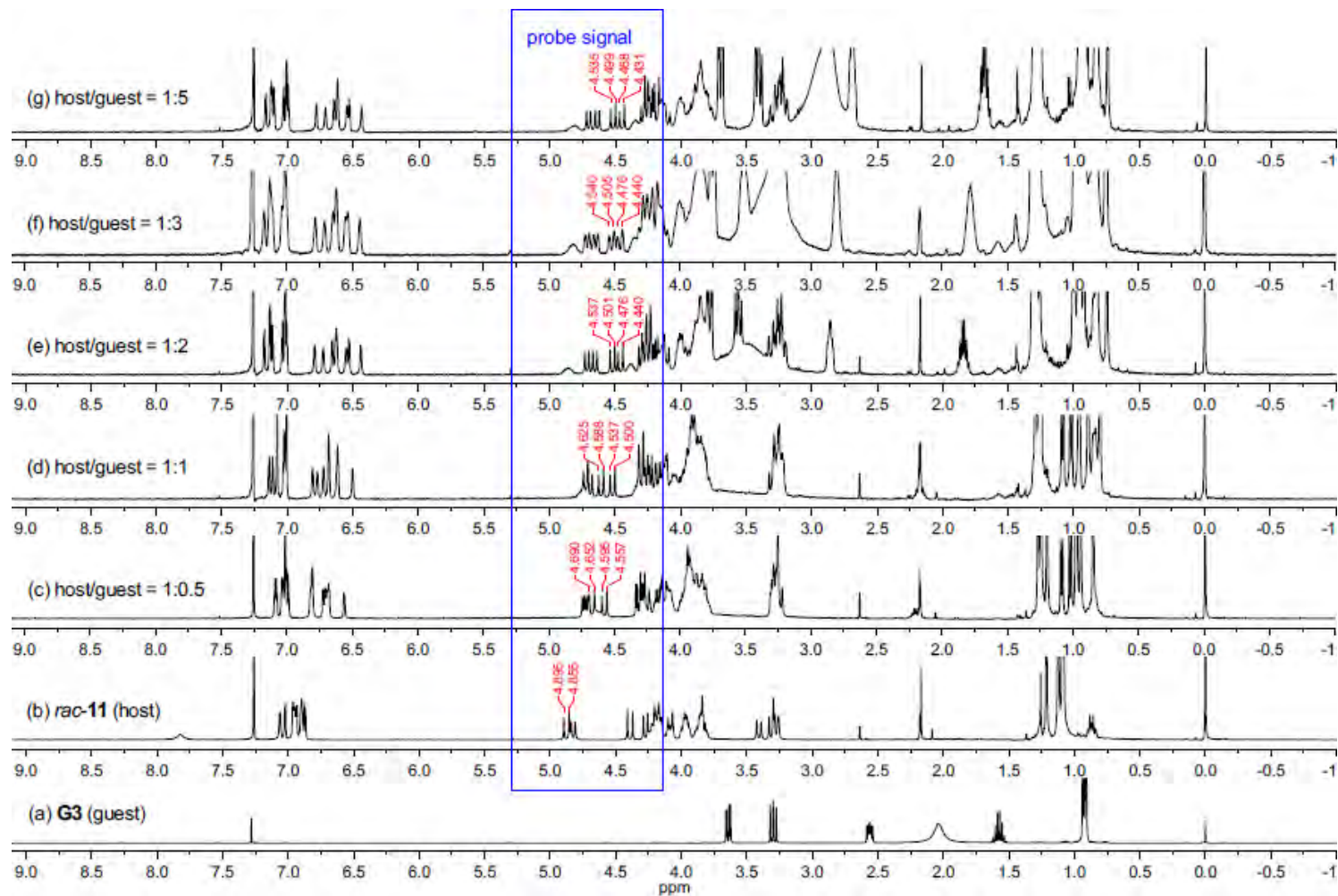


**Fig. S-48** <sup>1</sup>H NMR spectra (CDCl<sub>3</sub>, 400 MHz, 25 °C) of (±)-**12** (host, 10 mM) in the presence of increasing equivalents of (*S*)-**G3** (guest): (a) (*S*)-**G3**; (b) (±)-**12**; (c) host/guest = 1:0.5; (d) host/guest = 1:1; (e) host/guest = 1:2; (f) host/guest = 1:3; (g) host/guest = 1:5.

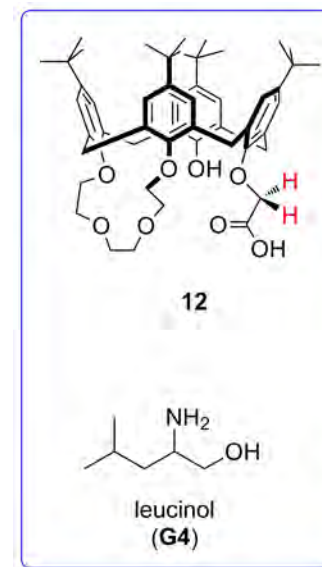
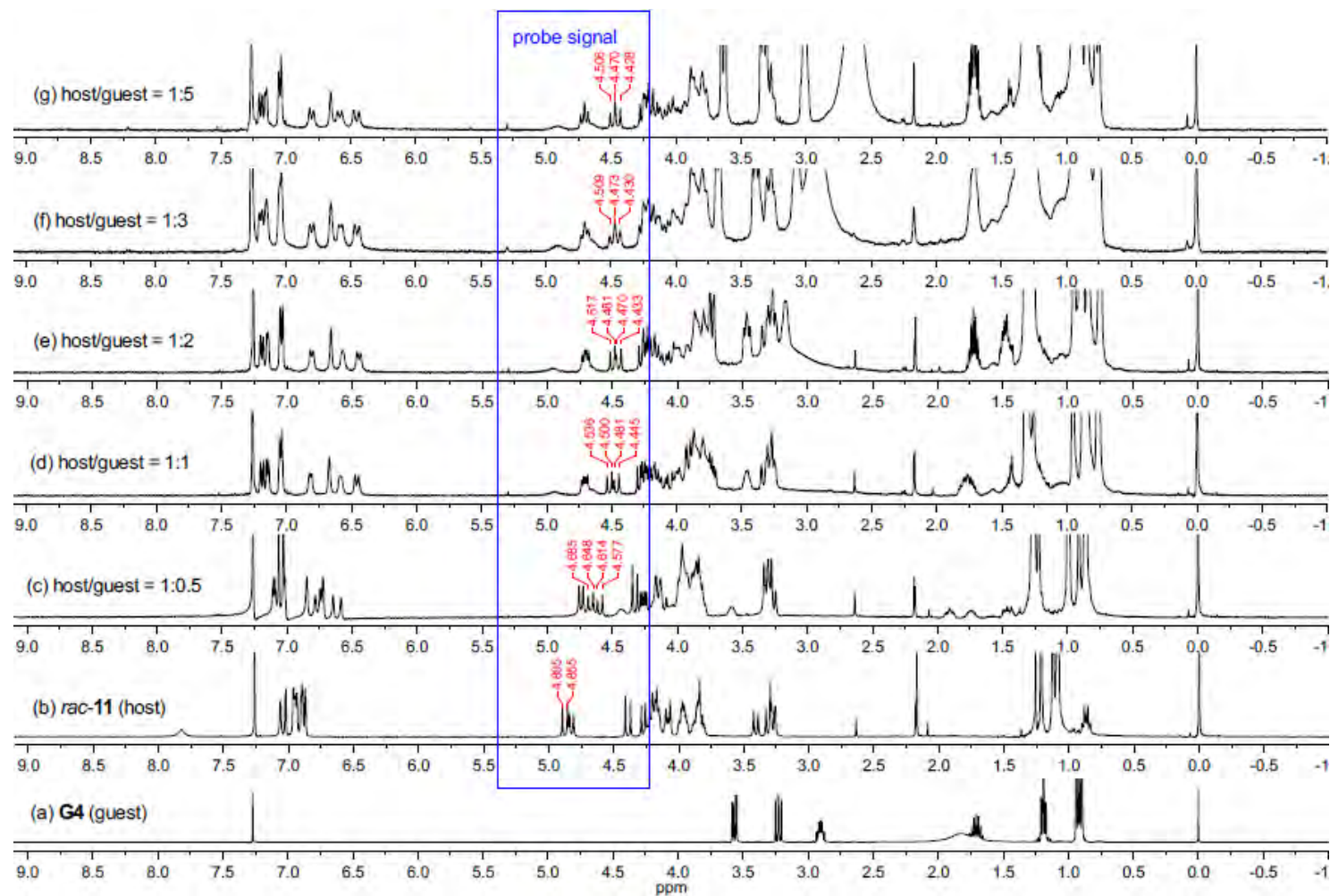


**Fig. S-49** <sup>1</sup>H NMR spectra (CDCl<sub>3</sub>, 400 MHz, 25 °C) of (±)-12 (host, 10 mM) in the presence of increasing equivalents of (*S*)-G4 (guest): (a) (*S*)-G4; (b) (±)-12; (c) host/guest = 1:0.5; (d) host/guest = 1:1; (e) host/guest = 1:2; (f) host/guest = 1:3; (g) host/guest = 1:5.

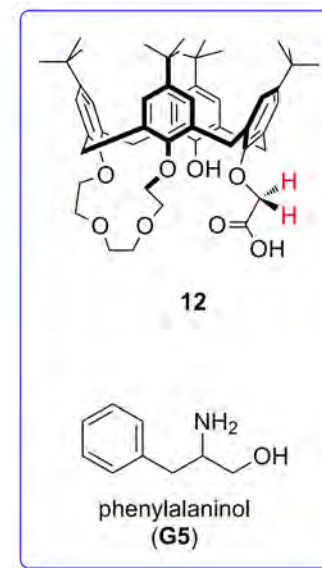
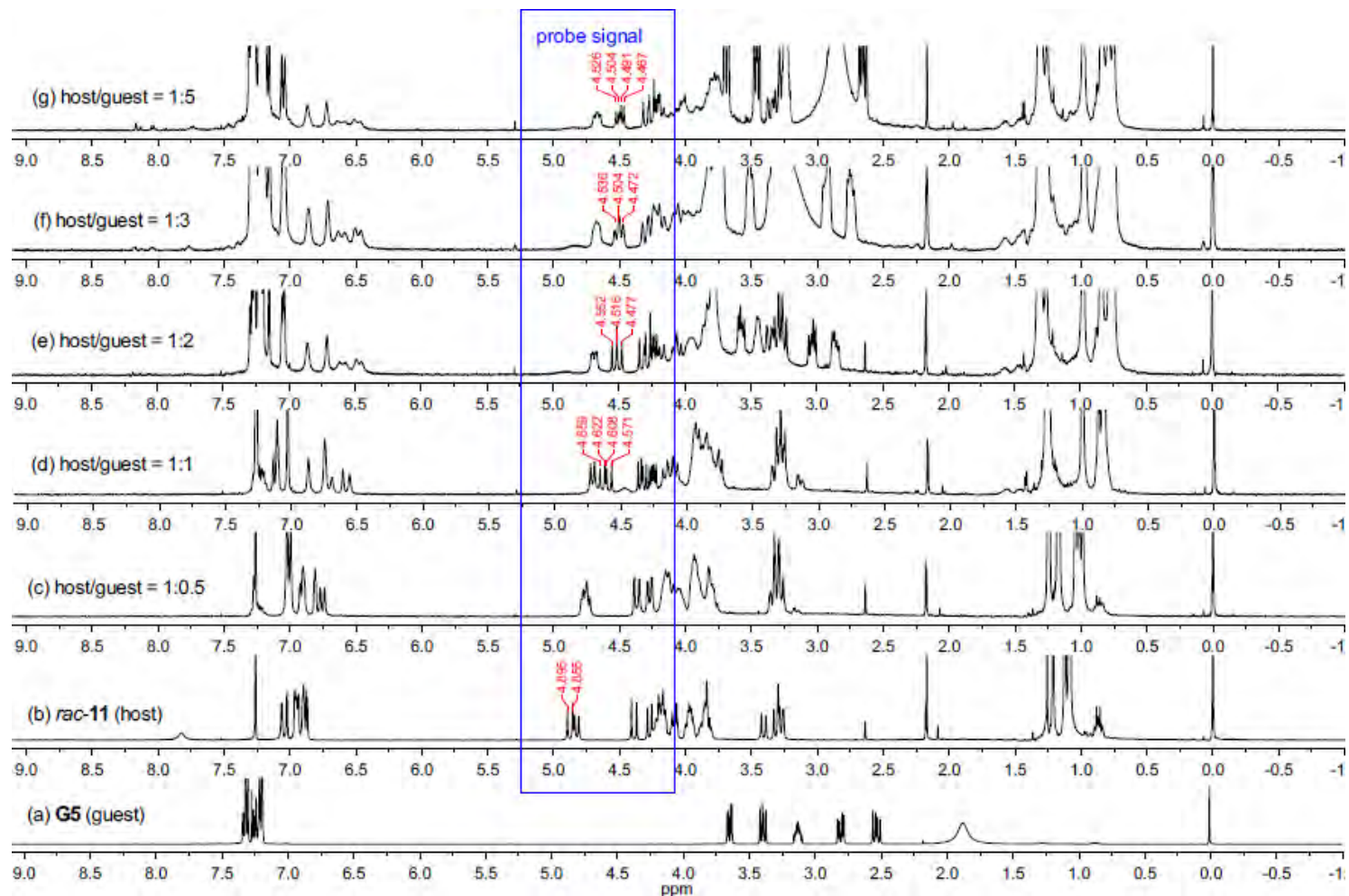


**Fig. S-50** <sup>1</sup>H NMR spectra (CDCl<sub>3</sub>, 400 MHz, 25 °C) of (±)-12 (host, 10 mM) in the presence of increasing equivalents of (S)-G5 (guest): (a) (S)-G5; (b) (±)-12; (c) host/guest = 1:0.5; (d) host/guest = 1:1; (e) host/guest = 1:2; (f) host/guest = 1:3; (g) host/guest = 1:5.



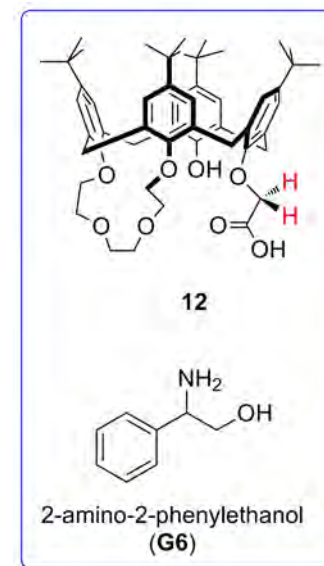
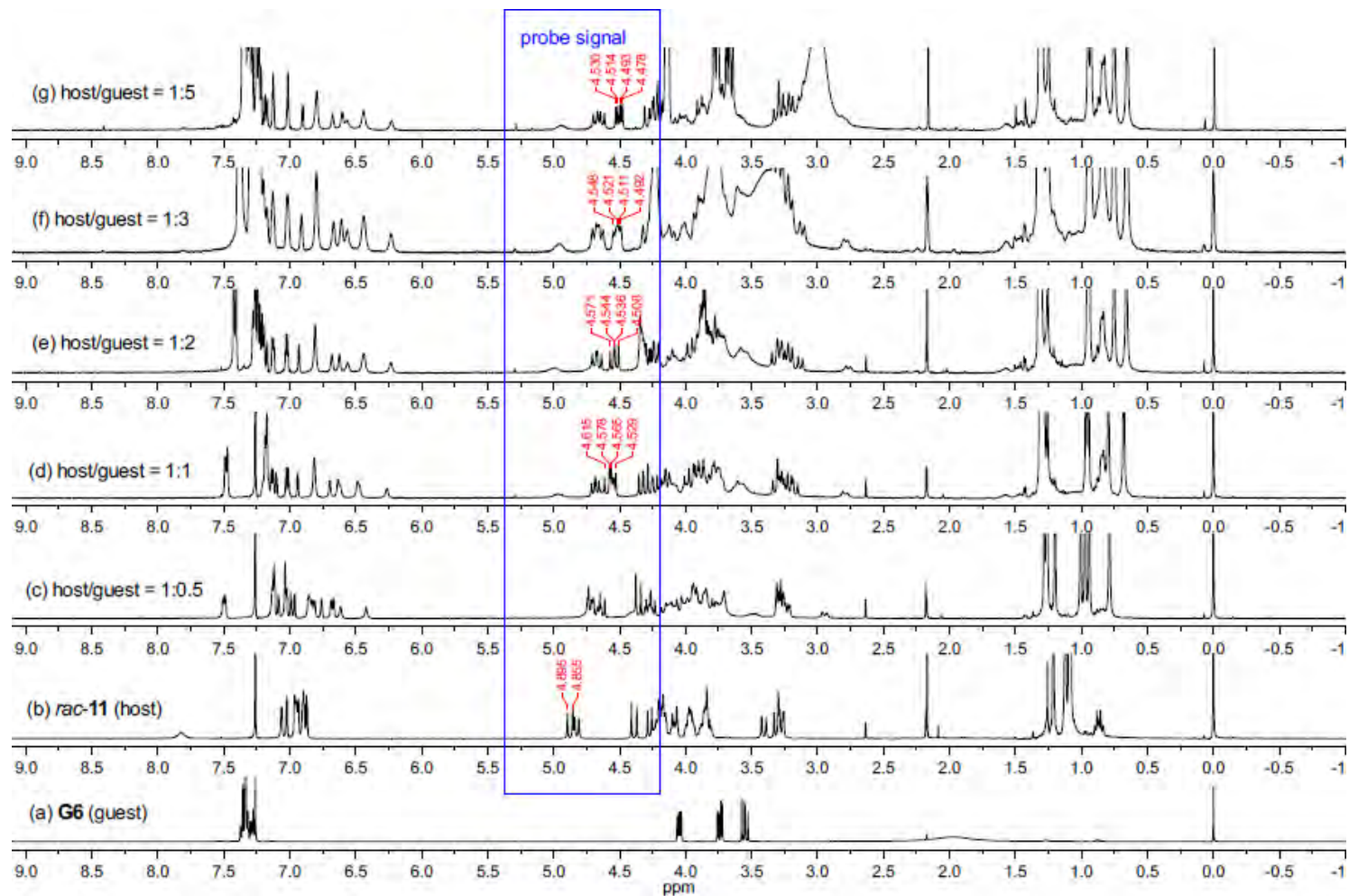


**Fig. S-51** <sup>1</sup>H NMR spectra (CDCl<sub>3</sub>, 400 MHz, 25 °C) of (±)-12 (host, 10 mM) in the presence of increasing equivalents of (*S*)-G6 (guest): (a) (*S*)-G6; (b) (±)-12; (c) host/guest = 1:0.5; (d) host/guest = 1:1; (e) host/guest = 1:2; (f) host/guest = 1:3; (g) host/guest = 1:5.

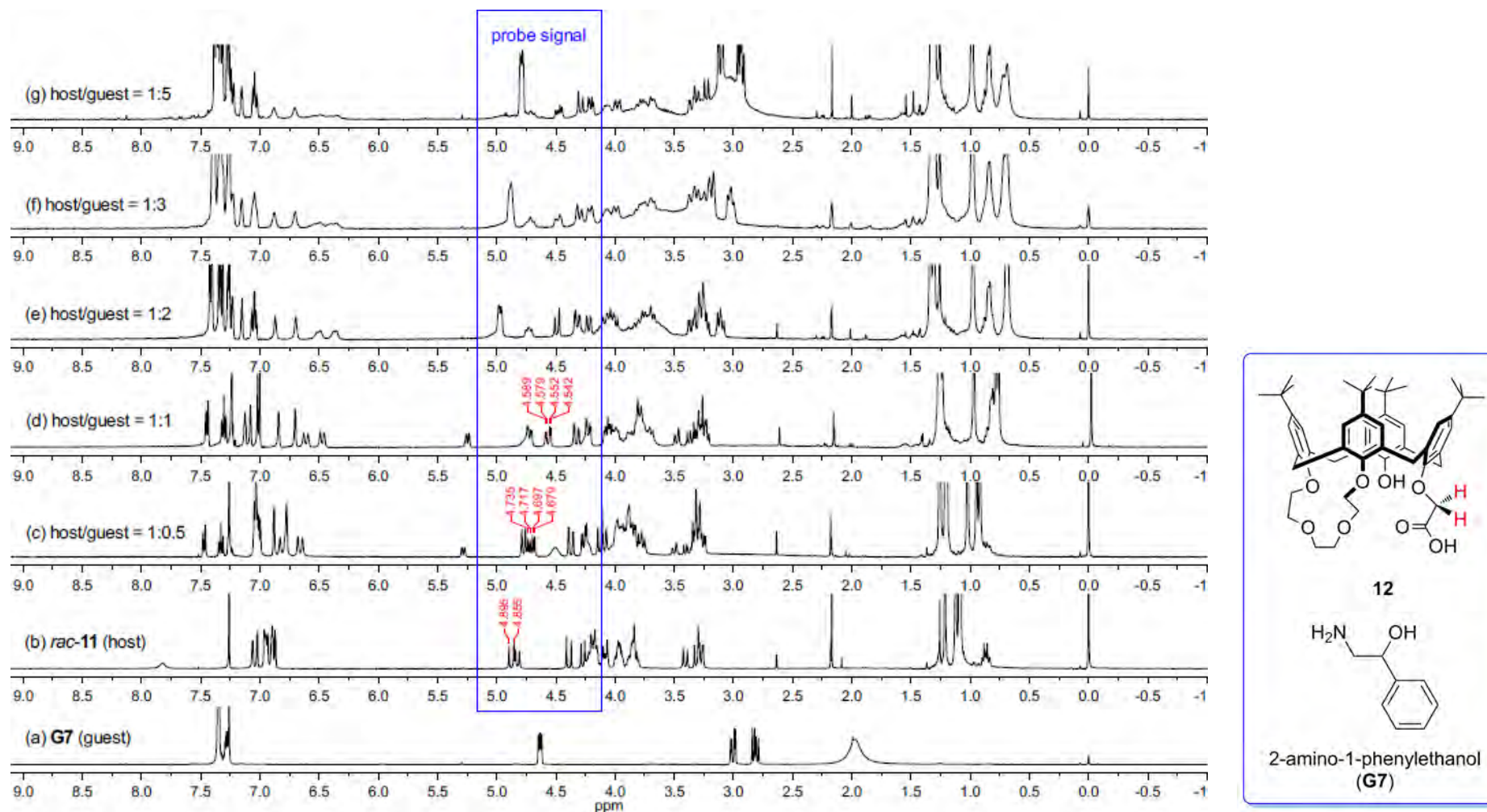


**Fig. S-52** <sup>1</sup>H NMR spectra (CDCl<sub>3</sub>, 400 MHz, 25 °C) of (±)-**12** (host, 10 mM) in the presence of increasing equivalents of (*R*)-**G7** (guest): (a) (*R*)-**G7**; (b) (±)-**12**; (c) host/guest = 1:0.5; (d) host/guest = 1:1; (e) host/guest = 1:2; (f) host/guest = 1:3; (g) host/guest = 1:5.

### C-6. $^1\text{H}$ NMR titration of ( $\pm$ )-**13** with **G1**–**G7**:

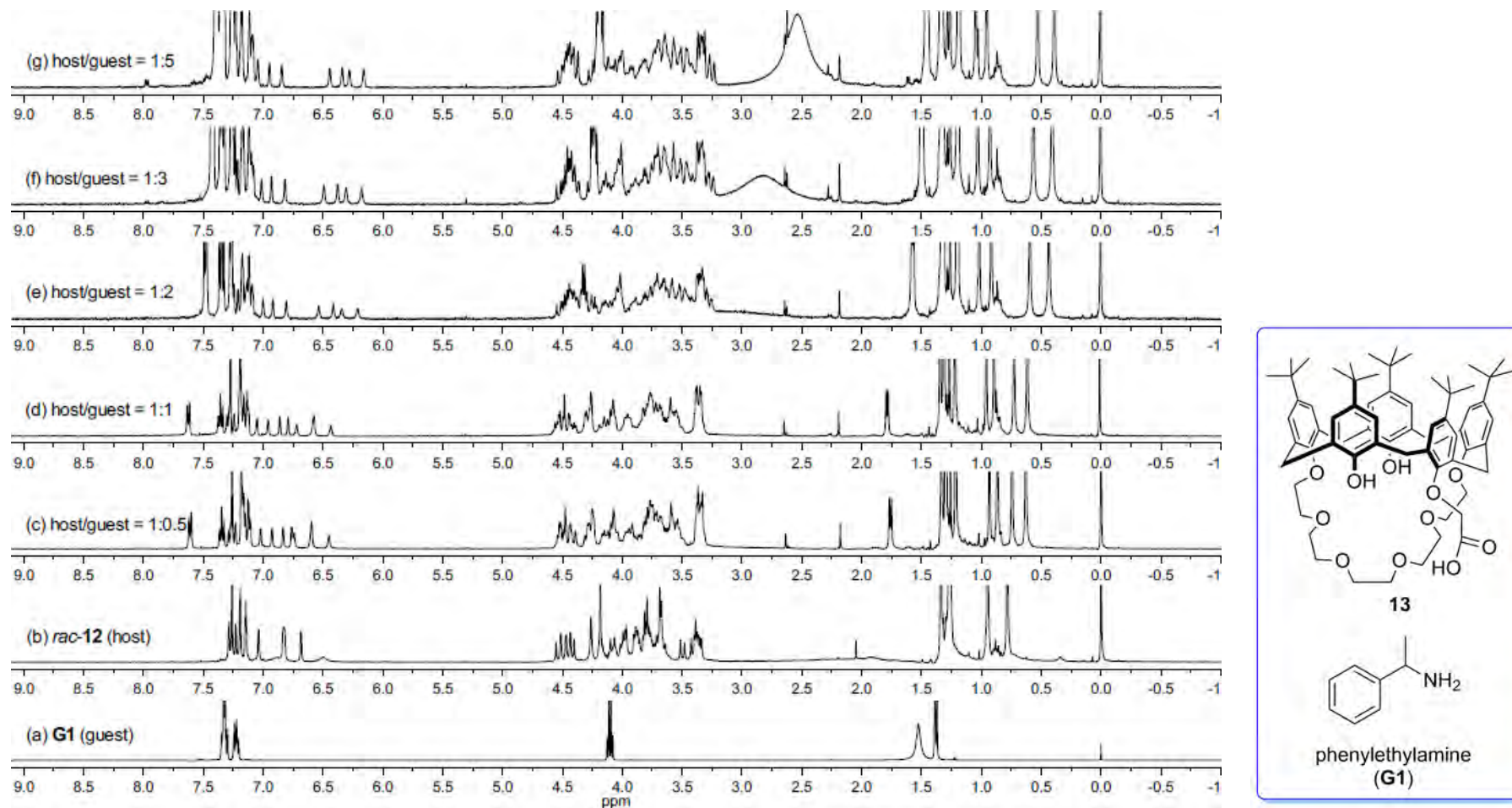


**Fig. S-53**  $^1\text{H}$  NMR spectra ( $\text{CDCl}_3$ , 400 MHz, 25 °C) of ( $\pm$ )-**13** (host, 10 mM) in the presence of increasing equivalents of (*R*)-**G1** (guest): (a) (*R*)-**G1**; (b) ( $\pm$ )-**13**; (c) host/guest = 1:0.5; (d) host/guest = 1:1; (e) host/guest = 1:2; (f) host/guest = 1:3; (g) host/guest = 1:5.

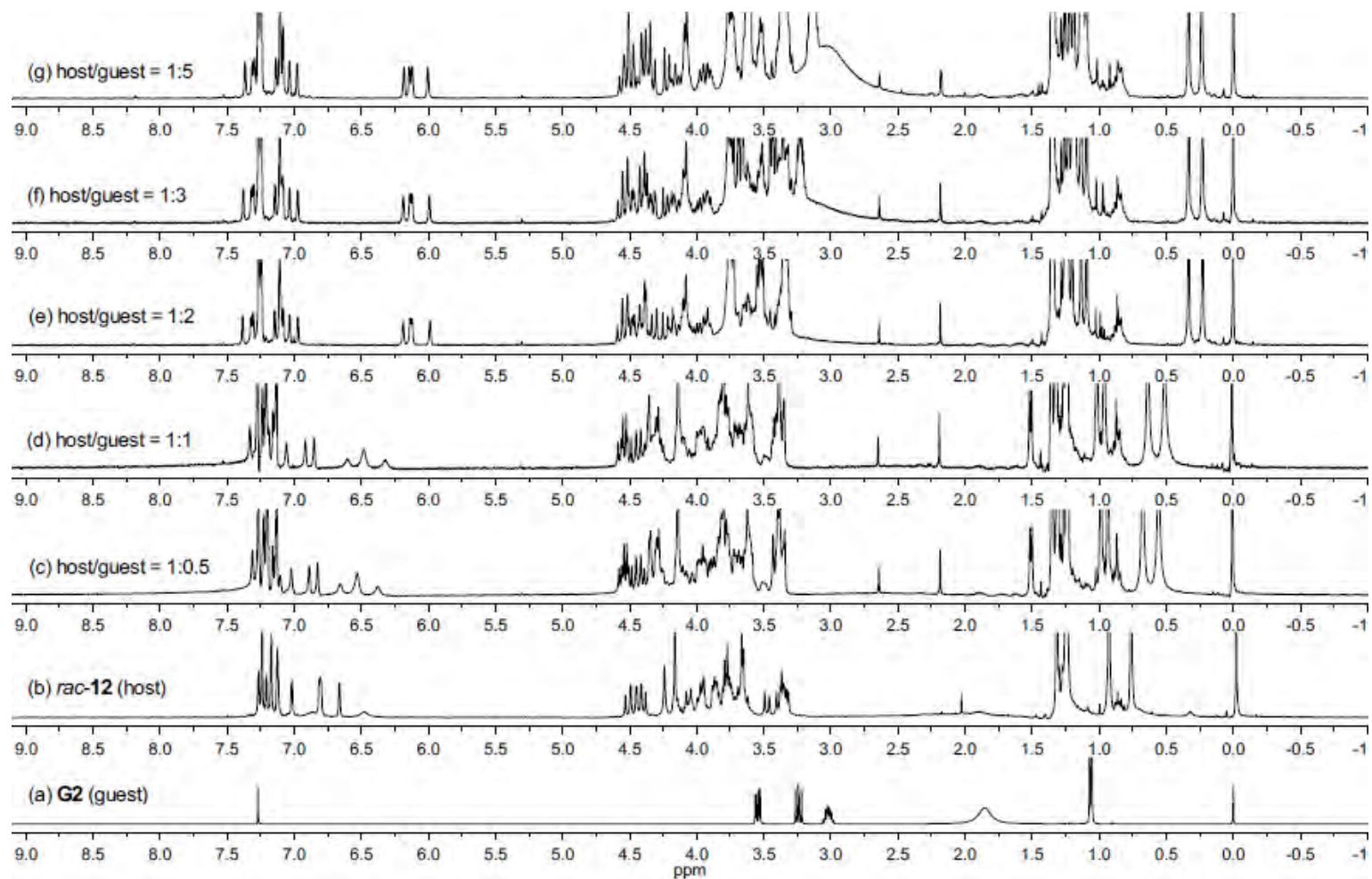


**Fig. S-54** <sup>1</sup>H NMR spectra (CDCl<sub>3</sub>, 400 MHz, 25 °C) of (±)-**13** (host, 10 mM) in the presence of increasing equivalents of (*S*)-**G2** (guest): (a) (*S*)-**G2**; (b) (±)-**13**; (c) host/guest = 1:0.5; (d) host/guest = 1:1; (e) host/guest = 1:2; (f) host/guest = 1:3; (g) host/guest = 1:5.

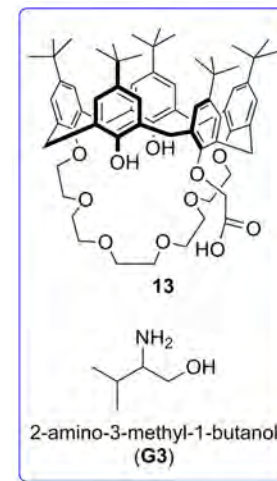
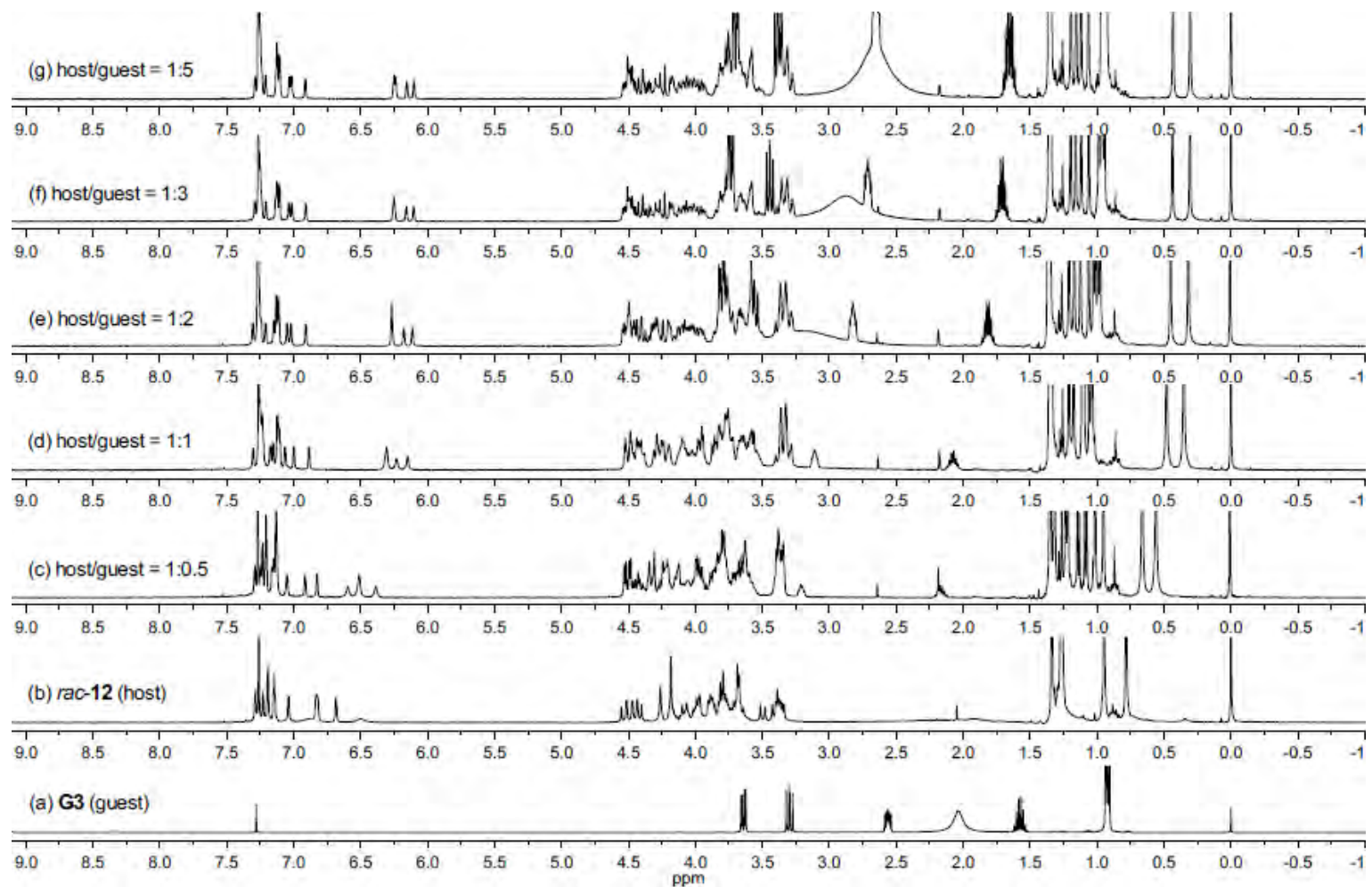


**Fig. S-55** <sup>1</sup>H NMR spectra (CDCl<sub>3</sub>, 400 MHz, 25 °C) of (±)-**13** (host, 10 mM) in the presence of increasing equivalents of (*S*)-**G3** (guest): (a) (*S*)-**G3**; (b) (±)-**13**; (c) host/guest = 1:0.5; (d) host/guest = 1:1; (e) host/guest = 1:2; (f) host/guest = 1:3; (g) host/guest = 1:5.

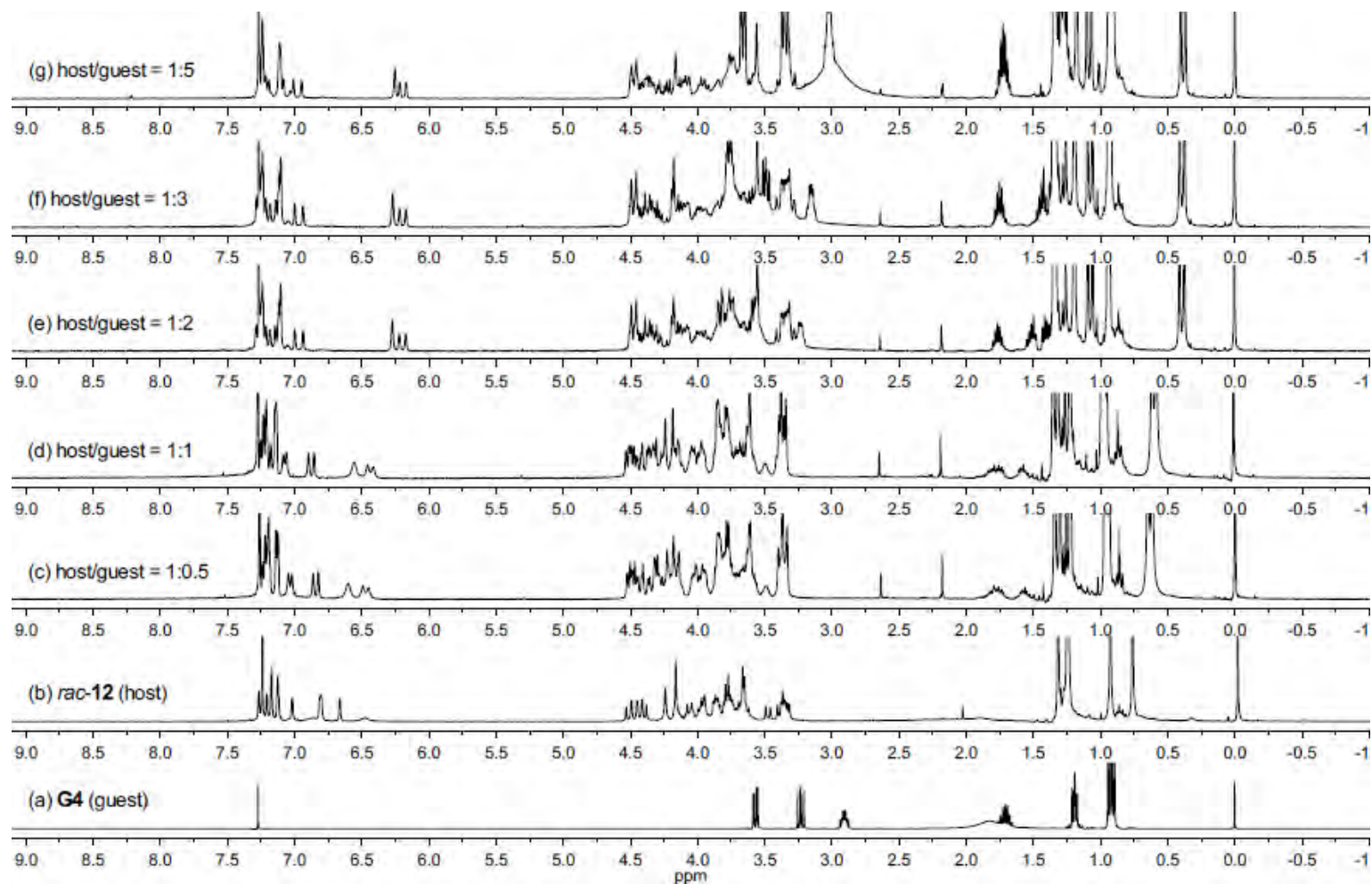


**Fig. S-56** <sup>1</sup>H NMR spectra (CDCl<sub>3</sub>, 400 MHz, 25 °C) of (±)-**13** (host, 10 mM) in the presence of increasing equivalents of (*S*)-**G4** (guest): (a) (*S*)-**G4**; (b) (±)-**13**; (c) host/guest = 1:0.5; (d) host/guest = 1:1; (e) host/guest = 1:2; (f) host/guest = 1:3; (g) host/guest = 1:5.

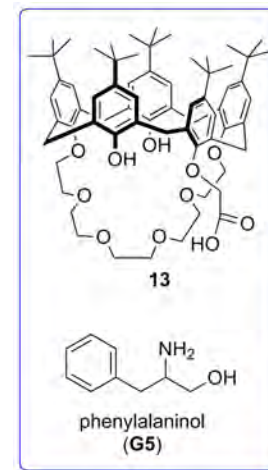
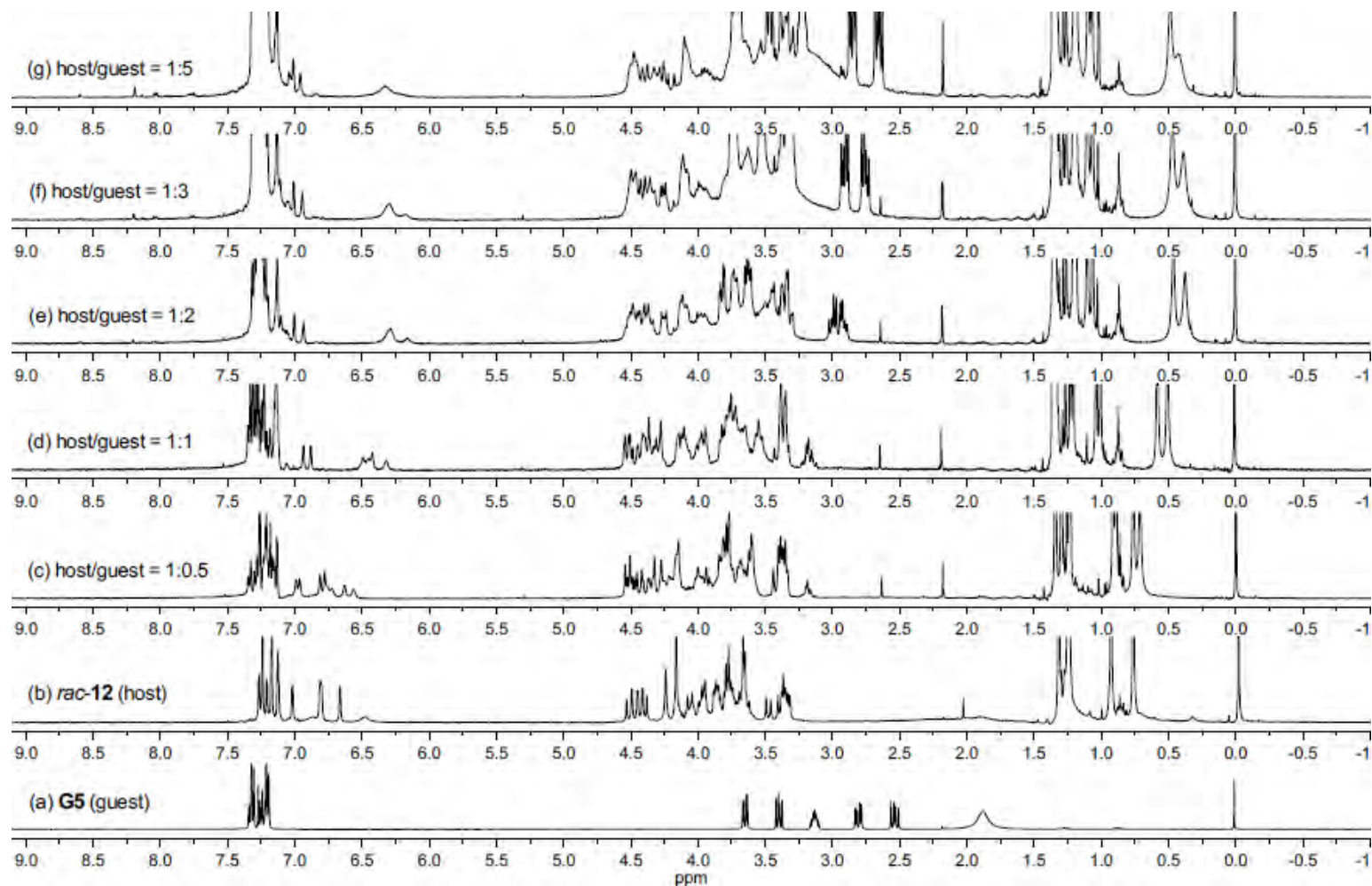


**Fig. S-57** <sup>1</sup>H NMR spectra (CDCl<sub>3</sub>, 400 MHz, 25 °C) of (±)-**13** (host, 10 mM) in the presence of increasing equivalents of (*S*)-**G5** (guest): (a) (*S*)-**G5**; (b) (±)-**13**; (c) host/guest = 1:0.5; (d) host/guest = 1:1; (e) host/guest = 1:2; (f) host/guest = 1:3; (g) host/guest = 1:5.

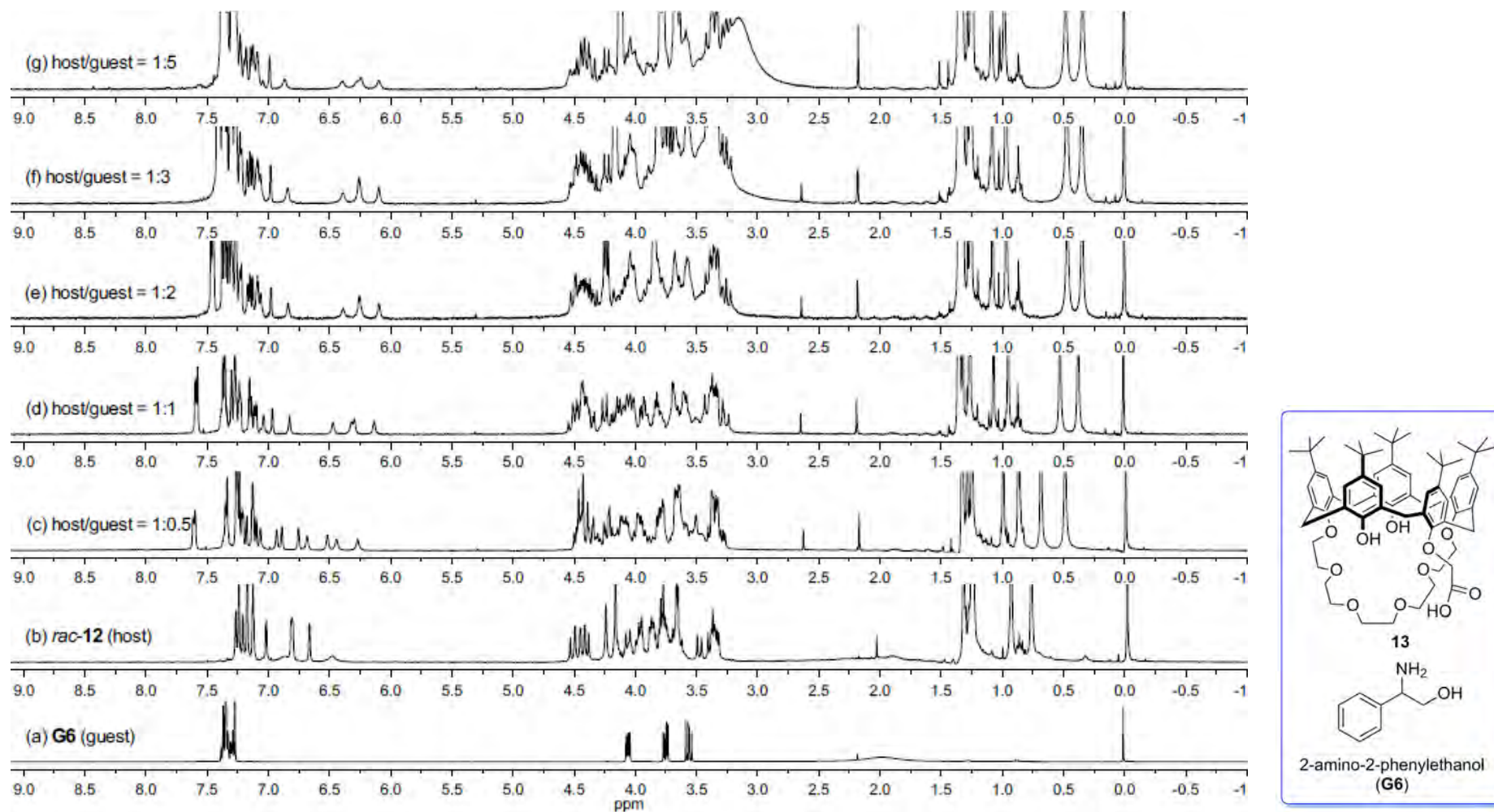


**Fig. S-58** <sup>1</sup>H NMR spectra (CDCl<sub>3</sub>, 400 MHz, 25 °C) of (±)-**13** (host, 10 mM) in the presence of increasing equivalents of (*S*)-**G6** (guest): (a) (*S*)-**G6**; (b) (±)-**13**; (c) host/guest = 1:0.5; (d) host/guest = 1:1; (e) host/guest = 1:2; (f) host/guest = 1:3; (g) host/guest = 1:5.



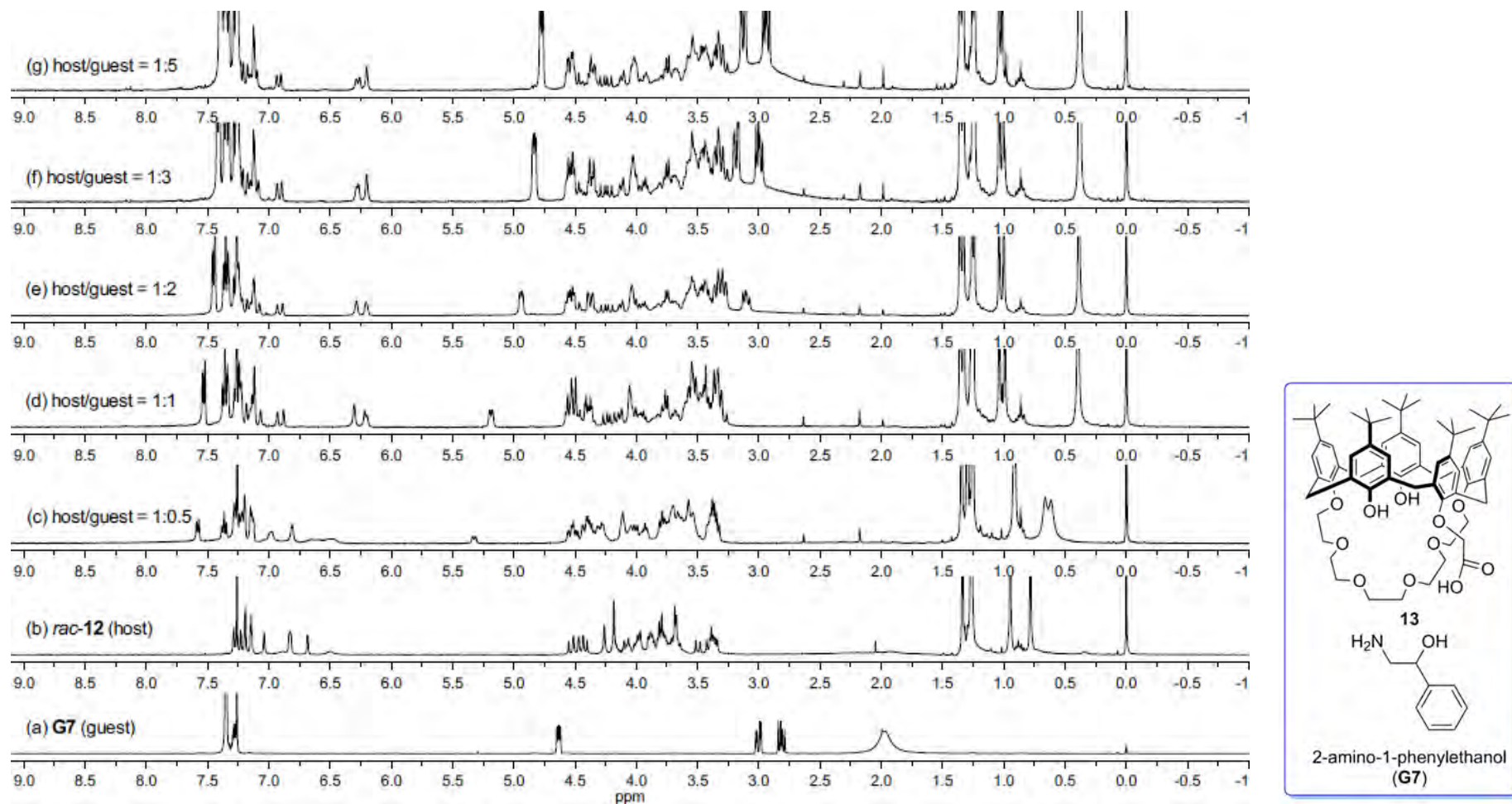


**Fig. S-59** <sup>1</sup>H NMR spectra (CDCl<sub>3</sub>, 400 MHz, 25 °C) of (±)-13 (host, 10 mM) in the presence of increasing equivalents of (*R*)-G7 (guest): (a) (*R*)-G7; (b) (±)-13; (c) host/guest = 1:0.5; (d) host/guest = 1:1; (e) host/guest = 1:2; (f) host/guest = 1:3; (g) host/guest = 1:5.

## Part D. Chiral recognition of enantiopure 10

### D-1. Job plot: (+)-(cS)-10 complexed with (S)- or (R)-G3:

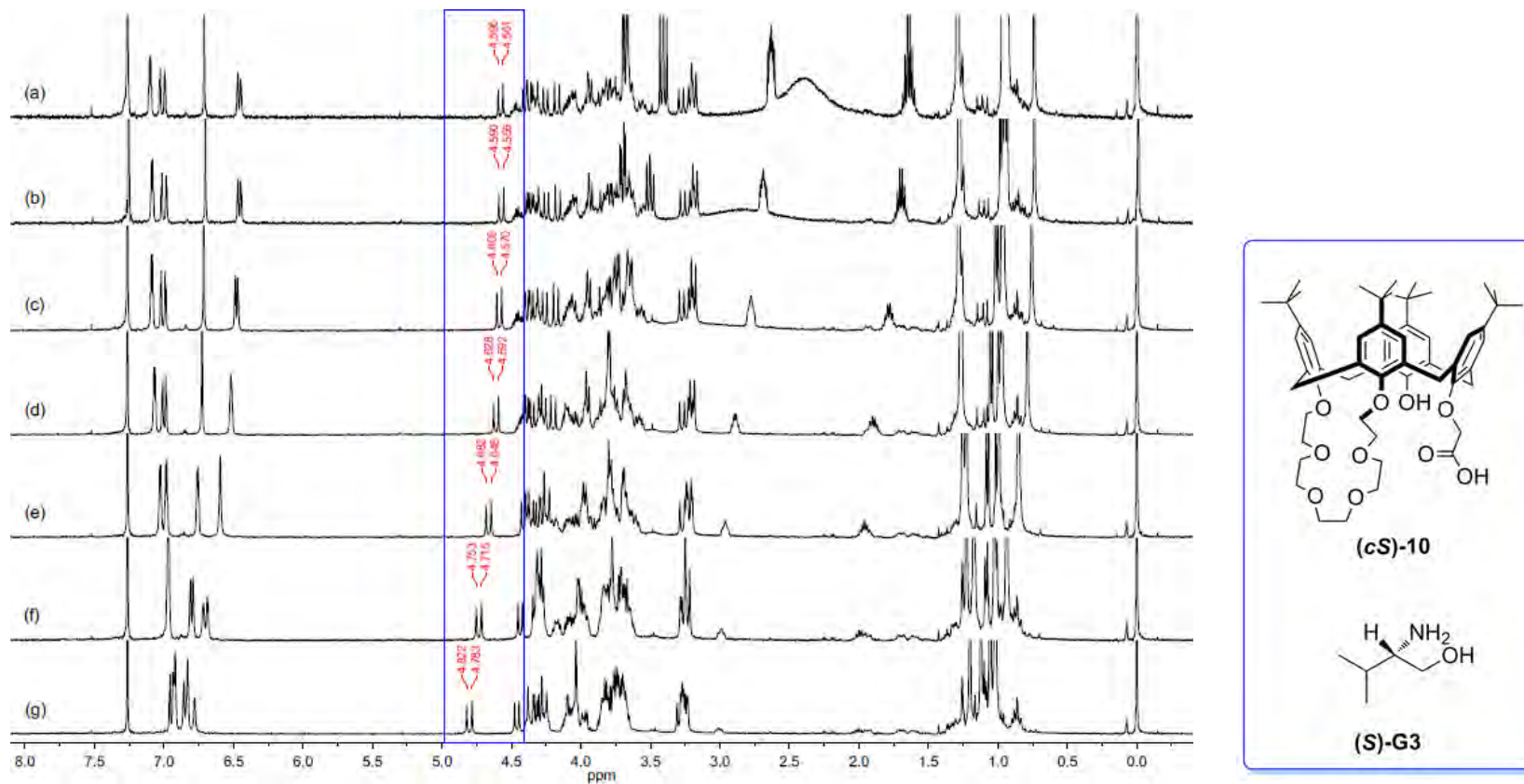


**Fig. S-60**  $^1\text{H}$  NMR spectra ( $\text{CDCl}_3$ , 400 MHz, 25 °C) recorded for Job plot for determination of the stoichiometric ratio of (+)-(cS)-10 complexed with (S)-G3. The total concentration of (+)-(cS)-10 and (S)-G3 was kept constant (10 mM, in  $\text{CDCl}_3$ ), while the molar fraction of the host (X) was continuously varied. X = (a) 20%; (b) 30%; (c) 40%; (d) 50%; (e) 60%; (f) 70%; (g) 80%.

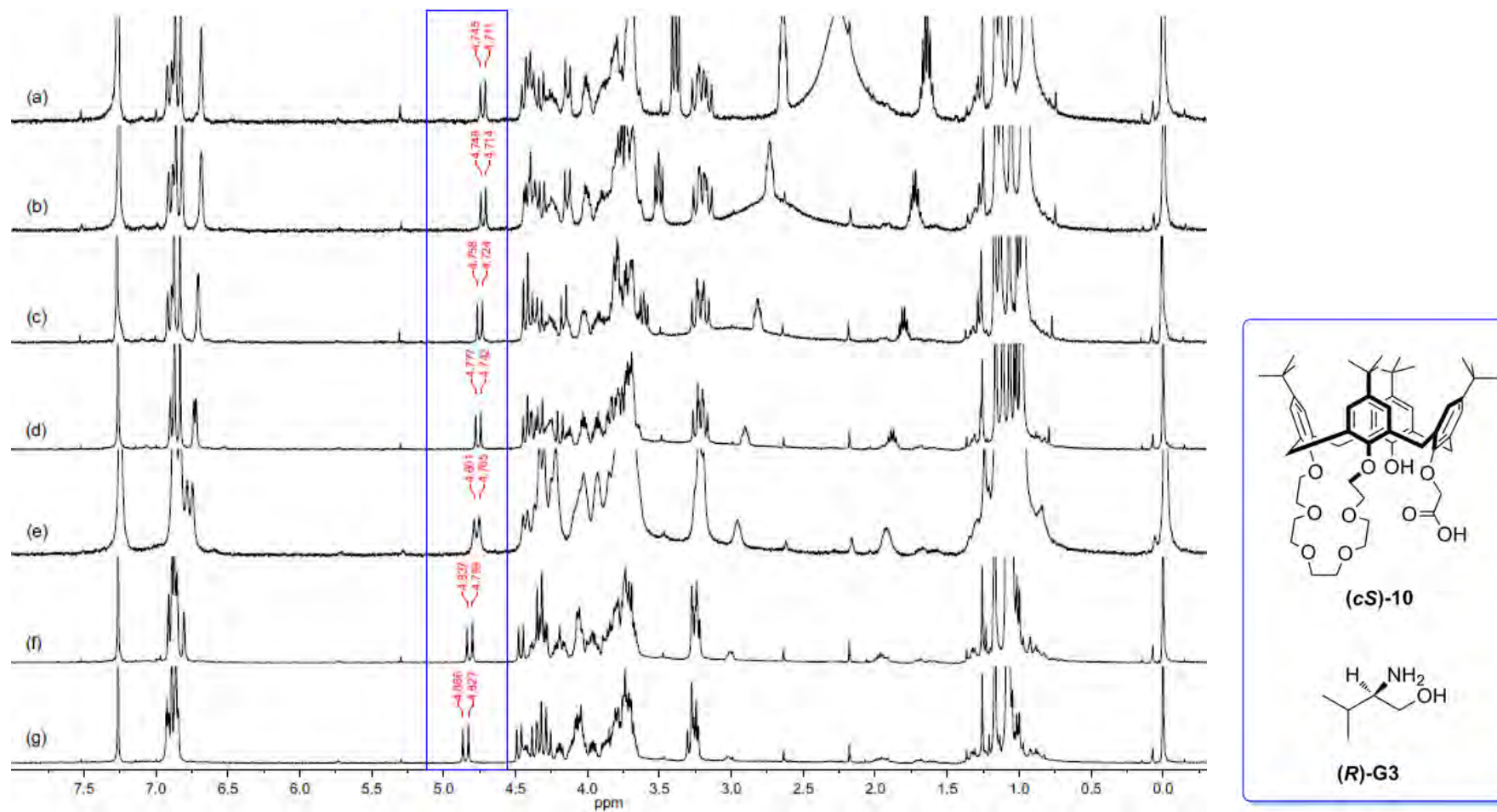


**Fig. S-61**  $^1\text{H}$  NMR spectra ( $\text{CDCl}_3$ , 400 MHz, 25 °C) recorded for Job plot for determination of the stoichiometric ratio of (+)-(cS)-10 complexed with (R)-G3. The total concentration of (+)-(cS)-10 and (R)-G3 was kept constant (10 mM, in  $\text{CDCl}_3$ ), while the molar fraction of the host (X) was continuously varied. X = (a) 20%; (b) 30%; (c) 40%; (d) 50%; (e) 60%; (f) 70%; (g) 80%.

**D-2. Job plot: (-)-(cR)-10 complexed with (S)- or (R)-G6:**

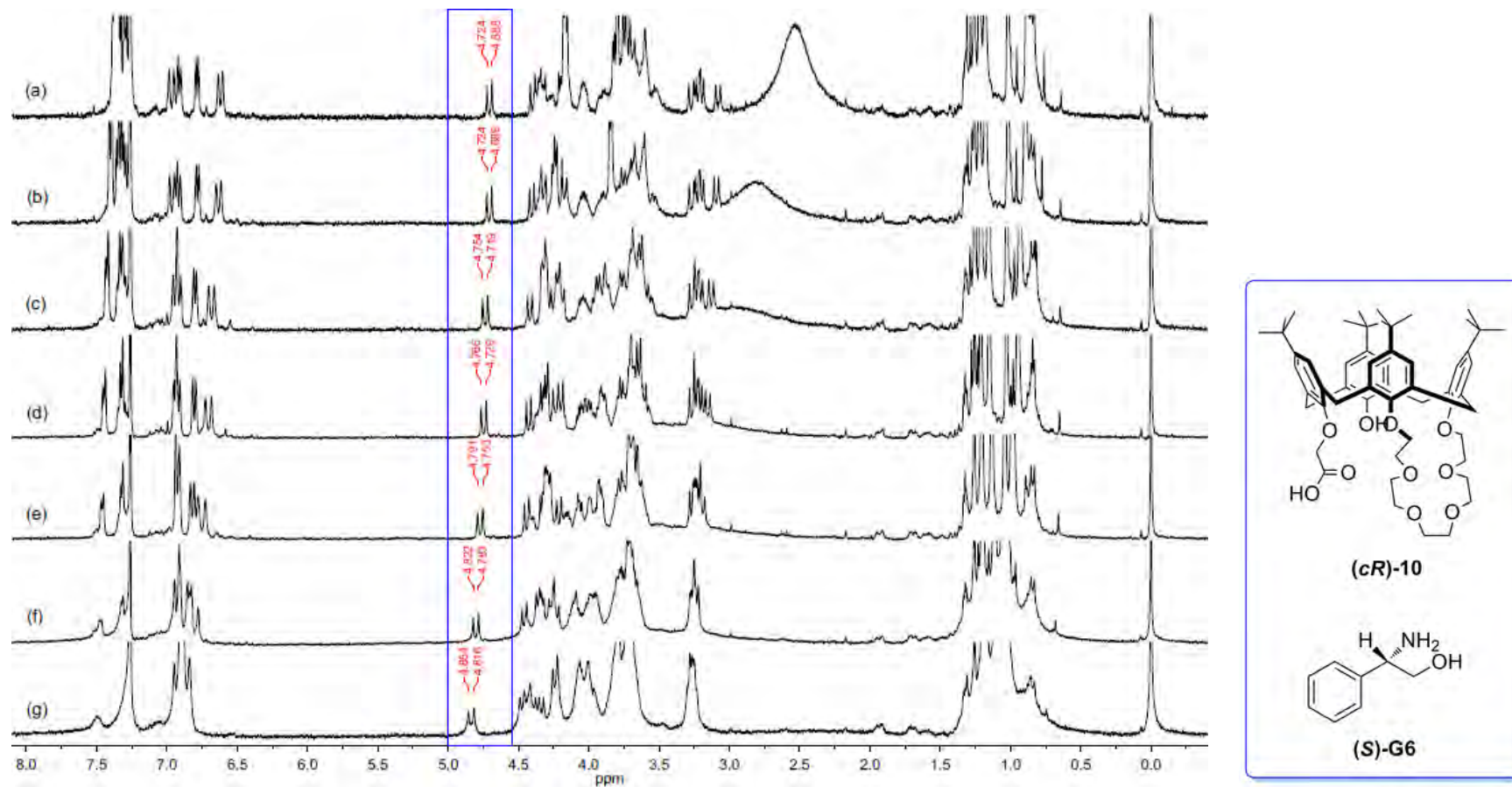


**Fig. S-62**  $^1\text{H}$  NMR spectra ( $\text{CDCl}_3$ , 400 MHz, 25 °C) recorded for Job plot for determination of the stoichiometric ratio of (-)-(cR)-10 complexed with (S)-G6. The total concentration of (-)-(cR)-10 and (S)-G6 was kept constant (10 mM, in  $\text{CDCl}_3$ ), while the molar fraction of the host (X) was continuously varied. X = (a) 20%; (b) 30%; (c) 40%; (d) 50%; (e) 60%; (f) 70%; (g) 80%.

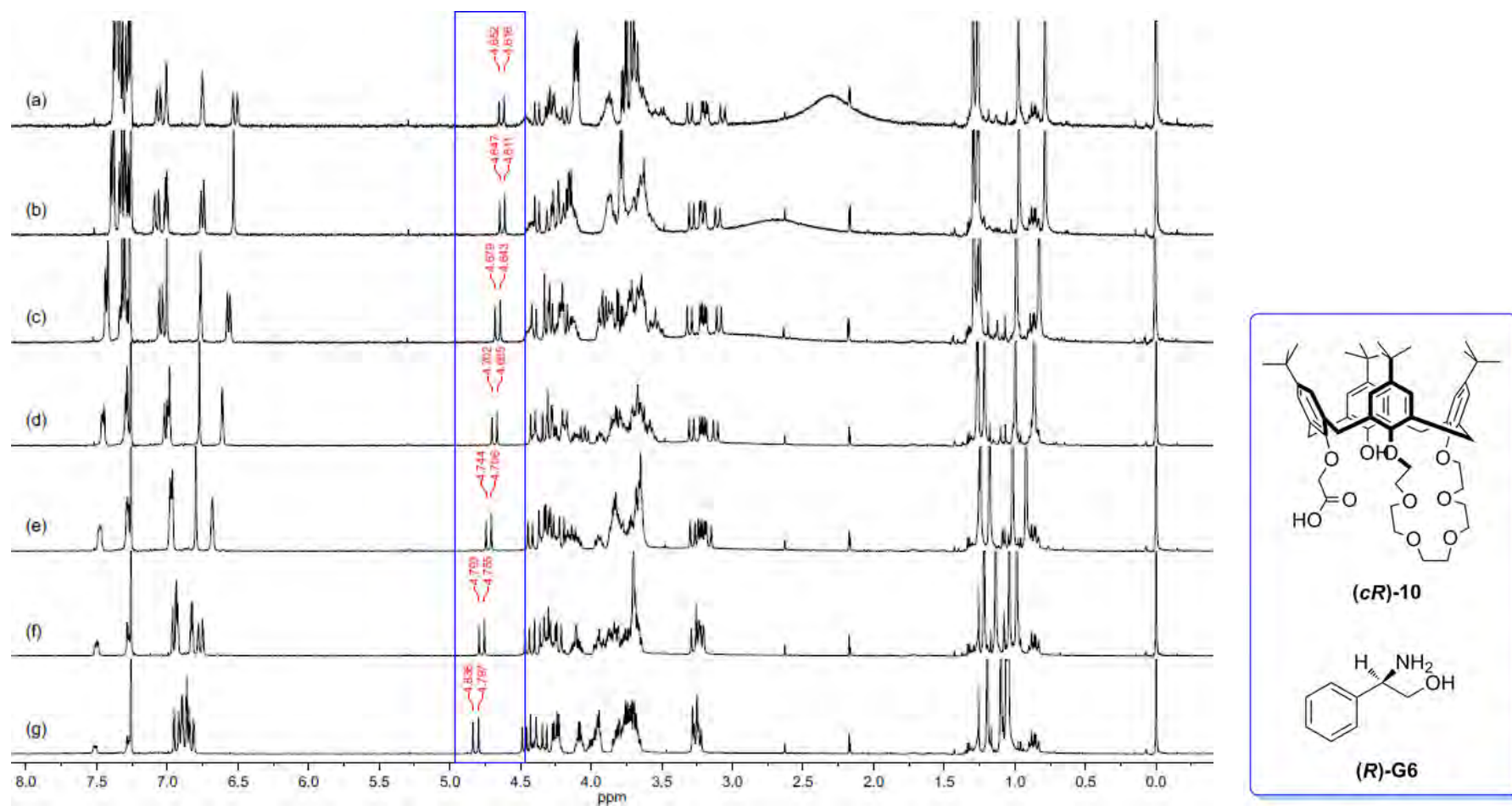


**Fig. S-63**  $^1\text{H}$  NMR spectra ( $\text{CDCl}_3$ , 400 MHz, 25  $^\circ\text{C}$ ) recorded for Job plot for determination of the stoichiometric ratio of  $(-)(cR)\text{-10}$  complexed with  $(R)\text{-G6}$ . The total concentration of  $(-)(cR)\text{-10}$  and  $(R)\text{-G6}$  was kept constant (10 mM, in  $\text{CDCl}_3$ ), while the molar fraction of the host (X) was continuously varied. X = (a) 20%; (b) 30%; (c) 40%; (d) 50%; (e) 60%; (f) 70%; (g) 80%.

### D-3. $^1\text{H}$ NMR titration and calculation of the association constants by nonlinear curve fitting method:

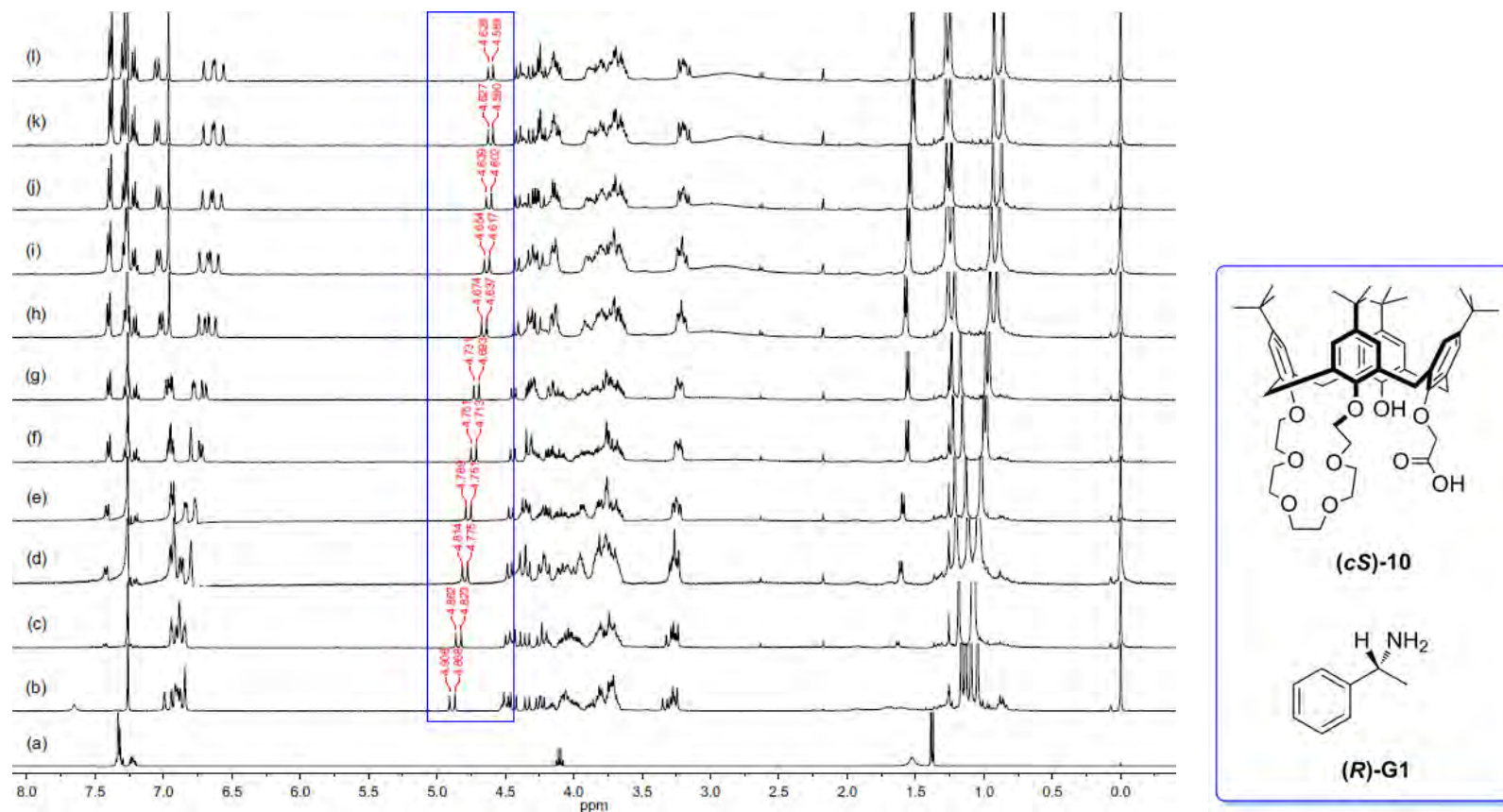


**Fig. S-64**  $^1\text{H}$  NMR spectra ( $\text{CDCl}_3$ , 400 MHz, 25 °C) of a constant concentration of (+)- $(cS)\text{-10}$  (5 mM) in the presence of increasing equivalents of specific guest: (a)  $(R)\text{-G1}$ ; (b) (+)- $(cS)\text{-10}$ ; (c) upon addition of 0.2 equiv of  $(R)\text{-G1}$ ; (d) upon addition of 0.4 equiv of  $(R)\text{-G1}$ ; (e) upon addition of 0.6 equiv of  $(R)\text{-G1}$ ; (f) upon addition of 0.8 equiv of  $(R)\text{-G1}$ ; (g) upon addition of 1.0 equiv of  $(R)\text{-G1}$ ; (h) upon addition of 1.2 equiv of  $(R)\text{-G1}$ ; (i) upon addition of 1.4 equiv of  $(R)\text{-G1}$ ; (j) upon addition of 1.6 equiv of  $(R)\text{-G1}$ ; (k) upon addition of 1.8 equiv of  $(R)\text{-G1}$ ; (l) upon addition of 2.0 equiv of  $(R)\text{-G1}$ .

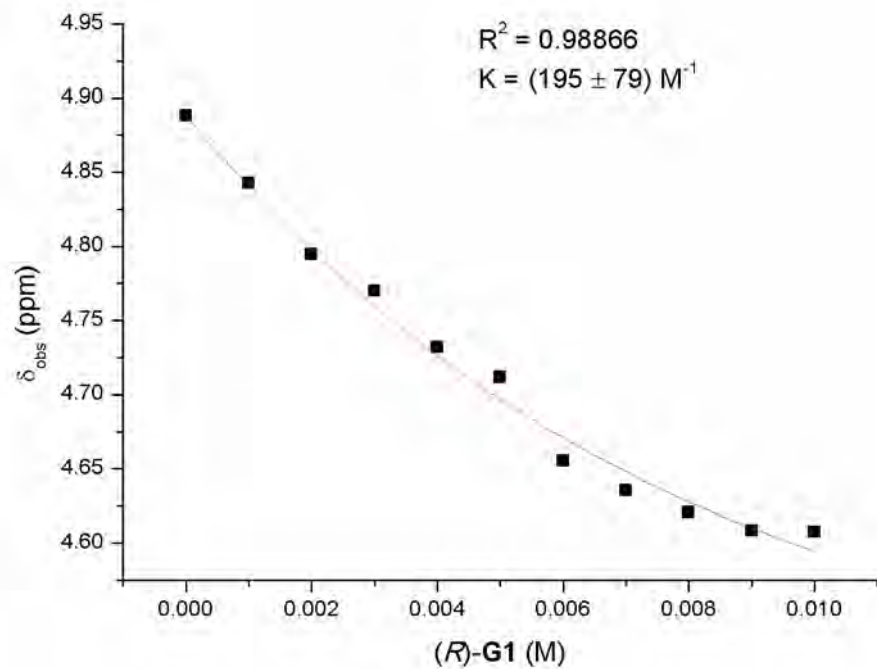


**Fig. S-65** The observed chemical shift changes of (+)-(cS)-**10** (5.0 mM) upon addition of (R)-**G1** (0–10.0 mM). The red solid line was obtained from nonlinear curve-fitting.

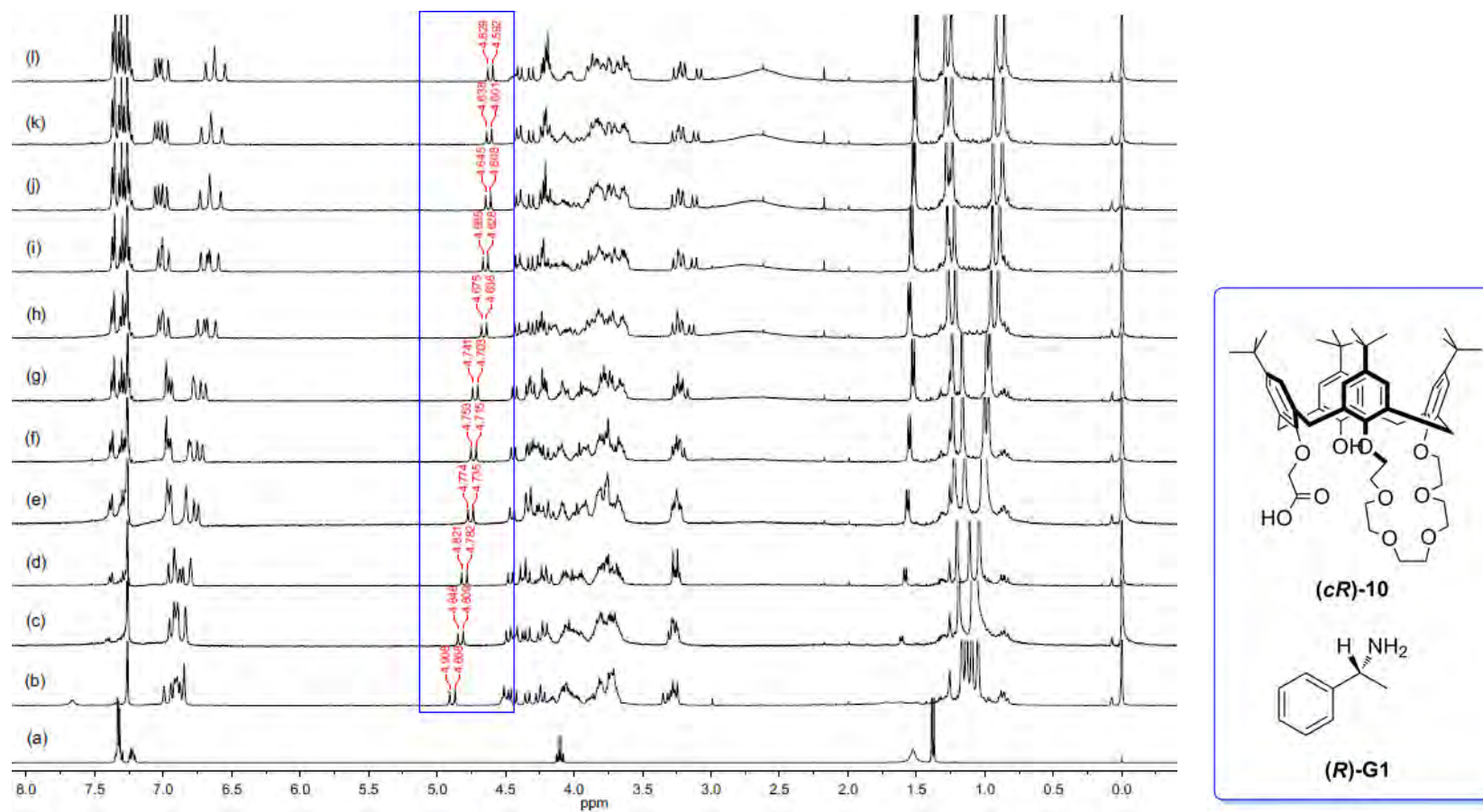


**Fig. S-66**  $^1\text{H}$  NMR spectra ( $\text{CDCl}_3$ , 400 MHz, 25 °C) of a constant concentration of (-)-(*cR*)-**10** (5 mM) in the presence of increasing equivalents of specific guest: (a) (*R*)-**G1**; (b) (-)-(*cR*)-**10**; (c) upon addition of 0.2 equiv of (*R*)-**G1**; (d) upon addition of 0.4 equiv of (*R*)-**G1**; (e) upon addition of 0.6 equiv of (*R*)-**G1**; (f) upon addition of 0.8 equiv of (*R*)-**G1**; (g) upon addition of 1.0 equiv of (*R*)-**G1**; (h) upon addition of 1.2 equiv of (*R*)-**G1**; (i) upon addition of 1.4 equiv of (*R*)-**G1**; (j) upon addition of 1.6 equiv of (*R*)-**G1**; (k) upon addition of 1.8 equiv of (*R*)-**G1**; (l) upon addition of 2.0 equiv of (*R*)-**G1**.



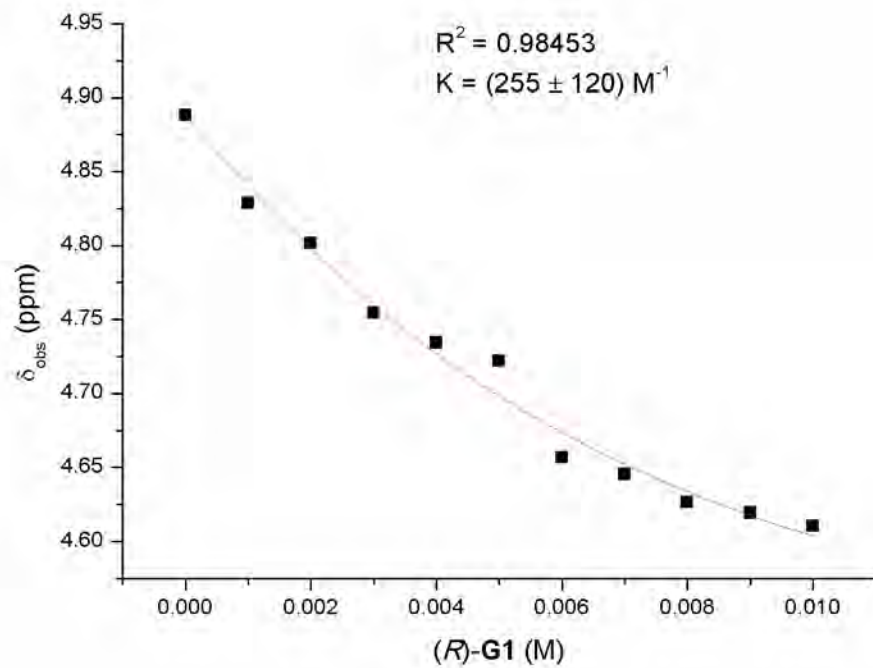


**Fig. S-67** The observed chemical shift changes of (-)-(cR)-**10** (5.0 mM) upon addition of (R)-**G1** (0–10.0 mM). The red solid line was obtained from nonlinear curve-fitting.



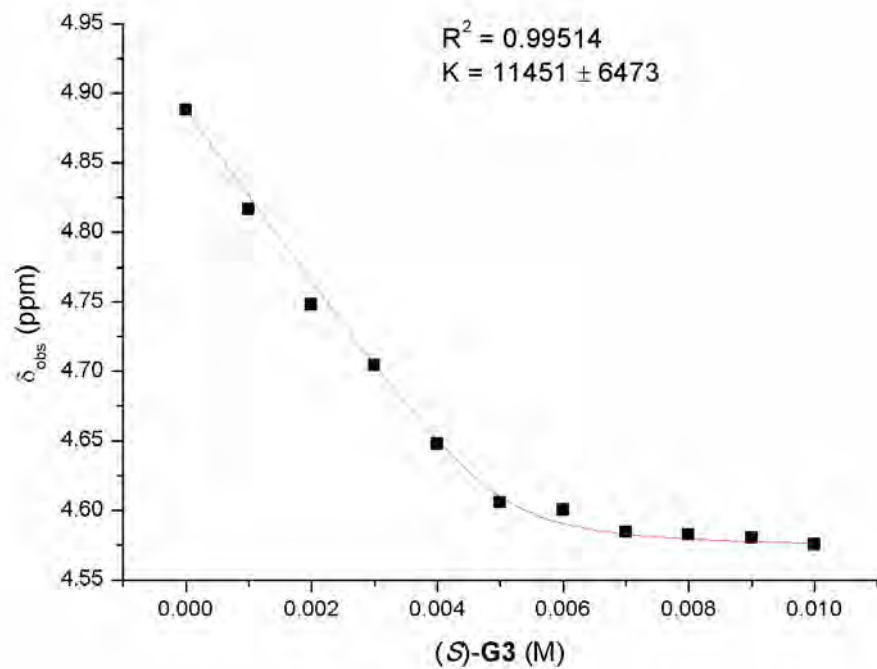


**Fig. S-69** The observed chemical shift changes of (+)-(cS)-**10** (5.0 mM) upon addition of (S)-**G3** (0–10.0 mM). The red solid line was obtained from nonlinear curve-fitting.

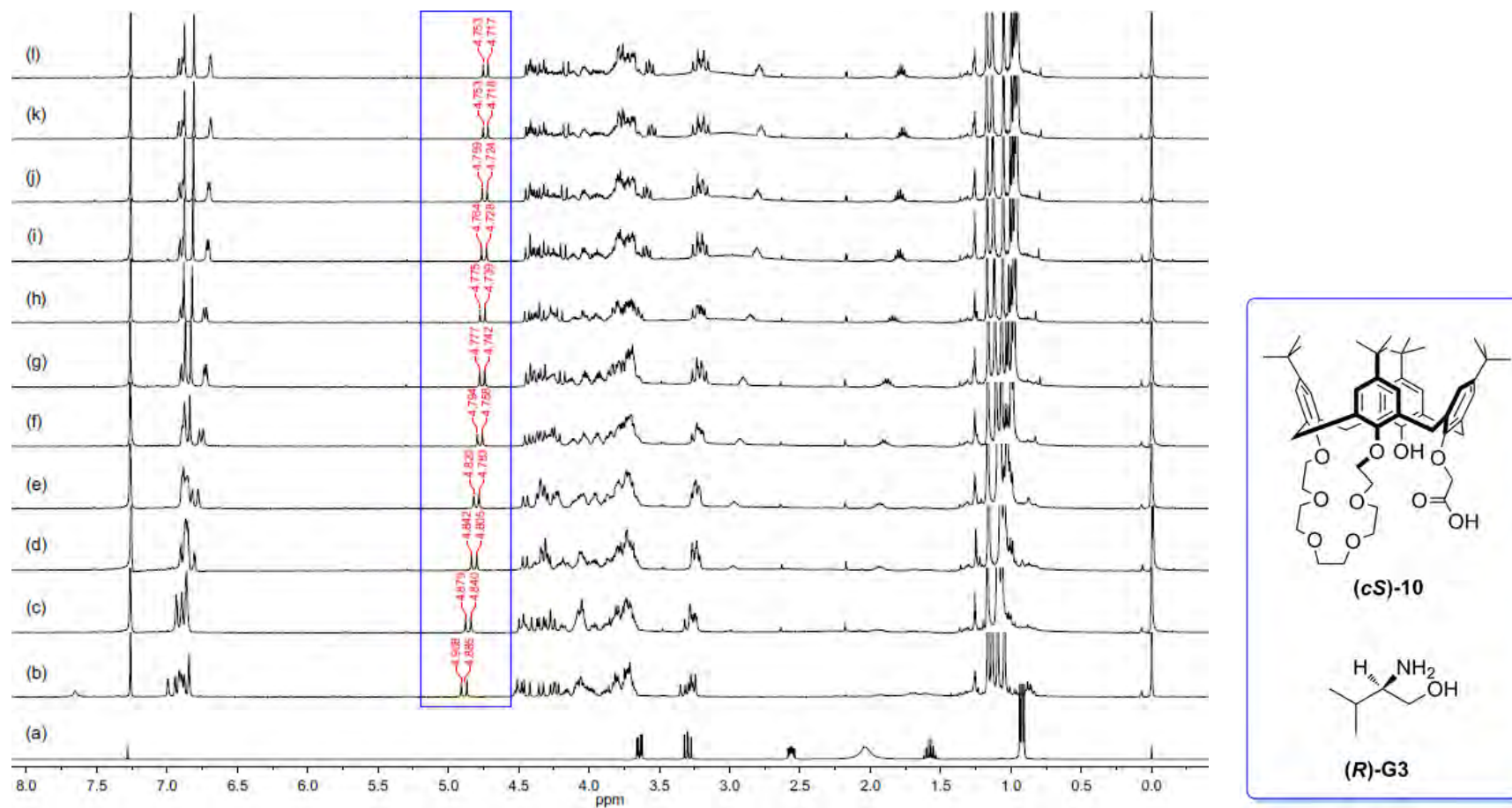


**Fig. S-70** <sup>1</sup>H NMR spectra (CDCl<sub>3</sub>, 400 MHz, 25 °C) of a constant concentration of (+)-(cS)-10 (5 mM) in the presence of increasing equivalents of specific guest: (a) (R)-G3; (b) (+)-(cS)-10; (c) upon addition of 0.2 equiv of (R)-G3; (d) upon addition of 0.4 equiv of (R)-G3; (e) upon addition of 0.6 equiv of (R)-G3; (f) upon addition of 0.8 equiv of (R)-G3; (g) upon addition of 1.0 equiv of (R)-G3; (h) upon addition of 1.2 equiv of (R)-G3; (i) upon addition of 1.4 equiv of (R)-G3; (j) upon addition of 1.6 equiv of (R)-G3; (k) upon addition of 1.8 equiv of (R)-G3; (l) upon addition of 2.0 equiv of (R)-G3.

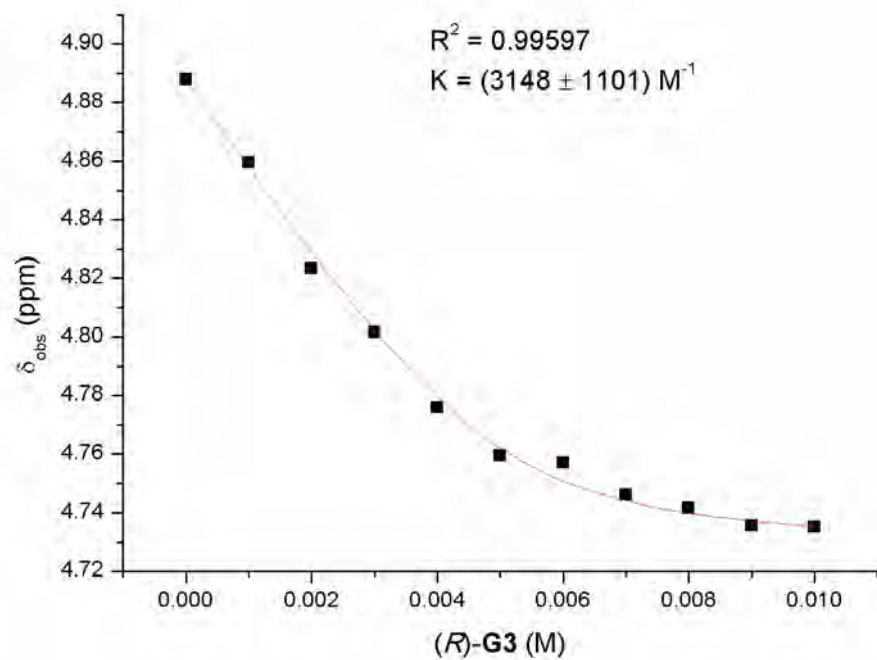


**Fig. S-71** The observed chemical shift changes of (+)-*cS*-**10** (5.0 mM) upon addition of (*R*)-**G3** (0–10.0 mM). The red solid line was obtained from nonlinear curve-fitting.

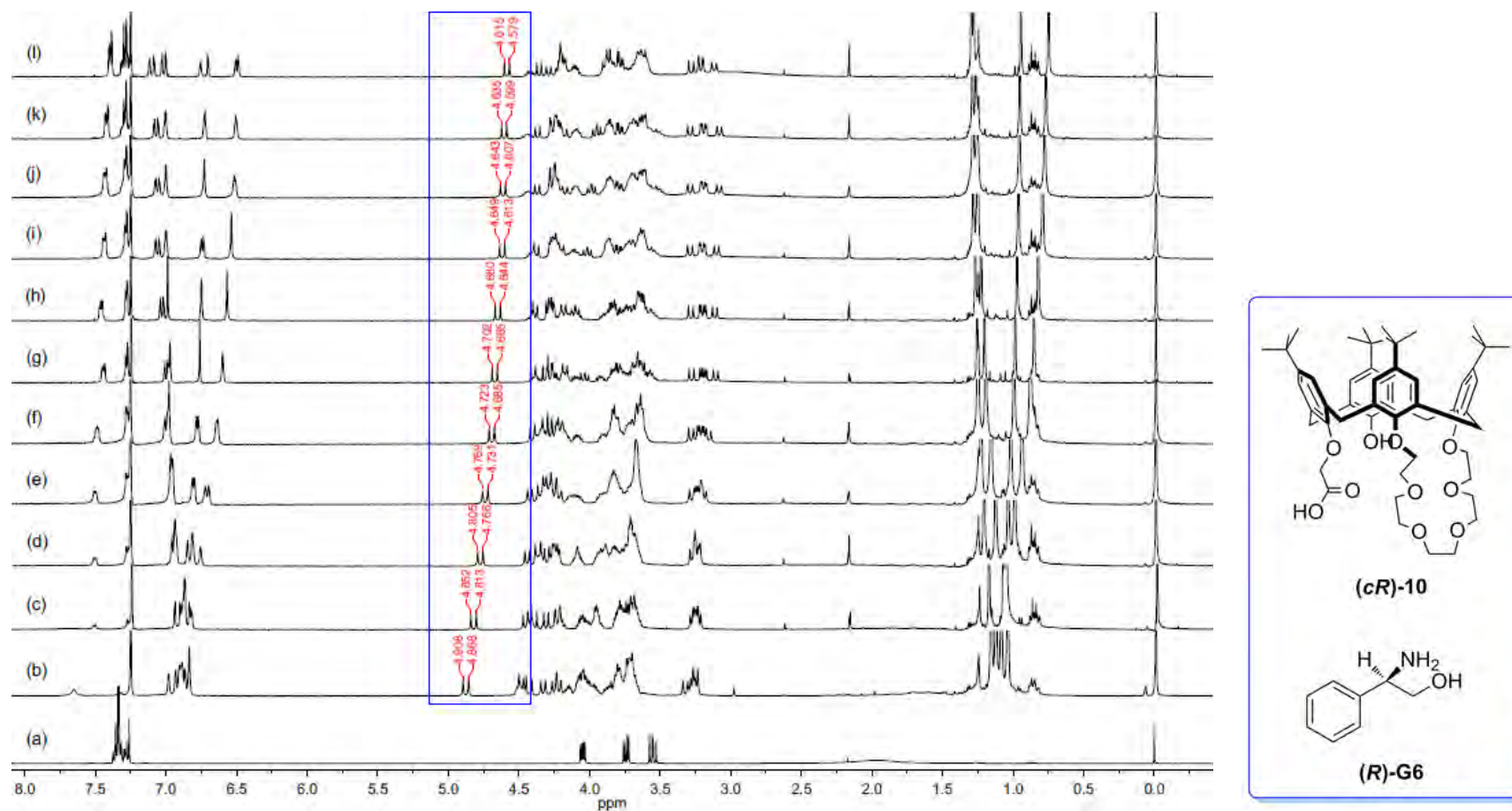


**Fig. S-72** <sup>1</sup>H NMR spectra (CDCl<sub>3</sub>, 400 MHz, 25 °C) of a constant concentration of (-)-(cR)-10 (5 mM) in the presence of increasing equivalents of specific guest: (a) (R)-G6; (b) (-)-(cR)-10; (c) upon addition of 0.2 equiv of (R)-G6; (d) upon addition of 0.4 equiv of (R)-G6; (e) upon addition of 0.6 equiv of (R)-G6; (f) upon addition of 0.8 equiv of (R)-G6; (g) upon addition of 1.0 equiv of (R)-G6; (h) upon addition of 1.2 equiv of (R)-G6; (i) upon addition of 1.4 equiv of (R)-G6; (j) upon addition of 1.6 equiv of (R)-G6; (k) upon addition of 1.8 equiv of (R)-G6; (l) upon addition of 2.0 equiv of (R)-G6.

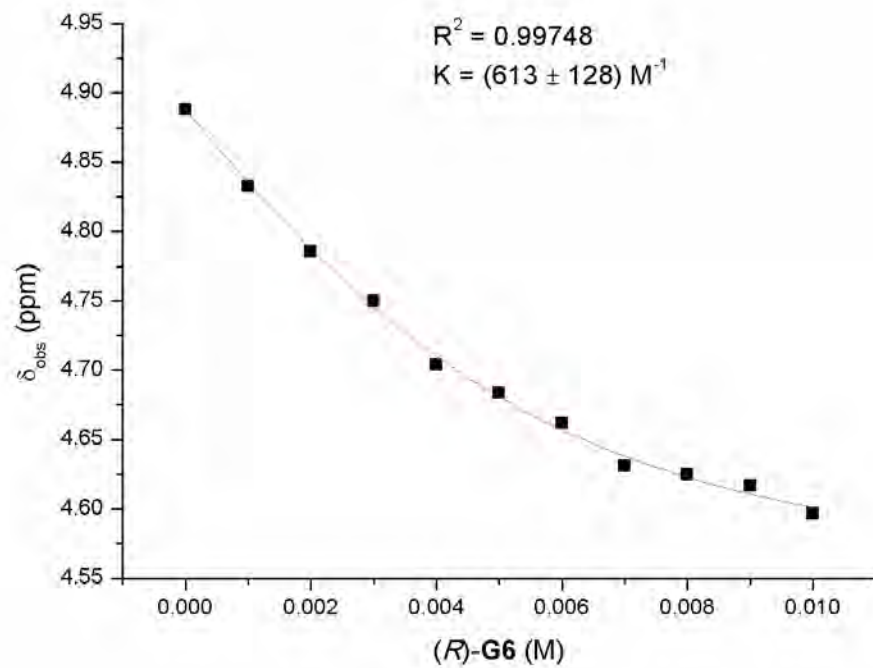


**Fig. S-73** The observed chemical shift changes of  $(-)\text{-}(cR)\text{-10}$  (5.0 mM) upon addition of  $(R)\text{-G6}$  (0–10.0 mM). The red solid line was obtained from nonlinear curve-fitting.

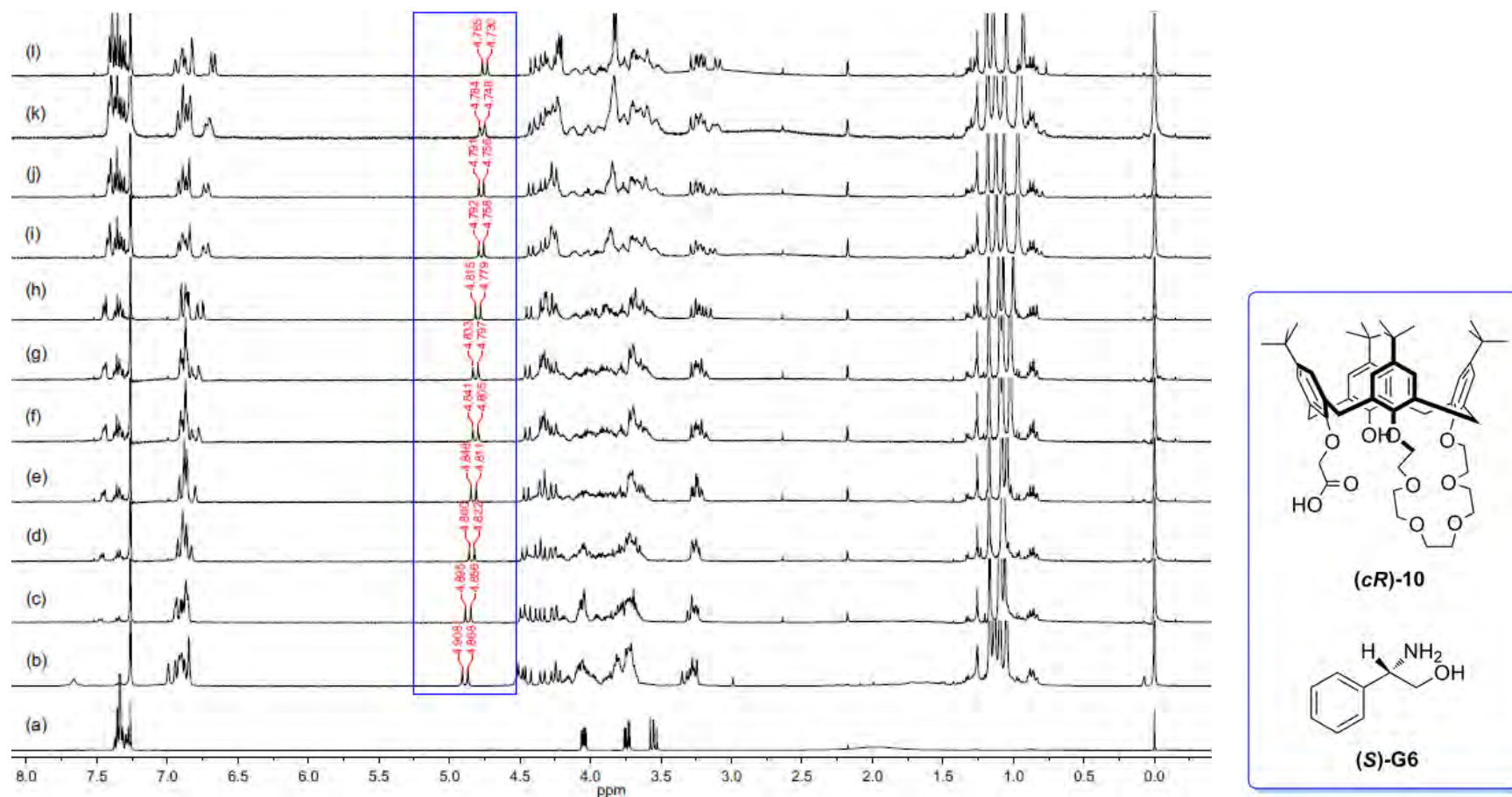


**Fig. S-74** <sup>1</sup>H NMR spectra (CDCl<sub>3</sub>, 400 MHz, 25 °C) of a constant concentration of (-)-(cR)-10 (5 mM) in the presence of increasing equivalents of specific guest: (a) (S)-G6; (b) (-)-(cR)-10; (c) upon addition of 0.2 equiv of (S)-G6; (d) upon addition of 0.4 equiv of (S)-G6; (e) upon addition of 0.6 equiv of (S)-G6; (f) upon addition of 0.8 equiv of (S)-G6; (g) upon addition of 1.0 equiv of (S)-G6; (h) upon addition of 1.2 equiv of (S)-G6; (i) upon addition of 1.4 equiv of (S)-G6; (j) upon addition of 1.6 equiv of (S)-G6; (k) upon addition of 1.8 equiv of (S)-G6; (l) upon addition of 2.0 equiv of (S)-G6.



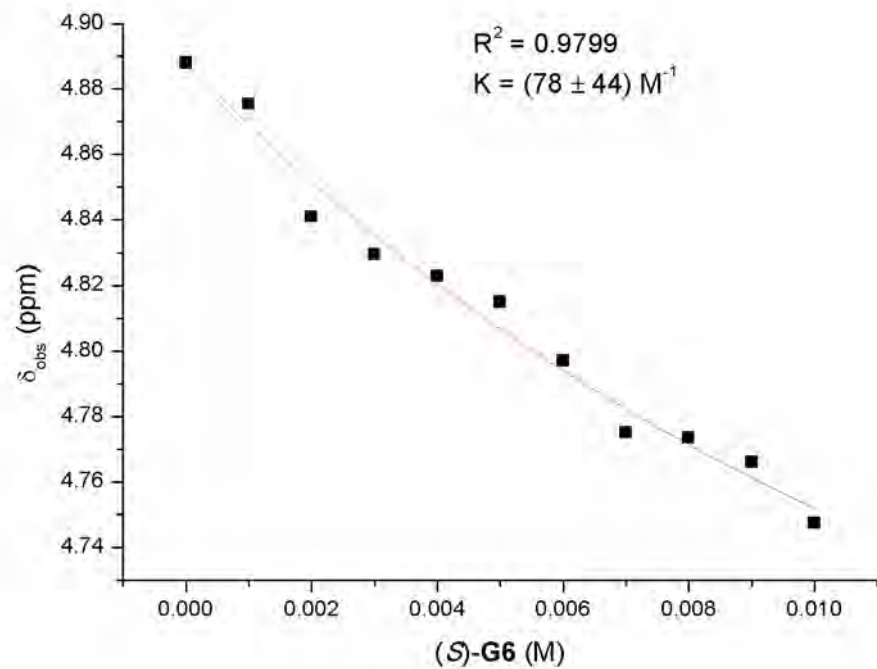


**Fig. S-75** The observed chemical shift changes of (-)-(cR)-**10** (5.0 mM) upon addition of (S)-**G6** (0–10.0 mM). The red solid line was obtained from nonlinear curve-fitting.

**D-4.  $^1\text{H}$  NMR spectra of (+)-(*cS*)-10 (5 mM) and (-)-(*cR*)-10 (5 mM) with varying enantiomeric composition of G3 for the drawing of the standard curves:**

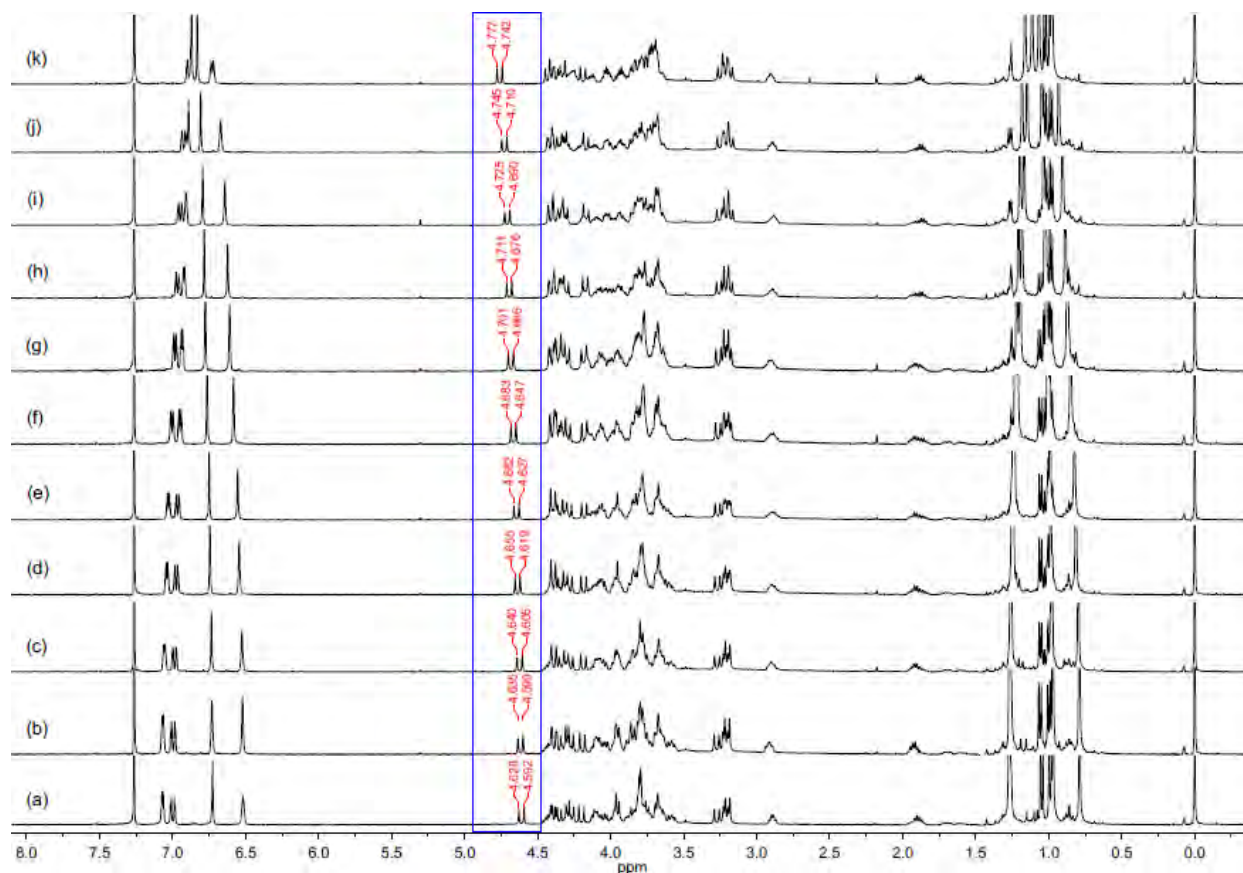


**Fig. S-76**  $^1\text{H}$  NMR spectra of (+)-(*cS*)-10 (5 mM) with varying enantiomeric composition ( $[\text{R}]/[\text{R}] + [\text{S}]$ ) of G3 (5 mM): (a) 0%; (b) 10%; (c) 20%; (d) 30%; (e) 40%; (f) 50%; (g) 60%; (h) 70%; (i) 80%; (j) 90%; (k) 100%.

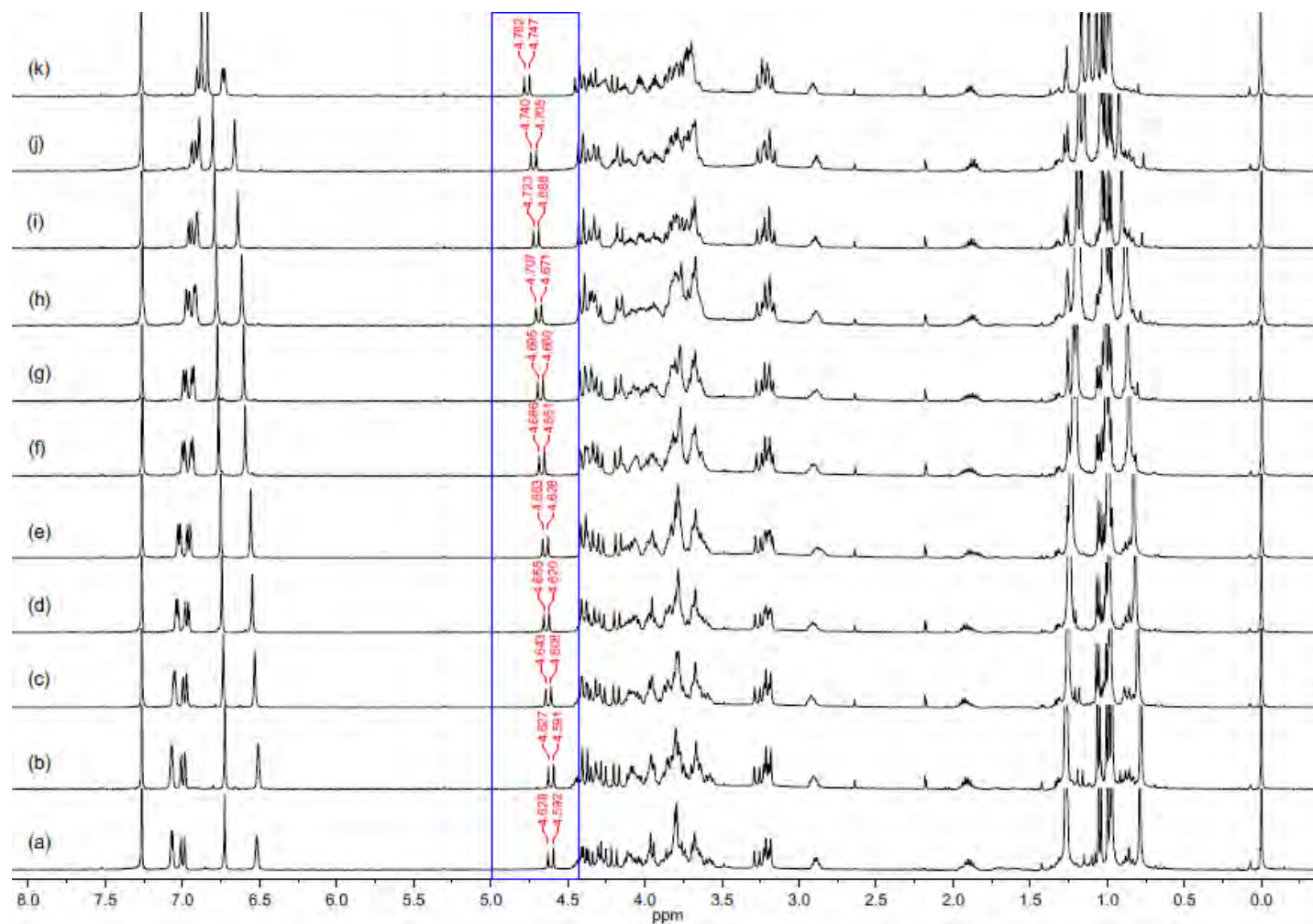


**Fig. S-77**  $^1\text{H}$  NMR spectra of  $(-)-(cR)\text{-10}$  (5 mM) with varying enantiomeric composition ( $[S]/[R] + [S]$ ) of **G3** (5 mM): (a) 0%; (b) 10%; (c) 20%; (d) 30%; (e) 40%; (f) 50%; (g) 60%; (h) 70%; (i) 80%; (j) 90%; (k) 100%.

## Part E. Nomenclature of the configuration of inherently chiral calix[4]crown-6 carboxylic acid **10**.

Herein we adopt the (*cR*)/(*cS*) nomenclature as was suggested by Mandolini, Schiaffino et al to describe the configuration of inherently chiral calix[4]arene **10**.<sup>1</sup> As is shown in Fig. S-78, the four methylene bridging carbons of **10** are labeled as a, b, c, and d in decreasing order of priority. An imaginary observer stand close to carbon d (the lowest priority) on the concave side of the calix[4]arene and see carbons a, b, and c in a counterclockwise sequence, so its configuration is designated as *cS* (here the prefix *c* stands for curvature). If a clockwise sequence is observed for a, b, and c, then the configuration is designated as *cR*.

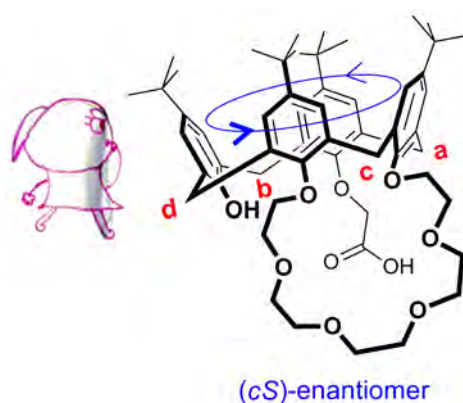


**Fig. S-78** A diagram for the (*cR*)/(*cS*) nomenclature of the configuration of the inherently chiral calix[4]crown-6 **10**.

### Reference

1. A. D. Cort, L. Mandolini, C. Pasquini and L. Schiaffino, *New J. Chem.*, 2004, **28**, 1198–1199.

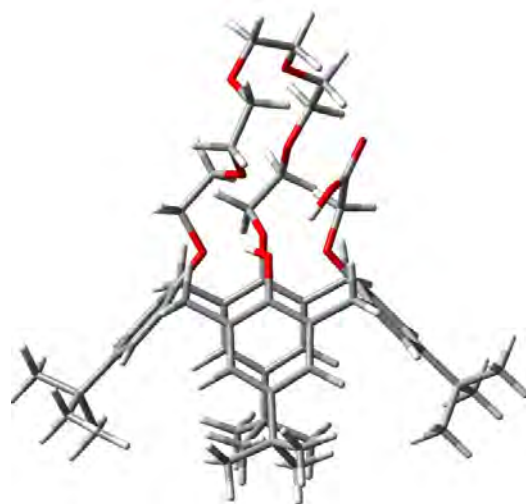
## Part F. DFT theoretical calculation details.

All calculations were performed by the Materials Studio software<sup>1</sup> and the Gaussian 09 program packages<sup>2</sup>. MD simulations based on the COMPASS force field at 300 K were employed to search the possible conformations of **10**. First 100 conformations with low energies were kept. Twelve conformations with lower energy were selected and their geometries were adjusted manually and optimized with the AM1 semi-empirical method. The geometries of the conformations with relative energy less than 6.0 kcal mol<sup>-1</sup> were optimized at DFT/B3LYP/6-31G(d) level, and frequency calculations were carried out to confirm these minima at the same level and to compute vibrational contributions to free energies at 298 K. The lower-energy conformers (i.e., with free energies less than 12 kJ mol<sup>-1</sup> from the minimum) were selected to predict ECD spectra. The population of different conformers follows a Boltzmann distribution. Electronic excitation energies and rotational strengths in CHCl<sub>3</sub> were calculated at TDDFT/B3LYP/6-31+G(d) level in velocity formalism for the first 60 states. The UV and CD curves were simulated by using the Gaussian function:<sup>3</sup>

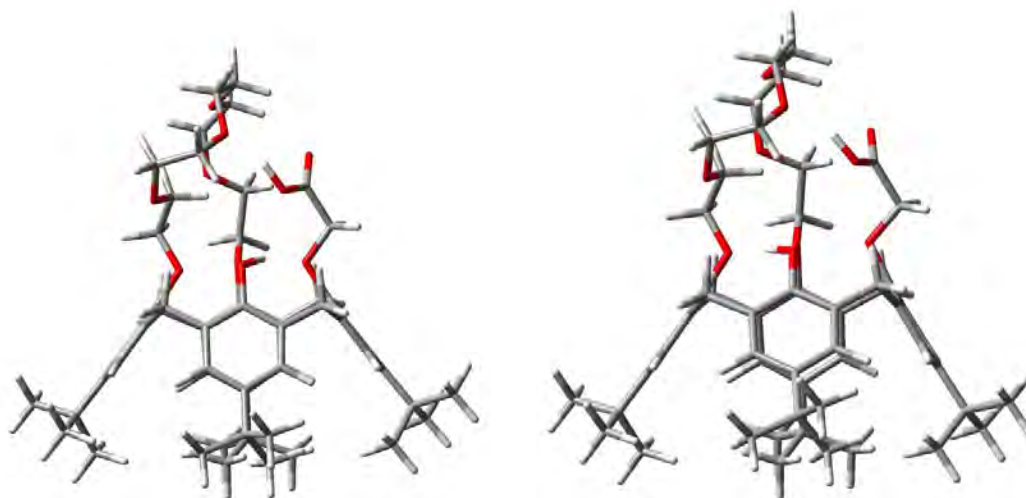
$$\Delta\varepsilon(E) = \frac{1}{2.296 \times 10^{-39}} \frac{1}{\sigma\sqrt{\pi}} \times \sum_i \Delta E_i R_i e^{-[(E-\Delta E_i)/\sigma]^2}$$

where  $\sigma$  is half the band width at  $1/e$  height and  $\Delta E_i$  and  $R_i$  are the excitation energies and rotatory strengths for transition  $i$ , respectively. Here a value of  $\sigma = 0.4$  eV. Because of the systematic errors of the theoretical transition energies as compared to the experimental ones, the spectra were red-shifted by 18nm.

In addition, host-guest interaction was modeled by DFT calculations. The full geometry optimization of the host, guests and complexes was performed at the B3LYP/6-31G(d) level. Since dispersion interactions were expected to be essential in the stereochemical control in some reactions, Grimme's DFT-D3(BJ) dispersion corrections were calculated using the DFTD3 program,<sup>4</sup> and D3 corrections were included for the discussion of enantioselectivity.



**(cS)-10-I**



**(cS)-10-II**

**(cS)-10-III**

**Fig. S-79** The geometries of the most stable conformers of *(cS)*-10 at TDDFT/B3LYP/6-31+G(d) level.

**Table S-1** Relative free energies and Boltzmann populations of the most stable conformers of *(cS)*-10.

conformers	Free energy (a.u.)	Free energy different (kcal/mol)	Boltzmann population (%)
<b>(cS)-10-I</b>	-2930.813446	0	91
<b>(cS)-10-II</b>	-2930.811202	1.41	8
<b>(cS)-10-III</b>	-2930.809516	2.47	1

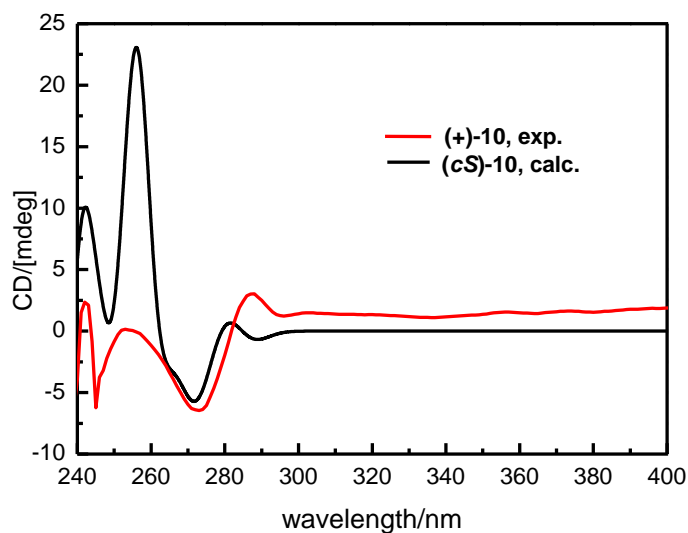


**Fig. S-80** A comparison of the measured and simulated ECD spectra of (*cS*)-**10** calculated at the TD-B3LYP/6-31+G(d)//B3LYP/6-31G(d) level of theory

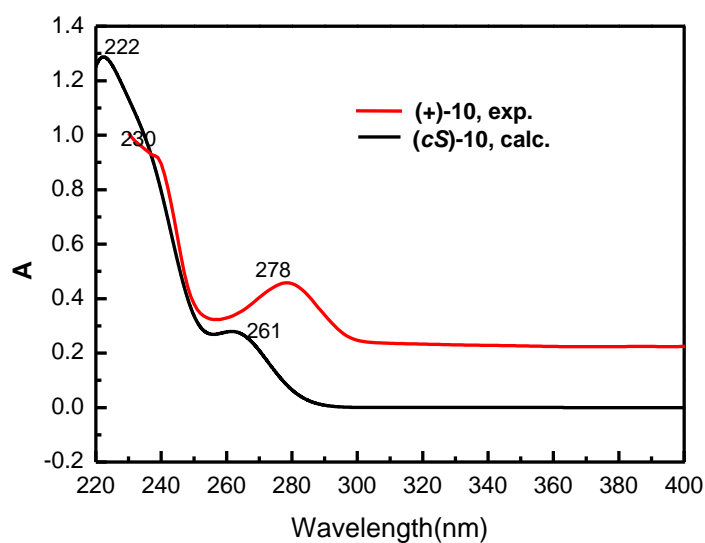


**Fig. S-81** A comparison of the measured and simulated UV spectra (right) of (*cS*)-**10** calculated at the TD-B3LYP/6-31+G(d)//B3LYP/6-31G(d) level of theory.

## References:

1. Accelrys Materials Studio by Accelrys Inc. Versions: 4.2.
2. Frisch, M. J.; Trucks, G. W.; Schlegel, H. B.; Scuseria, G. E.; Robb, M. A.; Cheeseman, J. R.; Montgomery, J. A., Jr.; Vreven, T.; Kudin, K. N.; Burant, J. C.; Millam, J. M.; Iyengar, S. S.; Tomasi, J.; Barone, V.; Mennucci, B.; Cossi, M.; Scalmani, G.; Rega, N.; Petersson, G. A.; Nakatsuji, H.; Hada, M.; Ehara, M.; Toyota, K.; Fukuda, R.; Hasegawa, J.; Ishida, M.; Nakajima,

T.; Honda, Y.; Kitao, O.; Nakai, H.; Klene, M.; Li, X.; Knox, J. E.; Hratchian, H. P.; Cross, J. B.; Bakken, V.; Adamo, C.; Jaramillo, J.; Gomperts, R.; Stratmann, R. E.; Yazyev, O.; Austin, A. J.; Cammi, R.; Pomelli, C.; Ochterski, J. W.; Ayala, P. Y.; Morokuma, K.; Voth, G. A.; Salvador, P.; Dannenberg, J. J.; Zakrzewski, V. G.; Dapprich, S.; Daniels, A. D.; Strain, M. C.; Farkas, O.; Malick, D. K.; Rabuck, A. D.; Raghavachari, K.; Foresman, J. B.; Ortiz, J. V.; Cui, Q.; Baboul, A. G.; Clifford, S.; Cioslowski, J.; Stefanov, B. B.; Liu, G.; Liashenko, A.; Piskorz, P.; Komaromi, I.; Martin, R. L.; Fox, D. J.; Keith, T.; Al-Laham, M. A.; Peng, C. Y.; Nanayakkara, A.; Challacombe, M.; Gill, P. M. W.; Johnson, B.; Chen, W.; Wong, M. W.; Gonzalez, C.; Pople, J. A. Gaussian03, revision A.1; Gaussian, Inc.: Pittsburgh, PA, **2009**.

3. Philip J. S.; Nobuyuki H. *Chirality*, **2010**, *22*, 229.

4. Grimme, S. DFTD3, V2.0 Rev 1; University Münster: Münster, Germany, **2010**.